



Universidade do Minho
Escola de Engenharia

Design of sustainable nano-based delivery systems and evaluation of their behaviour during *in vitro* digestion

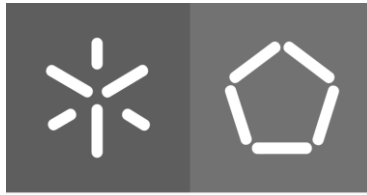
Alexandra Peixoto Ferreira

Design of sustainable nano-based delivery systems and evaluation of their behaviour during *in vitro* digestion

Alexandra Peixoto Ferreira

UMinho | 2022

October de 2022



Universidade do Minho
Escola de Engenharia

Alexandra Peixoto Ferreira

Design of sustainable nano-based delivery systems and evaluation of their behaviour during *in vitro* digestion

Dissertação de Mestrado

Mestrado em Biotecnologia

Trabalho efetuado sob a orientação da

Doutora Ana Cristina Braga Pinheiro

October de 2022

Direitos de autor e condições de utilização do trabalho por terceiros

Este é um trabalho académico que pode ser utilizado por terceiros desde que respeitadas as regras e boas práticas internacionalmente aceites, no que concerne aos direitos de autor e direitos conexos.

Assim, o presente trabalho pode ser utilizado nos termos previstos na licença abaixo indicada.

Caso o utilizador necessite de permissão para poder fazer um uso do trabalho em condições não previstas no licenciamento indicado, deverá contactar o autor, através do RepositóriUM da Universidade do Minho.

Licença concedida aos utilizadores deste trabalho



Atribuição
CC BY

<https://creativecommons.org/licenses/by/4.0/>

Agradecimentos

Com o concluir desta etapa gostaria de deixar os meus agradecimentos a todos os que contribuíram.

Em primeiro lugar, deixo o meu especial agradecimento à minha orientadora, Doutora Ana Cristina Pinheiro que me proporcionou a oportunidade de desenvolver este tema bem como a sua constante partilha de conhecimentos, incentivo à livre partilha de opiniões e confiança para desenvolver o trabalho com maior autonomia. Adicionalmente, este trabalho não poderia ter sido desenvolvido sem o apoio do Professor Doutor António Vicente que me permitiu utilizar as instalações do LIP e que demonstrou que mesmo sendo uma figura de autoridade é possível demonstrar amabilidade e companheirismo. O meu muito obrigada a ambos.

Também estou extremamente agradecida a todos os *Lipinhos* que desde o primeiro dia me fizeram sentir uma deles. Ao Vitor, Luís, Leandro, Francisco e Diogo, um muito obrigada pela disponibilidade em ajudar, apoio moral e companhia nas longas horas laboratoriais. Um especial agradecimento à Márcia, Raquel, Daniel e Jean-Michel que me acompanharam de mais de perto ao longo destes meses e contribuíram com o seu conhecimento teórico e prático na execução deste trabalho.

A nível mais pessoal gostaria de agradecer aos meus amigos, em especial à Sara, pela amizade, disponibilidade apesar da distância e paciência para me ouvir quando estava mais desanimada. Que venham mais anos de companheirismo e gargalhadas. Aos coleguinhas de bioinformática, Mónica, Tiago e Tiago obrigada por me fazerem sentir incluída, pelos serões de petiscadas e pelas longas explicações de tratamento estatístico.

Ao meu namorado, Miguel, obrigada pelo apoio incondicional, por me relembrares que por vezes é preciso abrandar e me alegrares nos dias de menor motivação recordando-me sempre do que sou capaz. Obrigada por teres entrado na minha vida e mostrares-me que o “improvável” funciona.

Por fim, mas não menos importante quero agradecer à minha família, por me permitirem fazer o percurso que quis sem restrições e ceticismos. Um especial agradecimento aos meus pais, por me mostrarem que para alcançar um objetivo é necessário esforço, dedicação e por vezes “bater com a cabeça na parede” sem desistir.

Statement of integrity

I hereby declare having conducted this academic work with integrity. I confirm that I have not used plagiarism or any form of undue use of information or falsification of results along the process leading to its elaboration.

I further declare that I have fully acknowledged the Code of Ethical Conduct of the University of Minho.

Resumo

A curcumina é um fitoquímico hidrofóbico obtido do açafrão da Índia, que demonstra efeitos benéficos contra a diabetes, cânceros do sistema gastrointestinal, úlceras gástricas, doença inflamatória intestinal e obesidade, bem como é segura, bem-aceite e de baixo custo sendo assim apelativa para a fortificação alimentar. Contudo, como apresenta baixa solubilidade e é foto instável, a sua encapsulação é benéfica. Além disso, a utilização de sistemas de encapsulação à base de plantas não só vai de encontro às tendências atuais de economia sustentável, que recorre a materiais abundantes, biodegradáveis, biocompatíveis e não-tóxicos mas também são materiais compatíveis para consumidores com dietas restritas. Neste trabalho, a curcumina foi encapsulada em dois nanosistemas de encapsulamento sustentáveis, especificamente nanopartículas lipídicas sólidas (SLNs) com base em cera de candelilla e nanopartículas de proteína de ervilha. Um desenho experimental foi implementado com o intuito de obter uma formulação otimizada de SLNs, tendo permitido determinar que a concentração de cera, de lecitina e de Tween 80 eram influentes na variabilidade dos parâmetros de resposta. Uma formulação composta por 4.2 % (w/w) de cera, 0.7 % (w/w) de curcumina e de 0.9 % (w/w) de lecitina e Tween 80, exibiu um tamanho de 179.2 ± 4.0 nm, índice de polidispersividade (PDI) de 0.191 ± 0.008 e ζ -potencial de -20.4 ± 0.3 mV. Apresentou ainda uma eficiência de encapsulação (EE) de 100 ± 0.6 % e estabilidade durante 27 dias. A bioacessibilidade, estabilidade e biodisponibilidade efetiva das SLNs foi de 67.4 ± 14.4 %, 5.3 ± 0.4 % e 3.6 ± 0.6 %, respetivamente. A baixa estabilidade pode refletir um *burst release* durante a fase gástrica. No final da fase gástrica, a libertação de ácidos gordos foi de 14.25 ± 6.38 %, um valor mais alto do que seria de esperar uma vez que a cera de candelilla é indicada como não digerível. As nanopartículas de proteína de ervilha foram otimizadas em relação à formulação, concentração de curcumina e pH. A formulação de pH 8 e concentração de curcumina inicial de 0.034 mg/mL foi escolhida por demonstrar um tamanho de 154.6 ± 6.5 nm, PDI de 0.312 ± 0.018 e ZP de -29.6 ± 2.7 mV, além da EE mais elevada (80.29 ± 8.54 %). Após 13 dias, o tamanho e ζ -potencial mantiveram-se e o PDI teve um aumento, pequeno, mas significativo. No fim da digestão *in vitro* obteve-se uma bioacessibilidade de 46.6 ± 27.7 %, estabilidade de 14.1 ± 2.9 % e biodisponibilidade efetiva de 5.0 ± 1.3 %. A digestibilidade das nanopartículas proteicas foi de 70.1 ± 16.6 %. Ambos os nanosistemas desenvolvidos demonstraram as características físicas desejadas, com tamanho pequeno, EE elevada, estáveis ao longo do tempo e bioacessibilidade relativamente altas.

Palavra-chave: curcumina, nanosistemas de entrega com base em plantas, nanopartículas lipídicas sólidas, nanopartículas proteicas, proteína de ervilha

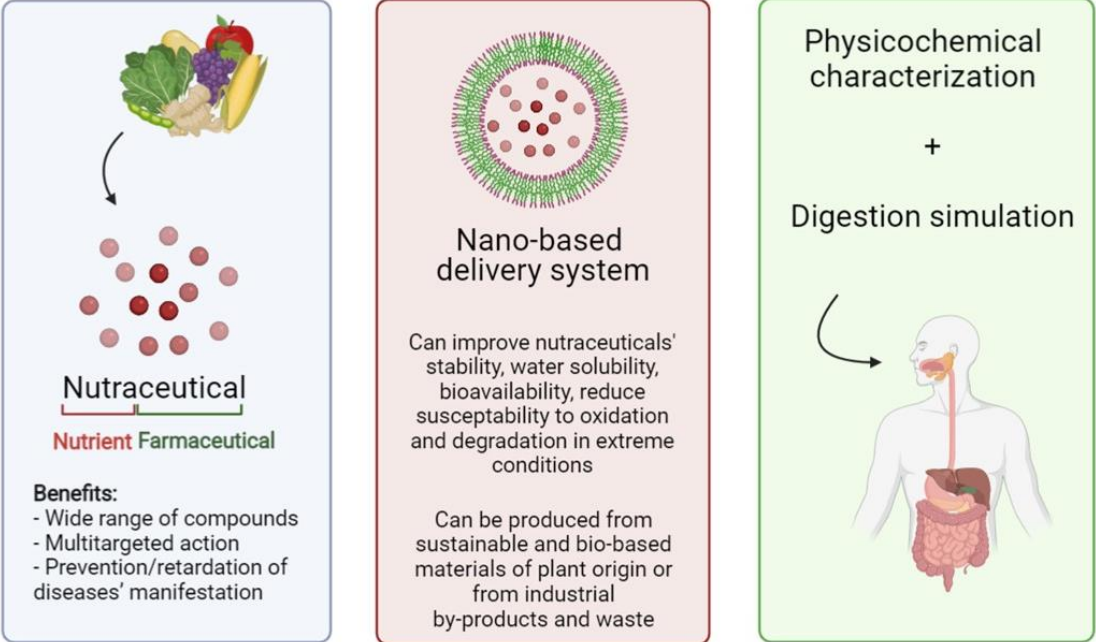
Abstract

Curcumin is a hydrophobic phytochemical obtained from the plant turmeric, whose beneficial effects against diabetes, gastrointestinal cancers, gastric ulcers, inflammatory bowel diseases and obesity as well as safety, tolerability and cost-effectiveness make it appealing for food fortification. Since this nutraceutical demonstrates low water solubility and photo instability, the encapsulation is seen as an optimal solution. Furthermore, the utilization of plant-based encapsulation materials not only is in accordance with the current tendencies of creating a more sustainable economy, while resourcing to abundant, biodegradable, biocompatible and non-toxic resources but also, they are appropriate for consumers with restricted diets (e.g. vegan, gluten or dairy free diet). In this work, curcumin was encapsulated in two sustainable bio-based nanodelivery systems, specifically solid lipid nanoparticles (SLNs) based on candelilla wax and pea protein nanoparticles. An experimental design was applied to optimize the SLNs formulation and allowed to determine that candelilla wax, lecithin and Tween 80 concentration significantly affected the response parameters variation. A formulation composed of 4.2 % (w/w) candelilla wax, 0.7 % (w/w) curcumin and 0.9 % (w/w) lecithin and Tween 80, demonstrated a size of 179.2 ± 4.0 nm, polydispersity index (PDI) of 0.191 ± 0.008 and a ζ -potential of -20.4 ± 0.3 mV. This formulation also demonstrated an encapsulation efficiency (EE) of 100.0 ± 0.6 % as well storage stability up to 27 days. SLNs bioaccessibility, stability and effective bioavailability was determined after *in vitro* digestion obtaining as results 67.4 ± 14.4 %, 5.3 ± 0.4 % and 3.6 ± 0.6 %, respectively. The low stability could reflect a burst release effect during gastric phase. At the end of intestinal phase, the free fatty acids release was 14.25 ± 6.38 %, a higher value than expected since candelilla wax is considered non-digestible. Pea protein formulations were optimized in terms of formulation, curcumin concentration and pH of formulation. The formulation with pH 8 and initial curcumin concentration of 0.034 mg/mL was selected since it demonstrated a size of 154.6 ± 6.5 nm, PDI of 0.312 ± 0.018 and ZP of -29.6 ± 2.7 mV. Additionally, it offered the highest EE (i.e. 80.29 ± 8.54 %). After 13 days of storage, the size and ZP were maintained and the PDI showed a slight but significant increase. At the end of *in vitro* digestion, a bioaccessibility of 46.6 ± 27.7 %, stability of 14.1 ± 2.9 % and effective bioavailability of 5.0 ± 1.3 % were obtained. The digestibility of PPI nanoparticles was 70.1 ± 16.6 %. Both biobased nanodelivery systems developed attained the proposed physical characteristics, with low particle sizes, high EE, stability over time and relatively high bioaccessibility.

Keywords: curcumin, pea protein, plant-based nanodelivery systems, protein nanoparticles, solid lipid nanoparticles

Graphical abstract

Design of sustainable nano-based delivery systems and evaluation of their behaviour during *in vitro* digestion



Index

Direitos de autor e condições de utilização do trabalho por terceiros	iv
Agradecimentos.....	v
Statement of integrity	vi
Resumo	vii
Abstract	viii
Graphical abstract	ix
Index	x
List of general nomenclature.....	xiii
List of tables	xv
List of figures	xvii
1. Motivation and objectives	20
1.1. Thesis motivation.....	21
1.2. Research aims.....	21
1.3. Thesis outline	22
2. Literature review	23
2.1 Nutraceuticals: Definition and health benefits	24
1.1.1. Phytochemicals	24
1.1.2. Vitamins	27
1.1.3. Lipids	28
1.1.4. Bioactive peptides.....	28
1.1.5. Prebiotics and probiotics	28
1.1.6. Minerals	29
2.2. Nutraceuticals: Limitations	29
2.3. Bio-based nanodelivery systems: Beneficial characteristics.....	30
2.4. Bio-based nanodelivery systems: Sustainable approach	31
2.5. Bio-based nanodelivery systems: Encapsulating materials	33
2.5.1. Polysaccharide-based delivery systems	33
2.5.2. Protein-based delivery systems	33
2.5.3. Lipid-based delivery systems.....	36
2.6. Bio-based nanodelivery systems: Encapsulation techniques	38
2.6.1. High shear homogenization	39
2.6.2. Cold gelation	39

2.7. Physicochemical characterization of biobased delivery systems	40
2.7.1. Particle size.....	40
2.7.2. Morphology	41
2.7.3. ζ -Potential	41
2.7.4. Structural alterations.....	41
2.7.5. Optical characterization.....	42
2.7.6. Encapsulation efficiency	42
2.8. Bio-based delivery systems' behaviour in the GI tract.....	42
3. Experimental approach.....	45
3.1. Materials.....	46
3.2. Encapsulation of curcumin in solid lipid nanoparticles.....	46
3.2.1. Preliminary assay to choose the plant wax	46
3.2.2. Experimental design.....	46
3.3. Encapsulation of curcumin in pea protein nanoparticles	47
3.3.1. Nanoparticle preparation	47
3.3.2. Curcumin encapsulation.....	48
3.4. Nanostructure's characterization	48
3.4.1. Particle size and polydispersity index	48
3.4.2. ζ -potential	49
3.4.3. Encapsulation efficiency	49
3.4.4. Stability assessment during storage of nanostructures.....	50
3.5. <i>In vitro</i> digestion	50
3.5.1. Digestion stock solutions	50
3.5.2. <i>In vitro</i> static digestion.....	51
3.5.3. Physicochemical characterization	51
3.5.4. Curcumin bioaccessibility, stability and effective bioavailability	51
3.5.5. Nanostructures' digestibility	52
3.6. Statistical analysis.....	53
3.6.1. Experimental design' statistical treatment	53
4. Results and discussion.....	55
4.1. Solid lipid nanoparticles for curcumin encapsulation	56
4.1.1. Preliminary assay: production of SLNs	56
4.1.2. Experimental design.....	57
4.2.1. Physicochemical characterization	59

4.2.2. Experimental design data analysis	63
4.3.2. <i>In vitro</i> digestion analysis.....	69
4.2. Encapsulation of curcumin in pea protein isolate nanoparticles.....	71
4.2.1. Formulation optimization	71
4.2.2. <i>In vitro</i> digestion of PPI nanoparticles	78
5. Conclusions and future remarks.....	83
5.1. Conclusions	84
5.2. Future remarks.....	85
6. References.....	87
7. Annexes.....	100

List of general nomenclature

AFM	Atomic force microscopy
B	Bioaccessibility
BA	Effective bioavailability
BBNDs	Biobased nanodelivery systems
BSA	Bovine serum albumin
CCRD	Central composite rotatable design
CLSM	Confocal laser electron microscopy
DDM	Dynamic digestion model
DH	Degree of hydrolysis
DLS	Dynamic light scattering
DSC	Differential scanning calorimetry
ED	Experimental design
EE	Encapsulation efficiency
FFA	Free fatty acids
GI	Gastrointestinal
GRAS	Generally recognized as safe
HSH	High shear homogenization
LDS	Lipid-based delivery systems
MLR	Multiple linear regression
NDS	Nanodelivery systems
PDS	Protein-based delivery systems
PDI	Polydispersity index
PLS	Partial least squares
PPI	Pea protein isolate
S	Stability
SDM	Static digestion model
SEM	Scanning electron microscopy
SGF	Simulated gastric fluid
SIF	Simulated intestinal fluid
SLNs	Solid lipid nanoparticles

SSF	Simulated salivary fluid
TEM	Transmission electron microscopy
TGA	Thermogravimetric analysis
VIP	Variable importance in projection
ZP	Zeta potential

List of tables

Table 1 – Nutraceuticals’ classification and description of compounds’ specific activity.....	25
Table 2 – Nutraceutical compounds or compound groups and their associated limitations.....	29
Table 3 – Examples of some encapsulating materials used for nutraceuticals’ encapsulation, with specification of the encapsulation technique and benefits verified.....	32
Table 4 – Some examples of lipidic delivery systems and their main characteristics.....	37
Table 5 – Top-down and bottom-up methods used in nanodelivery systems production.....	38
Table 6 - GI tract environmental conditions and their possible effect in the bio-based delivery system characteristics.....	42
Table 7 – Description of experimental design’ input variables and their imposed limits.....	47
Table 8 – Composition of the 27 assays of the experimental design.....	48
Table 9 – Particle mean size (nm), and respective standard deviation of solid lipid nanoparticles formulations based on with candelilla wax (27 formulations from experimental design). Statistically significant differences ($p > 0.05$) among values obtained for each parameter on the analysed days are indicated in lower case letters. Equal letters indicate that no statistically significant difference was identified through Tuckey Mean comparison test.....	60
Table 10 – Polydispersity index, and respective standard deviation, of solid lipid nanoparticles formulated with candelilla wax (27 formulations from experimental design). Statistically significant differences ($p > 0.05$) among values obtained for each parameter on the analysed days are indicated in lower case letters. Equal letters indicate that no statistically significant difference was identified through Tuckey Mean comparison test.....	61
Table 11 - ζ -Potential (mV), and respective standard deviation, of solid lipid nanoparticles formulated with candelilla wax (27 formulations from experimental design). Statistically significant differences ($p > 0.05$) among values obtained for each parameter on the analysed days are indicated in lower case letters. Equal letters indicate that no statistically significant difference was identified through Tuckey Mean comparison test.....	62

Table 12 – Encapsulation efficiency, of solid lipid nanoparticles formulated with candelilla wax (27 formulations from experimental design).....	63
Table 13 – Central composite rotatable design methodology employed on experimental design' data. The regression equation and respective determination coefficient for each dependent variable was attained by removal of non-statistically significant coefficients ($p < 0.05$).....	64
Table 14 – Multiple linear regressions' determination coefficients obtained for each dependent variable. based on the combination of one to four independent variables.....	66
Table 15 - Partial least squares analysis employed on the selected assays from the experimental design ($PDI < 0.5$). The resulting factors, variance explained from X effects and for Y responses, resulting from a standardized worlds iteration method, are indicated.....	67
Table 16 - Mean particle size, polydispersity index and ζ -Potential of the selected solid lipid nanoparticles (formulation E5), with respective standard deviation value, in the different in vitro gastrointestinal digestion phases. Different lowercase letters indicate statistically significant differences between digestion phases measurements.....	69
Table 17 – Experimental assays established conditions for determining the influence of final curcumin concentration (mg/mL) and final ethanol percentage (% w/v) on formulation E4.....	73
Table 18 – Curcumin's encapsulation efficiency. and respective standard deviation obtained for different formulations.....	77
Table 19 - Mean particle size, polydispersity index and ζ -Potential of PPI nanoparticles (formulation E9), in different in vitro gastrointestinal digestion phases. Different lowercase letters indicate statistically significant differences between digestion phases measurements ($p < 0.05$).....	80

List of figures

Figure 1 – Nutraceuticals' main advantages when encapsulated in nanodelivery systems.....	30
Figure 2 – Physical and Biological phenomena that occur during GI tract digestion.....	44
Figure 3 – Nanoparticles' size (A), polydispersity index (PDI) (B) and ζ -Potential (C). Statistically significant differences ($p>0.05$) among plant waxes, for each parameter, are indicated in lower case letters. Equal letters indicate that no statistically significant difference was identified through Tuckey Mean comparison test.....	56
Figure 4 – Stability assessment of solid lipid nanoparticle formulation based on candelilla wax. The particle size (A), polydispersity index (PDI) (B) and ζ -Potential (C) were evaluated during 37 days of storage. Statistically significant differences ($p > 0.05$) among values obtained for each parameter on the analysed days are indicated in lower case letters. Equal letters indicate that no statistically significant difference was identified through Tuckey Mean comparison test.....	58
Figure 5 – Nanoparticles apparent destabilization, indicated by black arrows, verified on day 27 after formulation. The formulation is composed of 3 % (w/w) candelilla wax, 0.10 % (w/w) curcumin and 1.5 % (w/w) of lecithin and Tween 80.....	59
Figure 6 – Variable importance in projection plot obtained as result of Partial Least Squares analysis of the selected experimental design assays.....	67
Figure 7 – Particles physical characterization of formulations E2, E3 and E4 of PPI nanoparticles. Mean particle size (A), polydispersity index (B) and ζ -Potential (C) were determined for each formulation. Formulation E2 and E4 correspond to the formulation's procedures initiated in a tenth of the total volume and in which the remaining water volume was added immediately or 2h after the calcium dichloride cross-linking. Formulation E3 has 85% of the total volume from the beginning. Different lowercase letters indicate significant difference ($p>0.05$) between formulations.....	72
Figure 8 – Mean particle size (A), polydispersity index (B) and ζ -Potential (C) of different PPI nanoparticles' formulations. E4 indicates the formulation without curcumin added while experiments T1, T3 and T4 had a final curcumin concentration of, respectively, 0.567, 0.113 and 0.000 mg/mL in final ethanol concentration of 8.95 % (w/v). In experiment T2, a final curcumin concentration of 0.567 mg/mL was obtained by direct addition of curcumin powder. T5 has a final curcumin and ethanol composition of	

0.013 mg/mL and 2 % (w/v). Different lowercase letters indicate significant difference ($p > 0.05$) between formulations.....74

Figure 9 – PPI nanoparticles mean particle size (A), polydispersity index (B) and ζ -Potential (C). Formulation E4 (green) corresponds to the formulation without curcumin, E6 (grey) and T5 (blue) correspond to the formulation with 0.013 mg/mL of curcumin added, respectively, before and after nanoparticles cross-linking induced by CaCl_2 . Different lowercase letters indicate statistically significant differences between formulations measurements ($p > 0.05$).....75

Figure 10 – Mean particle size (A), polydispersity index (B) and ζ -Potential (C) of different PPI nanoparticles' formulations. For formulations E8T1 (blue) and E8T2 (orange) crosslinking with CaCl_2 occurred at pH 7, with an initial curcumin concentration of 0.034 mg/mL and 0.078 mg/mL, respectively. For formulation E9 (green) and E10 (grey) crosslinking occurred at pH 8 and 9, respectively, and both formulations had an initial concentration of curcumin of 0.034 mg/mL. The formulations without curcumin (NCur) are represented in lighter colour tone while the formulations with curcumin encapsulated (WCur) are represented in a darker colour tone. Different lowercase letters indicate statistically significant differences between formulations measurements ($p > 0.05$).....76

Figure 11 – Mean particle size (A). polydispersity index (B) and ζ -potential (C) of different PPI nanoparticles' formulations. The formulations E6 and E4T5 curcumin adding of 0.013 mg/mL occurred, respectively, before and after nanoparticles cross-linking induced by CaCl_2 at pH7. Formulations E8T1 and E8T2 crosslinking with CaCl_2 occurred at pH 7, with an initial curcumin concentration of 0.034 mg/mL and 0.078 mg/mL, correspondingly. For formulation E9 and E10 crosslinking occurred at pH 8 and 9, respectively, and both formulations had an initial concentration of curcumin of 0.034 mg/mL. The measurement days are colour coded: dark grey as day 0, orange as day 1, green as day 13, yellow as day 15 and blue as day 30. Different lowercase letters indicate statistically significant differences between measurement days of the same formulation ($p > 0.05$).....79

Figure 12 – Degree of hydrolysis over time of PPI nanoparticles (formulation E9) at gastric phase of in vitro digestion.....81

Figure A.1 – Calibration curve of curcumin in ethanol - absorbance at 430 nm versus curcumin concentration ($\mu\text{g/mL}$). The calibration curve equation is: Absorbance (430 nm) = 61174 [Curcumin] ($\mu\text{g/mL}$) + 0.0544 and the respective determination coefficient is 0.9997. The absorbance measurements were obtained in Cytation 3_Byotec equipment.....101

Figure A.2 – Demonstration of curcumin mean absorbance at 430 nm, solubilized in 47.5 and 50 % (w/v) of ethanol. Different lower case letters are indicative of statistically significant differences ($p > 0.5$).....101

Figure A.3 – Calibration curve of curcumin in ethanol - absorbance at 430 nm versus curcumin concentration ($\mu\text{g/ml}$). The calibration curve equation is: Absorbance (430 nm) = 186.51 [Curcumin] (g/mL) – 0.01 and the respective determination coefficient is 0.9995. The absorbance measurements were obtained in Genesys 50 (Thermo scientific, USA) UV-Vis spectrophotometer.....102

Figure A.4 – Calibration curve of curcumin in chloroform – absorbance at 430 nm versus curcumin concentration ($\mu\text{g/ml}$). The calibration curve equation is: Absorbance (430 nm) = 0.1163 [Curcumin] ($\mu\text{g/ml}$) + 0.0126 and the respective determination coefficient is 0.9994 The absorbance measurements were obtained in DR 2800 (Hach Lange, USA) UV-Vis spectrophotometer.....102

Figure A.5 – Calibration curve of protein - absorbance at 750 nm versus BSA concentration ($\mu\text{g/ml}$) resultant from Lowry assay method. The calibration curve equation is the following: Absorbance (750 nm) = 0.0027 [Protein] (mg/L) + 0.0302 and the respective determination coefficient is 0.9899. The absorbance measurements were obtained in Cytation 3_Byotek equipment.....103

1. Motivation and objectives

1.1. Thesis motivation

Food industry modifications are occurring in the sense of developing novel products with new functionalities that satisfy the growing necessity of consumers for healthier and sustainable foods. Nutraceuticals are a wide range of natural and nutritional food compounds which demonstrate natural and nutritional food components which contain beneficial biological activity that helps keeping normal physiological functions [1]–[4]. Many of these compounds prevent or retard diseases' manifestation by acting as enzyme cofactors and substrates, eliminating toxic substances, improving nutrients absorption, and supporting gastrointestinal (GI) tract microflora [5], [6]. Curcumin is a hydrophobic phytochemical obtained from the plant turmeric whose beneficial effects (*i.e.* anti-inflammatory, antiviral, antioxidant and wound healing) are greatly studied [7], [8]. However, its bioavailability is greatly hindered by the low water solubility and photo instability.

Biobased nanodelivery systems, such as lipid- or protein-based, appear as an advantageous solution since they can mitigate curcumin limitations as well as protect it from external causes of degradation and enhance its cellular uptake [7], [9]. Nanoencapsulation could be employed into food or beverages as a way of evading the sensorial perception between original and fortified product [10].

Animal-based products are major contributors of food related Green House Gas emission, hence the substitution by plant based sources can be the solution for reducing the negative environmental impact of food while nurturing a more sustainable future [11], [12]. In addition to sustainability, bio-based materials of plant origin, have several interesting features such as high abundance in nature, diversified group of characteristics, biocompatibility and biodegradability [13]–[15]. [16], [17]. Nonetheless, these biobased nanodelivery systems must be physicochemical characterize and their behaviour during digestion must be determine no assess their suitability as food fortification systems.

1.2. Research aims

This work aims to develop different sustainable biobased nanodelivery systems (BBNDs), from plant origin, characterizing them and evaluating their behaviour during *in vitro* digestion. Specific aims include:

1. Development and optimization of solid lipid nanoparticles as well as pea protein nanoparticles for curcumin encapsulation.
2. Physicochemical characterization of the developed nanostructures.
3. Evaluation of nanostructures' storage stability.

4. Evaluation of selected nanostructures behaviour during *in vitro* digestion.

1.3. Thesis outline

This thesis is organized in 7 chapters. In chapter 1 is indicated the thesis motivation, research aims and thesis outline. Chapter 2 provides an overview of biobased nanodelivery systems' characteristics and application as nutraceuticals encapsulation systems, amplifying their beneficial effects while decreasing their limitations. Chapter 3 provides the procedures and materials utilized during the experimental approach, whose results are indicated in the following chapter (Chapter 4). Chapter 5 indicates the main conclusions of the experimental approach and suggestions for future work. Chapter 6 and 7 consist of the references and annexes, respectively.

2. Literature review

2. Literature review

Health care, nutrition and environmental issues are considered leading interests of the new generations, thus further attention should be taken into research associated with these topics [3], [18]. Particularly, the increasing consumers' awareness on food nutritional value and sustainability; presence of synthetic additives, potential toxicity and health impact is altering the way food is perceived and consumed [16], [18], [19].

European and International entities (i.e. United Nations Sustainable Development Goals 2030 and the European Green Deal) propose on creating a more sustainable economy with focus on changing unsustainable consumption and production pattern. The scientific, technological, and innovative work is the forefront of novel substance or products' development. The products ought to be functional, nutritional, safe, cost-effective and sustainable, parameters that ensure acceptance by consumers and comply with regulations [20]. Accordingly, food fortification with nutraceuticals dispersed within their matrix achieved through encapsulation has appealed to the scientific and general population scrutiny [16], [18]. Hence, the improvement and/or lengthened maintenance of their beneficial characteristics using sustainable bio-based nanodelivery systems could be the basis of the food industry's upheaval [18].

2.1 Nutraceuticals: Definition and health benefits

The term nutraceutical was firstly introduced by Stephen DeFelice, through a combination of the words nutrient and pharmaceutical, being described as "food or part of a food that provides medical or health benefits, including the prevention and/or treatment of a disease" [3], [6], [21]. Currently, nutraceuticals are defined as natural and nutritional food components which contain beneficial biological activity that helps keeping normal physiological functions [1]–[3]. Nutraceuticals differ from pharmaceuticals because they possess multitargeted action and low concentration of the active constituent [6]. A wide range of compounds are described as nutraceuticals, such as phytochemicals, vitamins, bioactive peptides, prebiotics, probiotics, and essential minerals, possessing different targets and mechanisms of action (Table 1) [2], [5], [18], [19], [22]. Many of these compounds prevent or retard diseases' manifestation by acting as enzyme cofactors and substrates, eliminating toxic substances, improving nutrients absorption, and supporting gastrointestinal (GI) tract microflora [5], [6].

1.1.1. Phytochemicals

Phytochemicals are a large group of compounds, such as resveratrol, carotenoids, polyphenols, flavonoids and isoflavones. They exert high antioxidant, anti-inflammatory, anticarcinogenic, antiaging and antithrombotic activity since they serve as substrates or cofactors for many enzymes involved in

biochemical reactions, help to eliminate unwanted toxic substances, scavenge oxygen and nitrogen free radicals, interact with cellular receptors and many others [5], [6], [22]. Additionally, they act as pigments and flavour precursors [6].

Table 1 – Nutraceuticals' classification and description of compounds' specific activity

Classification	Compounds	Specific activity	Reference
Polyphenol	Curcumin	Antioxidant; anticarcinogenic; anti-diabetic; anti-inflammatory; cardioprotective; immunomodulatory	[5], [8], [23], [24]
	Resveratrol	Anticarcinogenic, anti-inflammatory, anti-diabetic, anti-aging activity; Chronic disease prevention	[25], [26]
	Quercetin	Antioxidant, anti-inflammatory and anticarcinogenic activity; cardiovascular protection	[25], [27]
Carotenoid	Lutein	Antioxidant; cataracts and atherosclerosis prevention	[5]
	β -Carotene	Antioxidant, skin protection; immune modulation; degenerative diseases prevention	[22], [28]
	Lycopene	Antioxidant; cardiovascular disease prevention	
Flavonoid	Anthocyanin	Antioxidant activity; chronic disease prevention such as cancer and cardiovascular disease	
Vitamin	Vitamin D	Calcium and phosphate metabolism; formation of osteoblasts; Foetal development; normal function of nerve system, pancreas, and immune system	[22]
	Folic acid	Intervenes in cell division and growth during pregnancy and infancy	
	Vitamin E	Antioxidant activity	
	Vitamin C	Antioxidant activity; essential cofactor in fatty acids biosynthesis	[25]
Lipids	Docosahexaenoic acid	Cardiovascular protection	[22], [29]
	LC-PUFAS	Modulators of local and systemic inflammation in obesity	[30]
	Phosphatidylcholine	Increases cholesterol efflux; Inhibits fatty acid synthesis; Stimulates the oxidation of cholesterol to bile salts	[25]

Bioactive peptide	Lunasin	Antineoplastic; antioxidant activity; inhibition of lipid peroxidation; metal ion chelation	[31]
	VPP and IPP	High blood pressure reduction	
	α -Lactalbumin	Analgesic activity	
	β -Lactotensin	Cholesterol lowering action	
Prebiotic	Fructooligosaccharides	Restoration of normal intestinal microbiota; Improvement of glucose tolerance and insulin sensitivity	[25], [32]
	Chitosan	Regulates lipid-related pathways; facilitates protection of the tight junctions in the gut	[25]
	Pectin	Enhances the abundance of <i>Bacterioides</i> , <i>Olsenella</i> and <i>bifidobacteria</i> ;	
Probiotic	<i>Lactobacillus delbrueckii</i>	Aid in lactose digestion	[33]
Essential minerals	Chromium	Potentiates the insulin action, improving glucose tolerance	[22]
	Selenium	Intervenes in iodine metabolism in the thyroid	

Phenolic compounds, such as polyphenolic and flavonoids, are associated with antioxidant, anticarcinogenic, anti-inflammatory, antiaging and antithrombotic activity [22]. Their strong antioxidant activity prevents cellular damage and reduces inflammation, which is associated with the inhibition of oxidative stress and lipid peroxidation in the liver [25]. Flavonoids are associated with angiotensin-converting enzyme blocking, consequently, they prevent platelet aggregation [29]. Furthermore, they also protect and strengthen the cardiovascular system and reduce the risk of estrogenic-induced cancers [29].

Carotenoids are a structurally and functionally diverse phytochemical group, that cannot be synthesised by humans [22]. Generally, these compounds contain antioxidant and immunomodulation activities which are associated with degenerative diseases prevention [22], [34], [35]. Moreover, this pigmented molecules not only regulate adipocyte differentiation, energy dissipation and fat oxidation but also signal oxidation and express inflammatory mediators [25], [28].

Isoflavones are structurally and functionally similar molecules to human estrogen, but with mild estrogenic properties. An high intake of these strong antioxidant compounds is associated with lower incidence of type II diabetes, osteoporosis and some cancers, such as endometrial, prostate cancer, breast cancer and others [29], [36]. Extensive reviews about flavonoids [37], polyphenols [38], [39], resveratrol [26],

carotenoids [28], [35] and isoflavones [36], [40] characteristics, beneficial effects and activity can be found elsewhere.

1.1.1.1. Curcumin

Curcumin is a hydrophobic phytochemical obtained from the plant turmeric (*Curcuma longa*). This polyphenol is commonly used as a spice, food colouring and as traditional medicine [23]. Curcumin's nutraceutical effects (*i.e.* anti-inflammatory, antiviral, antioxidant and wound healing) are greatly studied, especially the pharmacological properties [7], [8]. Transcription factors, inflammatory mediators, and enzymes (e.g. protein kinases, protein reductase and histone acetyl transferases) are common targets of curcumin activity. Its comprehensive activity is associated with its epigenetic regulation role [8].

Numerous phytochemicals, including curcumin, demonstrate anticancer effects along with fewer detrimental effects to normal living cells than other chemotherapeutic agents [7]. Positive effects in the prevention as well in all stages of this disease were associated with the anti-inflammatory and anticancer properties [7]. Additionally, it demonstrates chemosensitization and radiosensitization effects [8]. Moreover, its beneficial effects against diabetes, gastrointestinal cancers, gastric ulcers, inflammatory bowel diseases and obesity as well as safety, tolerability and cost-effectiveness makes it appealing for food fortification [8], [23], [41].

However, curcumin bioavailability is greatly hindered by its low water solubility and photo instability [23]. This polyphenol is quickly degraded in neutral and alkaline solutions, converting in bicyclopentadione and other minor compound such as ferulic acid, feruloyl methane and vanillin [23]. Although, some of the metabolites and degradation products demonstrate beneficial activity, curcumin exhibits higher antiproliferative effect and antioxidant activity [23]. Therefore, the encapsulation of this nutraceutical is seen as a solution to improve curcumins' solubility, bioavailability and pharmacokinetic attributes. Several, curcumin-loaded nanodelivery systems (NDS), based on have been reported in the literature [7], [42].

1.1.2. Vitamins

Vitamins possess an essential role in normal growth and life maintenance, not to mention they have the double function of nutrients and disease control agents [34]. Some elements of this large group of organic compounds act similarly to hormones or mineral metabolism regulators, regulate cell and tissue growth and differentiation, and others display antioxidant activity. However, most of vitamins serve as precursors for enzymes' cofactors [22]. Lipid soluble vitamins, such as vitamin A, D and E regulate mineral metabolism, control the redox balance, administer tissue differentiation and immunomodulate

[25]. Additionally, water-soluble vitamins, such as vitamin C or vitamin B complex, scavenge reactive oxygen species preventing low-density lipids oxidation and serve as enzyme cofactors [25].

1.1.3. Lipids

Lipids are a chemically diverse group of hydrophobic molecules [30]. These compounds are constituents of cell membranes, are an energy source and act as signalling molecules [22], [30]. Polyunsaturated fatty acids are cell membrane components that demonstrate beneficial lipid-reducing effects. Phytosterols, plant analogs of cholesterol, not only exhibit modulatory action of lipid peroxidation and mitigate oxidative stress but also, regulate the endothelial activation markers and are inflammation markers [25], [30].

1.1.4. Bioactive peptides

Peptides are small and polar molecules, obtained by hydrolysis of dietary proteins, that exhibit high absorption and variable hydrophobicity [25]. Bioactive peptides are a diverse group of food proteins' hydrolysates that present various physiological properties such as cell proliferation' control, antioxidant, antimicrobial, antihypertensive, anticholesterolemic, and other [31]. Extensive review on bioactive peptides was done by other authors [31].

1.1.5. Prebiotics and probiotics

Probiotics are live microorganisms that have beneficial effects on the host, when administered in adequate amounts [33]. These microorganisms support a healthy digestive tract and a healthy immune system by creating a more favourable gut environment and stabilizing the gut community, protecting the host against invading and pathogenic microorganisms [33], [43].

Prebiotics are fermentable oligosaccharides, non-digestible by the human digestive tract organs, that exert beneficial effects on intestinal microorganisms' microenvironment and in their relative abundance, beneficiating the host well-being and health [25], [32], [43]. Some organic acids, such as acetate, propionate and *n*-butyrate, obtained by hydrolysis of non-digestible carbohydrates can modulate colonocyte function, gut homeostasis, the immune system, renal physiology and other [32].

Synbiotics are defined as "a mixture comprising live microorganisms and substrate(s) selectively utilized by host microorganisms that confers a health benefit on the host" [25], [43]. This combination of prebiotic and probiotics exhibit complementary or synergistic behaviour and selectively stimulate the proliferation of one or more probiotic taxa [25], [43]. An extensive review on probiotics [33], [44], prebiotics [32], [45] and synbiotics [43], [46] can be found elsewhere.

1.1.6. Minerals

Minerals play an important role in physiological and biochemical processes such as water and electrolyte balance, metabolic catalysis, oxygen binding, hormone functions but also in bone and teeth development, muscle strength and membrane formation [22], [47]. These micronutrients are required in low quantities however they are necessary to essential functions such as nerve impulse transmission, formation of erythrocyte cells, regulation of glucose levels and blood pressure [47]. Extensive review was done by Gharibzahedi & Jafari (2017).

2.2. Nutraceuticals: Limitations

Nutraceuticals' major limitations are related to poor stability and bioavailability in food systems, susceptibility to oxidation through heat, oxygen, light or humidity influence, high volatility, low water solubility, degradation in extreme conditions during digestion and undesirable taste and flavour (Table 2) [2], [5], [18], [19], [34].

Consequently, when a specific compound and its benefits are desirable, its characteristics, limitations and possible interactions with other compounds, when integrated in the food matrix must be considered [17]. Furthermore, stability must be assured during foods' production process, storage and digestion so that the maximum quantity of bioactive compound reaches the desired target [17]–[19], [41].

Table 2 – Nutraceutical compounds and their associated limitations

Nutraceuticals	Limiting factors	References
Carotenoids	Chemical structure changes due to environmental and processual stress (oxygen, pH, light, and temperature variation)	[34]
Phytochemicals	Low bioavailability; Poor dissolution in gastrointestinal tract	[3]
Polyphenols	Instability; Unpleasant taste	[2]
Vitamins	Low stability and water solubility; Sensitivity to oxidation; Loss of functions due to temperature, light, or humidity variation	[22], [34]
Anthocyanins	Chemical structure changes associated with polymeric forms, oxygen, pH, light and temperature; Dependency on cofactors and/or ascorbic acid	[22]
Bioactive peptides	Denaturation and conformational changes during processing, storage and consumption; rapid elimination by renal function	[2], [31]
Probiotics	Microorganisms' viability is dependent on the matrix, temperature, pH and oxygen level	[43]
Prebiotics	Effects are dependent on host and environmental factors	[32]
Minerals	Bioavailability and stability changes due to interaction with other compounds	[2], [5]
Phytosterols	Low solubility in aqueous-based solutions	[2]

2.3. Bio-based nanodelivery systems: Beneficial characteristics

Different strategies may be applied to overcome nutraceuticals' limitations such as the utilization of nanodelivery systems, absorption enhancement technologies and excipient foods [2]. The nanoencapsulation of nutraceuticals in NDS is a very promising strategy since it offers several advantages (Figure 1). The entrapment of nutraceuticals demonstrates an enhancement of their stability and bioavailability, once it facilitates the entering through biological barriers and simultaneously avoids precocious metabolic modifications during storage and digestion [3], [48], [49].

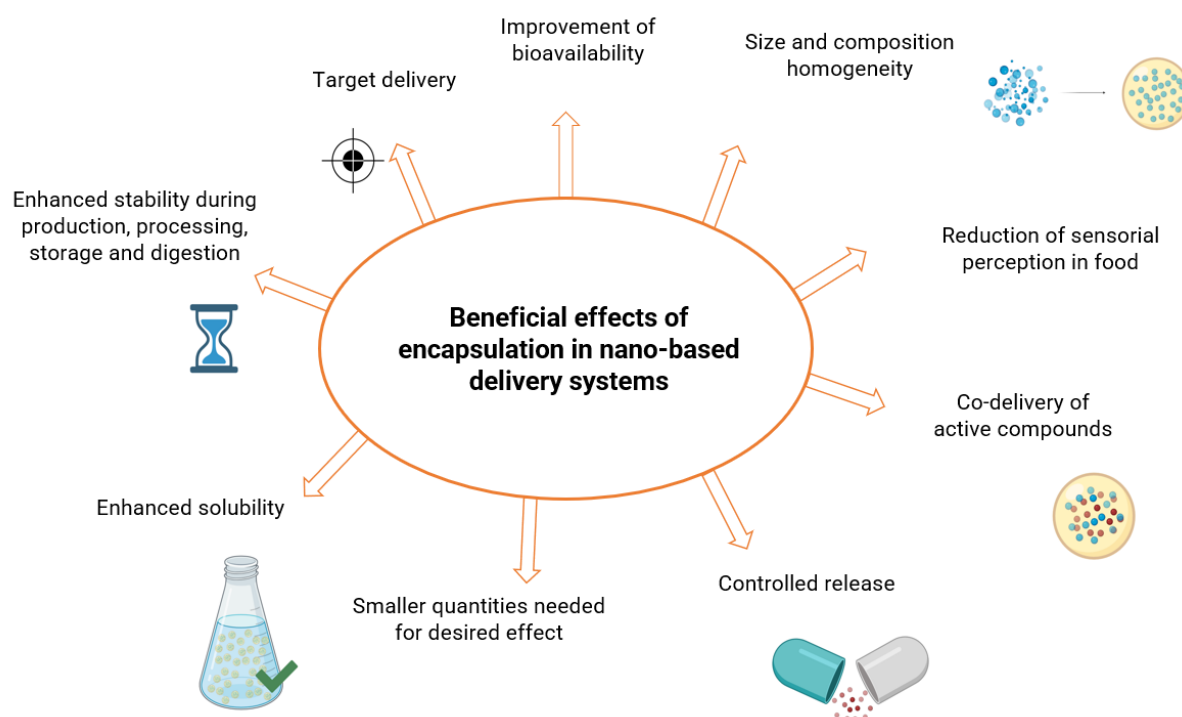


Figure 1 – Nutraceuticals' main advantages when encapsulated in nanodelivery systems.

During NDS selection, their food-grade status, cost effectiveness and industrial feasibility must be considered [2], [16], [50]. In opposition to pharmaceutical industry in which NDS are widely applied, in the food industry all components must be classified as food grade and the processing operations must be adjusted [2], [5], [19], [48]. Furthermore, the physical and chemical stability, aqueous solubility, the interaction with the nutraceutical and the food matrix, the adequate residence time in GI tract, absorption rate and releasing profile at the desirable site of action must be considered [2], [5], [18].

Food grade materials can be obtained from bio-based materials (polysaccharides, proteins and lipids), in isolated or associated complexes, or from other materials that are Generally Recognized as Safe (GRAS) such as mineral salts, cyclodextrins and low molecular weight emulsifiers [2], [5], [16]. Bio-based

nanodelivery systems (BBNDS) contain a wide range of compositions, sizes, structures, functions, physico-chemical and biological properties [5], [16], [19]. These compounds present biodegradability, high loading capacity and low toxicity [19]. The release rate is linearly dependent on the surface area and inversely proportional to delivery systems' particle size [5], [34]. Additionally, some compounds also possess intrinsic nutraceutical activity [3]. Therefore, the utilization of BBNDS not only can effectively protect the nutraceuticals from external factors but they are also considered safer than inorganic nanoparticles since most of them are already present in food [2], [3], [16], [19]. Some recently studied nutraceuticals' NDS with proven benefits are reported in Table 3.

2.4. Bio-based nanodelivery systems: Sustainable approach

The rapid increasing population' growth and simultaneous depletion of natural resources is inducing a soaring effort in agricultural and food industry [51]. On one hand, developing countries have recurrent food shortages which culminate in hunger and malnutrition [16], [52]. On the other hand, developed countries have low purchase price, an excessive production and pervasive consumption of low nutritional value food [52]. Additionally, the inefficient use of natural resources by the food industry results in a high amount of waste, by-products and co-products without an intended use [51].

In this sense, the production of fortified food with sustainable and BBNDS emerges as an interesting solution [52]. In addition to sustainability, bio-based materials, specifically from plant origin, have several interesting features such as high abundance in nature, diversified group of characteristics, biocompatibility and biodegradability [13]–[15]. Similarly, food production' residues can be used as delivery systems' materials since they are rich in nutraceuticals and bio-based materials (polysaccharides, proteins and lipids) [51], [53], [54]. Conjointly, it could reduce the cost of production by simultaneously adding value to industrial residues [16], [17].

Thusly, the utilization of sustainable and BBNDS could not only reduce the necessary amount of nutraceuticals ingested to exert beneficial effects, avoiding any adverse exposure to environmental conditions, but also reduce costs of production and of residues' treatment [16], [17]. However, consideration should be given to possible variations in composition and quality of the initial source along with discrepancies resulting from differences in conditions and processes used to obtain the compound of interest [2].

Table 3 – Examples of some encapsulating materials used for nutraceuticals' encapsulation, with specification of the encapsulation technique and benefits verified

Encapsulating material	Nutraceutical encapsulated	Encapsulation technique	Advantages	Reference	
Polysaccharide-based delivery system	Starch	β -Carotene	Nanoprecipitation	Controlled release under gastric conditions	[55]
	Starch	Catechin	Ultrasonication	Retention of properties and controlled release in the intestine	[56]
	Chitosan	L-Ascorbic acid	Ionic gelation	Increased stability under heat processing	[57]
Protein-based delivery system	Zein	Curcumin	Electrohydrodynamic atomization	Encapsulation efficiency ranging from 85 to 90 %; No significant changes of the nanoparticles or curcumin' content were verified	[58]
	Casein	Folic acid	Coacervation	Increased bioavailability;	[59]
	Whey protein	Vitamin D3	Nanoemulsion	Increased bioavailability	[60]
	Whey protein	Astaxanthin oleoresin	Spray drying	Encapsulation efficiency of 58.7%; High antioxidant stability in pH ranging from 4 to 7	[61]
	Octyltanoat and precinol	Vitamin A palmitate	Hot homogenization	The nanostructured lipid carrier demonstrated 98.5 % encapsulation efficiency and stability during two months at 25°C	[62]
	Pea protein	Vitamin D	Nanoemulsion	High encapsulation efficiency (94-96 %); high cellular uptake	[60]
	Gelatine - pectin complex	Lycopene	Complex coacervation	93.2 % encapsulation efficiency	[63]
	Whey protein - gum acacia complex	β -Carotene	Complex coacervation	Encapsulation efficiency of 80 %; Protection during storage and sustained release of nutraceutical	[64]
	Mealworm protein - chitosan complex	Curcumin	Electrostatic deposition	Increased stability and protection during gastric phase	[24]
	Lipid-based delivery system	Corn oil	Curcumin	Homogenization	Increased bioavailability
Vegetable oil		Probiotics	Spray chilling	Protection during digestion or when exposed to environmental stresses	[66]
Vegetable oil		Vitamin D3	Spray chilling	Avoids decomposition at higher temperatures; increased stability during storage	[67]

2.5. Bio-based nanodelivery systems: Encapsulating materials

2.5.1. Polysaccharide-based delivery systems

Polysaccharides are long chains of monosaccharides units which differ in composition, molecular weight, type of chain (linear or branched), glycosidic bond (α or β) and linkage [17], [68], [69]. The concentration, solubility and charge have influence in intra and intermolecular interactions, therefore chemical modifications can be applied to improve interactions capability or specific properties [68]. These high molecular weight polymers can be sourced from plants (i.e., starch, cellulose, pectin, gum arabic) but also from microorganisms (alginate, cellulose, chitosan and dextran), animals (chitosan) and algae (carrageenan) [16]. Chitosan is the most widely used polysaccharide in nanoencapsulation due to its mucoadhesive properties, pH stimulation and ability to form particles with size under 200 nm which can penetrate the intestinal epithelium through tight junctions [16]. Starch, a major component of food, can be adjusted to a specific application since it acquires different properties based on its source and processing conditions [16]. Polysaccharides are versatile molecules which can bind and entrap hydrophobic and hydrophilic nutraceuticals [17]. Additionally, they can self-assemble and are suitable for high temperature processes and resistant to gastric and intestinal conditions [17]. However, they can be affected by the pH and ionic strength of the solution, and their composition and properties can vary with source and method of extraction [17]. Extensive review about various polysaccharides used as delivery-systems can be found elsewhere [17], [42].

2.5.2. Protein-based delivery systems

Proteins are amino acid based polymers, linked by peptide bonds, with a range of functional groups and amphiphilic behaviour [17], [68], [69]. The type, number and sequence of amino acids determine the molecular characteristics and consequently, proteins present a wide variety of functional properties [69]. Their structure and physicochemical characteristics enhance binding and, consequently, the encapsulation of molecules, ions or ligands [70]. Protein based nanoparticles are preferred for medical, food and cosmetic applications not only because bioactive molecules can be added through covalent, ionic or hydrogen bonds but also because surface modification can be employed [71].

The encapsulation in protein-based delivery systems (PDS) can enhance the adhesion properties since some proteins are able to bind specifically to sugar-residues in the surface of epithelial cells [22]. The binding of calcium or calcium phosphates to casein can facilitate target-activated release when in acidic conditions such as the stomach [70]. Their solubility is mainly affected by pH and the interactions in solution are dependent on associative bonds (disulfate bonds, hydrogen bonds, attraction-repulsion forces) [68]. They can interact with both hydrophilic and hydrophobic compounds, for instance, whey

protein can improve the retention of hydrophobic compounds [17], [68]. Likewise, the physicochemical properties of encapsulating compounds and bioactive molecules have an important role on their interaction, and therefore on the nanoparticle formation, encapsulation efficiency and their food matrix compatibility [72].

Various techniques can be applied in protein-based delivery systems formation such as nanoemulsification, coacervation, cross-linking, antisolvent precipitation, electrospraying and electrospinning [70], [73]. The reduction of PDS' size has demonstrated to increase biorecognition, bioavailability, bioadhesion and stability [5], [70]. The rate, extent and trigger mechanism of nutraceuticals release is dependent on protease activity and GI tract environmental conditions (i.e. pH, temperature, ionic strength) [17], [70]. It must be considered that proteins' behaviour is affected by pH and temperature, they are sensitive to flocculation (near their isoelectric point, at high salt concentrations or when heated), they demonstrate poor resistance to intestinal conditions and some proteins may originate allergic reactions [17], [49]. Extensive review about PDS can be found elsewhere [17], [70].

Furthermore, proteins and polysaccharides can be used individually or in complexes based on interactions of their charged functional groups [22], [74]. The environmental conditions (i.e., pH, ionic strength, temperature) and molecular characteristics (i.e., molecular weight, biopolymer charge density, biopolymer flexibility, concentration, and ratio) have influence in their associative interactions [17], [74]. Most of these complexes are formed in low pH hence these structures can protect nutraceuticals from acidic conditions during gastric digestion [74]. Additionally, the complexes formed by electrostatic interactions can present targeted and controlled release of nutraceuticals in determined environments [74]. Protein-saccharides complexes were extensively reviewed by other authors [68].

2.5.2.1. Pea Protein nanoparticles

The most studied proteins are gelatine, collagen, whey protein, casein and zein [68], [70]. Recently, there has been an increasing interest in the use of plant proteins since novel products can be produced while abiding to restricted diets (e.g. vegan diet) as well as supporting the current expanding sustainable tendency of food and pharmaceutical industries [15], [73]. Additionally, the utilization of plant-based proteins offers a lower risk of contamination with infectious pathogens [73].

Although soy protein remains the most consumed plant protein, pea protein is widely accepted due to the easy availability, high nutritional value and low allergenicity [24], [25], [71], [75]. It also demonstrates a great potential since it contains a high content of essential amino acids and generates less concerns about genetic modifications than soy protein [76]–[78]. The high essential amino acids content, especially

of lysine, could be advantageously used for overcoming cereal protein deficiency in this amino acid [75], [79].

This plant protein not only has good emulsification properties, substituting non-vegetarian friendly emulsifiers, but also demonstrates interesting gelation, foaming, thermal stability and water holding characteristics [76], [78]. Additionally, pea protein isolate can be extracted from peas without additional degreasing steps, unlike canola or soy proteins, attaining an inexpensive, broadly available and more sustainable protein isolate [78], [80].

Pea protein nanostructures have been developed through various techniques and reported in the literature. Li and co-workers (2021) used potassium metabisulfite to induce the self-assembly of pea protein isolate nanoparticles. They verified that the size of the nanoparticles increased from 124 to 298 nm with the increase of potassium metabisulfite concentration (0 to 8 mM) [81]. Pea protein nanoparticles, with a size range between 267 and 337 nm and stability of 4 weeks, were also produced using ethanol-induced desolvation [82].

Pea protein poor water solubility is a major challenge, however, the inherent hydrophobicity makes it suitable for encapsulating small phenolic compounds, such as curcumin, due to increased availability of binding sites [77], [83], [84]. Fan and colleagues (2020) developed pea-protein nanoparticles through calcium-induced crosslinking to encapsulate resveratrol, an easily degraded, lipophilic and isomerized bioactive polyphenol. They evaluated the influence of calcium concentration and pH on formulations physical characteristics and were able to develop nanoparticles with reduced size and PDI (< 200 nm) as well as good encapsulation efficiency [85]. Walia & Chen (2020) encapsulated vitamin D in pea protein stabilized nanoemulsions, obtaining nanostructures with size between 170 and 350 nm, good stability, and high encapsulation efficiency (> 92 %). In this study, it was also observed a decrease in particles size with the increase of pea protein concentration [60]. Wei and colleagues (2020) developed core-shell pea protein carboxymethylated corn fiber gum composites for curcumin delivery. At pH 7.0, they obtained pea protein nanoparticles with a size of 220 nm, curcumin-loaded pea protein nanoparticles with 211 nm and nanocomposites with 270 nm. The pH change from 7.0 to 3.0 during formulation, demonstrated to increase the encapsulation efficiency [86]. Yi and colleagues (2020) also verified that pea protein nanoparticles size significantly increased with thermal treatment, pectin complexation and curcumin encapsulation [79].

Additionally, the protein hydrophobicity may also be used to develop sustained-release delivery systems, as demonstrated with zein and gliadin proteins, without further chemical treatment to harden and,

consequently, no toxic chemical crosslinkers use [14], [15]. The encapsulation properties may also be enhanced through physical, chemical or enzymatic modifications which change the solubility, surface activity and amphiphilicity of the proteins [14].

2.5.3. Lipid-based delivery systems

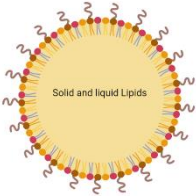
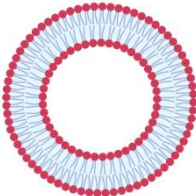
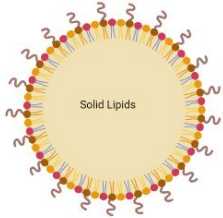
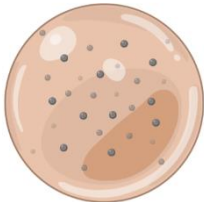
Lipid is a wide range classification of macromolecules that are synthesized from ketoacyl and isoprene groups and are soluble in nonpolar solvents, possessing hydrophobic or amphiphilic behaviour. Most lipid-based delivery systems (LDS) are created through emulsions, that is the dispersion of small spherical droplets of one liquid in another, which it is immiscible with [41], [69]. LDS demonstrate different physicochemical properties and functional attributes associated not only with the type and concentration of oil and emulsifier but also with the production method (Table 4).

LDS are suitable for encapsulation of hydrophobic and/or lipophilic nutraceuticals such as carotenoids, polyphenols and flavonoids [41]. Additionally, there are established production methods, they don't require organic solvents during processing and they can be produced in larger scale with reduced costs [50], [69], [87]. The use of triglycerides enables the rapid digestion within the small intestine, release of the nutraceuticals and an enhanced absorption [50]. Low-energy methods have been proven to not be appropriate to formulate nanoemulsions from natural emulsifiers due to their solubility characteristics and phase behaviour [49]. Lipid nanoparticles are kinetically stable but thermodynamically unstable and consequently they tend to lose their stability during storage [69], [88]. However, they possess higher stability to gravitational separation and droplet aggregation than conventional emulsions [41]. The stability of LDS can be improved by reducing the size of the particles while increasing the density of the oil and viscosity of the water phase [22]. Lipidic delivery systems were extensively review by other authors [41], [69], [89], [90].

2.5.3.1. *Candelilla wax based solid lipid nanoparticles*

Solid lipid nanoparticles (SLNs) are delivery systems composed of lipids that are solid at room temperature which are usually stabilized by the addition of surfactants or polymers [7]. SLNs have a wide utilization in cosmetic and pharmaceutical as well as promising prospects in food fortification due to their easy scale-up product production and avoidance of organic solvents during formulation [91], [92]. Other advantages include the high stability *in vivo*, as it remains solid at body temperature, possibility of autoclaving or sterilization and modulation of their release profile [92]. The solid state of the matrix not only increases the physical stability, comparatively with other lipidic nanoparticles, while avoiding destabilization, but also protects against chemical reactions [93].

Table 4 – Some examples of lipidic delivery systems and their main characteristics

Designation	Characteristics	References
Nanostructured lipid carriers		
	<p>Solid matrices composed of solid and liquid lipids, with an outer shell of surfactants; Can improve nutraceuticals' resistance to chemical degradation and demonstrate sustained release rate; They have a disordered structure which confers an higher loading capacity;</p>	<p>[22], [87], [94]</p>
Nanoliposomes		
	<p>Colloidal dispersions containing small lipid nanoparticles comprised of concentric lipidic bilayer(s) formed by self-association of phospholipid molecules in water; Can entrap, protect, and release hydrophilic, hydrophobic and amphiphilic nutraceuticals; Requires high surfactant concentration; Can be produced by Mozari method, sonication, high pressure homogenization and others; Poor economic feasibility, stability, encapsulation efficiency and loading capacity</p>	<p>[5], [10], [87]</p>
Solid lipid nanoparticles		
	<p>Solid lipid spheres with external phospholipids and surfactants; High water content (70-95 %); The solid lipid core can solubilize lipophilic compounds; Improves bioavailability of water insoluble nutraceuticals; May change shape, increasing susceptibility to aggregation; can be produced by high pressure homogenization, hot and cold high pressure, ultrasonication and microemulsion</p>	<p>[87], [94], [95]</p>
Nanoemulsions		
	<p>Colloidal systems formed by heterogeneous system emulsifiers; Can be obtained through low or high-energy approaches; They are optically transparent but are affected by pH, temperature, and salts concentration; The small size avoids gravitation separation; Can only be formulated from high concentrations of synthetic surfactants; Thermodynamically unstable in comparison to microemulsions; Susceptible to droplet growth through Ostwald separation</p>	<p>[87], [94]</p>

The employment of bio-based compounds of plant origin as delivery systems can improve and/or maintain nutraceuticals' beneficial characteristics, while being more sustainable, comparatively with animal waxes. Additionally, SLNs produced from plant waxes are biocompatible, nontoxic and abundant [91]. The utilization of plant-based lipids offers a healthier source of saturated fatty acids with low quantities of trans fats. Furthermore, the utilization of low lipid concentrations or non-digestible solid fats is concordant with the current low-fat consumption trends [96].

Candelilla wax is obtained from the leaves of *Euphorbia antisyphilitica* and *Euphorbia cerifera* typically found in Mexico and Texas, USA [93], [97], [98]. It is a FDA approved gelator, employed as a binder, glazing agent or food coating material [93], [97], [98]. This highly hydrophobic plant wax has demonstrated health benefits, biodegradability and non-toxicity [96]. The arid climatic conditions of Mexico and northeast of USA restrict the agricultural practices, hence the harvest and commercialization of candelilla wax could contribute to the economic development of the region [99], [100]. In addition, alternative extraction methods with citric acid were developed to avoid the utilization of sulfuric acid (traditional method), resulting in a low impurity wax, with a safer and eco-friendlier process [99], [100].

2.6. Bio-based nanodelivery systems: Encapsulation techniques

Depending on the nutraceuticals and encapsulation materials' characteristics different procedures may be employed to produce BBNDs [5], [34]. Also, two different approaches can be applied: *bottom-up* and *top-down*. *Bottom-up* technique originates larger structures through sequential addition of atoms or molecules, achieved through chemical synthesis, self-assembly and positional assembly of molecules [5], [34], [48]. *Top-down* technique involves size reduction and shaping of structures by physically processing the materials with precise tools and energy application [5], [48]. The technique utilized in the production of the delivery system may modulate and influence their properties such as structure of the particle, shape, surface properties and moisture content [5], [68]. Conjointly, many nutraceuticals are sensitive to heat and high temperatures, therefore encapsulation procedure' selection is a key step to avoid loss of activity [2]. *Top-down* and *bottom-up* methods are indicated in Table 5 and were extensively reviewed by other authors [5], [48], [89], [101].

Table 5 – *Top-down and bottom-up methods used in nanodelivery systems production*

Top-Down methods	Bottom-up methods
Emulsification	Coacervation
Ultrasonication	Microemulsions
Microfluidization	Phase inversion
Solvent evaporation	Mozafari method
Microchannel emulsification	Supercritical fluid
High pressure homogenization	Nanoprecipitation
High shear homogenization	Inclusion complexation
	Antisolvent precipitation

There is still room for improvement of BBNDs associated with not only the optimization of the formulation in order to increase nutraceuticals' bioavailability and stability, but also to assess the risk of their use in food [19]. The combination of two delivery systems could be a new approach to encapsulate nutraceuticals with higher stability and a more efficient controlled release [19], [49]. For examples, the stability of nanoemulsions can be improved through coating with a layer of biopolymers, such as peptides or polysaccharides [49]. Furthermore, it is necessary to understand the modifications that occur to the delivery system and/or nutraceutical during processing, storage and digestion in order to improve their performance and conclude about their safety [19].

2.6.1. High shear homogenization

High shear homogenization (HSH) is a technique in which the high velocity of the rotor induces the axial suction of the solution inside the dispersion head, followed by its radial squeezing through the rotor-stator openings. Due to the high acceleration forces, the material is exposed to shear forces and strong turbulence which ensures great mixture of the solution [102]. Comparatively with high pressure homogenization, it requires less energy and time consumption [103]. The utilization of longer processing times increases the solution temperature, due to the absorbed energy, and does not significantly affect the solutions particles fineness [102].

Mai and colleagues (2021) employed HSH technique to develop SLNs with encapsulated gac-oil, composed of a high content of the hydrophobic compounds β -carotene and lycopene. The adjustment of homogenization temperature and time allowed to obtain various formulations with size inferior to 200 nm and stability of 60 days [104]. Triplett and co-workers (2009) were also to produce SLNs through HSH to encapsulate β -carotene [105]. Under the same solid lipid to surfactant ratio, the speed and time define the final SLNs characteristics [106].

2.6.2. Cold gelation

Protein nanostructures can produce nanostructures through denaturation of globular proteins, resorting to temperature, acid addition, ionic strength modification or enzymatic activity. The characteristics of the nanostructures will depend on the heating settings (i.e. direct or indirect heating, temperature, heating rate, treatment time) as well as the environmental conditions (e.g. pH and ionic strength) [107], [108].

Ionotropic gelation, also known as cold gelation, induces nanostructures formation through addition of salt ions to the protein solution. This method requires a pre-denaturation step, based on temperature, pressure or enzymatic activity, to induce protein unfolding [107]–[109]. Then, the process occurs at a

pH above the isoelectric point of the protein, so that the salts ions induce gelation through minimization of the electrostatic repulsive forces between molecules. Divalent ions tend to be more efficient as intermolecular crosslinking agents than monovalent cations ions, since they can bind specifically to proteins [107], [108]. This procedure does not require the utilization of organic solvents and can be employed after addition to a food matrix, therefore being suitable for food industry [109].

2.7. Physicochemical characterization of biobased delivery systems

In order to select the most appropriate BBNS for a determined application, it is required to know their physicochemical properties, such as composition, size, structure, interactions established, interfacial properties and physical state of the nutraceutical and of the food matrix [16], [19], [87], [110].

2.7.1. Particle size

Particle size and size distribution are important characteristics which can determine functional properties of the NDS, such as stability, structure, optical clarity, encapsulation and release characteristics [17], [34], [110], [111]. Particle size is an important attribute with implications on nanoparticles stability, bio-distribution, encapsulation efficiency, mucoadhesive and cellular uptake [112]. Polydispersity index (PDI) not only indicates the width of particles' size distribution, being values higher than 0.6 indicators of polydispersity and values under 0.3 indicators of mono-dispersity, but also the distribution of the particles in the matrix [34], [113]. Both particle size and PDI are physical characteristics with impact on bulk properties, product performance, stability and final appearance of food grade or pharmaceutical-grade products [112].

Smaller particles generally have a better dissolution behaviour, possibly associated with the increase of surface area to volume ratio [34], [89]. In order to validate size measurements, it is recommended scanning electron microscopy (SEM) to micrometer sized delivery systems and transmission electron microscopy (TEM) to nanometer sized particles [111]. Dynamic light scattering (DLS) can be used to ascertain the size distribution of particles dispersed or dissolved in a liquid [70], [89], [110]. This biophysical technique determines the specific size-dependent fluctuation intervals of a laser light scattered by the samples' particles, by simultaneously recording and quantifying the light dispersion [114], [115]. Consequently, the light diffusion resulting from the Brownian movements of samples' particles can be employed to determine the average particle size in the sample [114], [116]. Although it can quantify aggregates formation it does not provide functional information of the detected aggregates on bioactivity [117].

2.7.2. Morphology

Morphology and colour are associated with organoleptic properties, stability and bioavailability [111]. The morphology of formulations can be analysed by microscopy techniques, such as atomic force microscopy (AFM) or confocal laser electron microscopy (CLSM) [70], [110], [111]. AFM can provide images from both lateral and vertical positions without any preparation, however CLSM requires the addition of fluorescent dyes to study the morphology [110]. SEM and TEM are the most employed techniques to analyse particles morphology [87], [89]. Morphology assessment can be complemented by thermal analysis, utilizing differential scanning calorimetry (DSC), or thermogravimetric analysis (TGA) [89], [111]. DSC determines the variation of temperature and energy in the phase transition, indicating the crystallization state of the particles, fusion range, purity and homogeneity [87], [88]. Therefore it can be used to determine the location and physical state of the encapsulated compound [89].

2.7.3. ζ -Potential

The electrical characteristics of the delivery system can influence different properties such as stability, release and adhesion to solid or biological surfaces [110]. Zeta potential (ZP) represents the electrokinetic potential, that is, the electric potential in the interfacial double layer of a dispersed particle versus a point in the continuous phase [34], [118], [119]. This parameter represents the degree of repulsion between charged particles in a dispersion [119], [120]. Parameters such as ionic strength, pH and type and concentration of encapsulating materials exert effects in the surface charges and electrostatic interactions resulting in ZP variation [34], [121]. In general, a ZP superior to +30 mV or inferior to -30 mV lead to more stable complexes [34], [110]. It should be noticed that ZP is not an absolute measurement of nanoparticles stability since other factors such as materials properties and the use of surfactants affect the physical stability [122].

2.7.4. Structural alterations

Functional groups' alterations resulting from encapsulation and/or non-covalent intermolecular interactions (i.e. hydrogen bonds, electrostatic or hydrophobic interactions) can be determined by Fourier transform infrared spectrometry (FTIR) analysis [24]. Infrared and Raman spectra can provide important knowledge about conformational changes and consequently infer about structural stability [89]. The stability of the encapsulated nutraceuticals should be compared with the nutraceuticals alone to determine the stability improvement conferred by the delivery system against environmental agents such as temperature, oxygen and humidity [70].

2.7.5. Optical characterization

Optical characterization is dependent on various factors, such as suspensions' particle size, concentration or refractive index [110]. Measuring the selective absorption of visible light can indicate a higher turbidity, if there is a lower transmittance, or a lighter material when there is a greater reflectance [110]. It can be obtained by UV- visible spectrometry or image processing techniques [110] Sensorial tests can be applied to determine textural features and, complementarily, be correlated with viscosimetry and rheological measurements. Extensive review about characterization techniques of delivery systems was done by other authors [87], [110].

2.7.6. Encapsulation efficiency

It is also important to have defined parameters which indicate the after effects of encapsulating with a specific bio-based delivery system when compared to the free nutraceutical or other formulations [123]. The encapsulation efficiency is an important parameter which determines the effective loading of the nutraceutical into the delivery system [111]. This parameter can be determined by UV-vis spectrometry, TGA and high performance liquid chromatography [111]. Furthermore, physiochemical stability during storage indicates the time interval in which the delivery system sustains the initial characteristics being determinant to select the appropriate storage conditions and packaging [89]. Modifications in particle size, PDI, morphology and ZP are indicators of physiochemical instability [124].

2.8. Bio-based delivery systems' behaviour in the GI tract

During digestion, the BBNDs is exposed to various environmental conditions, with complex physicochemical and physiological processes, that can affect the nutraceutical activity (Table 6) [19]. Moreover, it must be recognized the alterations that occur within the GI tract and the repercussions in the absorption, distribution, metabolism, excretion and toxicity potential of the nutraceutical [16], [19].

Table 6 - GI tract environmental conditions and their possible effect in the bio-based delivery system characteristics

Environmental condition	Possible effect in the biobased delivery system
pH	Alteration of particles electrical charge and consequent changes in composition, structure and/or interactions established
Temperature	Changes in physical state, molecular conformation, or interactions between components
Composition and concentration of ions	Possible impact in electrostatic interactions through electrostatic screening or binding effect
Presence of enzymes	Premature digestion of components
Presence of surface-active components	Interfacial composition' alterations
Flow/force profile	Breaking down of the delivery system

Bioavailability is determined as the fraction of the unchanged nutraceutical or its bioactive metabolite that is absorbed and reaches the systemic circulation [17], [22], [89], [123]. This parameter is dependent on the materials used to encapsulate, the physical state of the delivery system and the surrounding matrix since they determine the chemical stability, solubility in the GI tract and absorption [2], [22]. Additionally, it can only be determined correctly by *in vivo* analysis [125]. Meanwhile, bioaccessibility corresponds to the amount of a compound that is released from the food matrix in the GI tract and becomes available for absorption [89]. Usually, it is the rate limiting factor of bioactivity, being both parameters positively correlated [125]. It can be determined by *in vitro* assays providing important data about the phenomena and mechanism underlying bioavailability [125].

Ideally, *in vivo* digestion models should be used since they provide reliable, accurate and direct results. However, they present not only higher cost, technical constraints and poor reproducibility but also require ethical evaluation [5], [19], [124]. To select the appropriate type of *in vivo* models, it must consider the type of functional and nutritional properties to assay [89].

Currently, *in vitro* digestion models are the most applied GI systems to understand the physicochemical behaviour of BBNS under GI tract conditions [5], [19], [101]. These digestion models allow to obtain inexpensive, fast and reproducible results due to the utilization of standardized methods [124]. Bioaccessibility can be determined by *in vitro* or, alternatively, by *ex vivo* models utilizing tissues, cell cultures and artificial membranes [5], [124]. Due to the inherent complexity of human GI tract (Figure 2), the design and making of an ideal *in vitro* digestion system is difficult requiring further efforts and technological advances. *In vitro* digestion models are divided into static or dynamic depending on their complexity [5].

In vitro static digestion models (SDM) use glass containers to mimic human digestion requiring simpler protocol execution and lower costs [124]. Additionally, they allow to assess multiple samples simultaneously [5], [19]. The physiological parameters, such as ratio of food to digestion fluids, pH and enzymatic concentration, are kept constant during the digestion modelling [125]. Generally, SDM procedures are based on Miller (1981), COST INFOGEST network method or INFOGEST 2.0 being mainly used for mechanical studies and hypothesis building with specific applications [5], [125]–[127].

Since SDM do not replicate the human digestive system mechanical forces and dynamic conditions, different *in vitro* dynamic digestion models (DDM) have been created in the last years [5], [124], [125]. These dynamic aspects can influence the bioactivity and bioavailability of the nutraceutical, which would not be reflected in the values determined by SDM [125]. Commonly, these models contain a multi-

chamber systems, in which each compartment simulates a different environment [5]. DDM can simulate pH change, transit time, enzyme secretion and microbial activity continuously [124]. These digestion models are based on *in vivo* data and adjusted accordingly [124]. Some DDM contain external pumping of water and flexible walls that allows to regulate temperature and mimic peristaltic movements [5]. It must be considered that not all DDM are able to mimic mechanical, kinetic and chemical physiological conditions of the digestive system simultaneously [124]. Different DDMs were explained by other authors [124], [125].

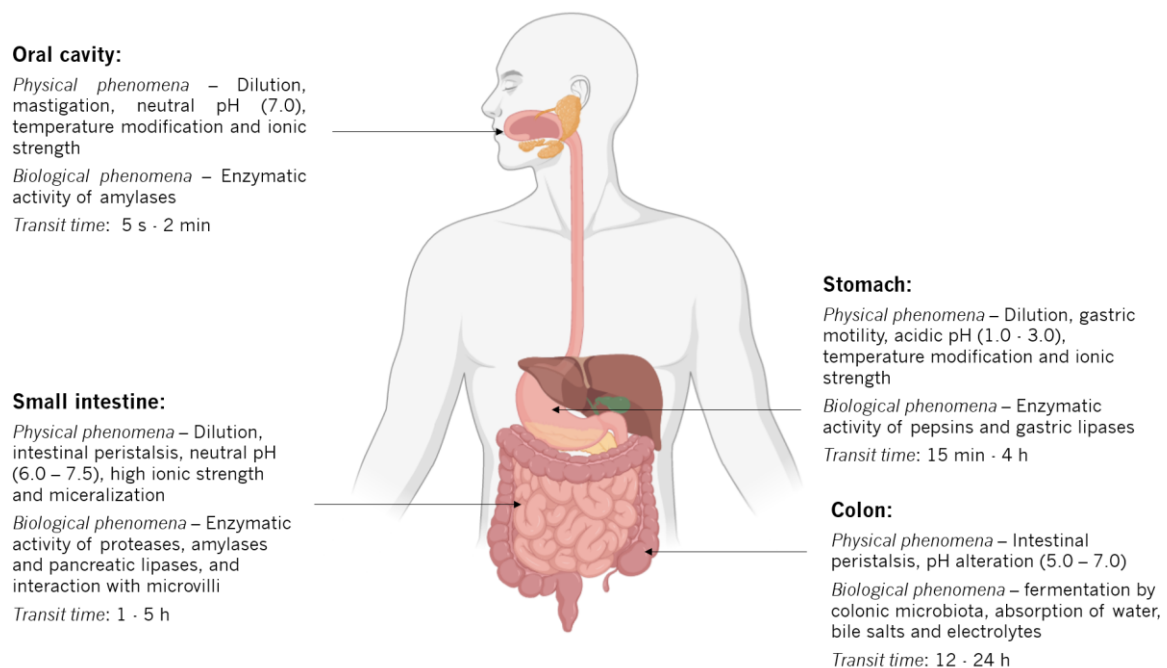


Figure 2 – Physical and Biological phenomena that occur during GI tract digestion.

The use of pH-stat titration method can complement the *in vitro* digestion by monitoring hydrolysis reactions, which releases or consumes protons [128]. An automatic system adds acidic or basic solution in order to maintain pH constant, and therefore the volume added can be related to the degree of hydrolysis [128]. This method allows to study the enzymatic digestion' kinetics in a simple, fast, reproducible and non-destructive manner [128].

3. Experimental approach

3.1. Materials

Curcumin (from *Curcuma longa* (Turmeric) powder), pepsin (from Porcine gastric mucosa), pancreatin (from porcine pancreas), bile (bile extract porcine) and bovine serum albumin were purchased from Sigma-Aldrich (St. Louis, MO, USA). Tween 80 was purchased from PanReac AppliChem ITW Reagents (Darmstadt, Germany). Candelilla wax was generously given by Ceras Marti (Barcelona, Spain), pea protein (Pisane®) by Cosucra™ (Warcroing, Belgium) and phospholipon 90G (soybean lecithin) by Lipoid (Ludwigshafen, Germany).

3.2. Encapsulation of curcumin in solid lipid nanoparticles

3.2.1. Preliminary assay to choose the plant wax

SLNs were prepared with three available plant waxes (i.e. Candelilla, carnauba and rice bran wax) according to Kheramandian and colleagues (2010) with some modifications [129]. A lipid solution composed of the selected plant wax (3.0 %, w/w), phospholipid 90G (1.5 % (w/w)) and curcumin (0.1 %, w/w) were melted in a water bath, at a temperature 10 °C above the wax' melting point, and under magnetic agitation. Simultaneously, Tween 80 (1.5 %, w/w) was solubilized in distilled water at the same temperature, followed by a homogenization in an Ultra-Turrax (T18, Ika Werke, Germany) during 2 min at 3 400 rpm. Then, the aqueous solution was added to the lipid solution and mixed at 18 000 rpm for 8 min in an Ultra-Turrax (T18, Ika Werke, Germany). At last, the mixture was gradually dispersed at a volume ratio of 1:10 in cold water at 2±1 °C and under stirring at 2 000 rpm for 5 min, followed by an additional 35 min at 800 rpm in a mechanical stirred. The SLNs were kept at 4 °C in the dark.

3.2.2. Experimental design

The development of novel formulations and their optimization is a variable dependent process. The conscious planning of experiments allows to determine the factors whose influence is significant and, if possible, quantify the impact in the response variables. At the beginning of 20th century, Ronald Fisher introduced the concept of applying statistical analysis during the planning stages of research instead at the end of the experiment [130]. Experimental design (ED) relies on a deliberate selection of one or more independent variables and observation of their impact on one or more dependent variable [131]. The controlled input factors of the process are systematically and purposely varied, and as result the connection between independent and dependent variables through mathematical functions enables the determination of the most influential factors, identification of optimal conditions for the desired output and identification of interaction effects between factors [130].

3.2.2.1. Preliminary tests: Curcumin' solubility assessment

Curcumin solubility in candelilla wax was determined through the successive addition of curcumin to a mixture of candelilla wax and lecithin (ratio of 1:1). Visual verification was used to assess the complete solubilization of curcumin in the wax. Curcumin visible remains, agglomerates or suspended particles were considered as indicators of non-solubilization. Also, if mixture separation occurred when vials were left without shaking the results were not considered as positive.

3.2.2.2. SLNs optimal formulation

The experimental design was created to identify a causal relationship between independent and dependent variables, while minimizing the number of required experiments. To obtain an optimal formulation, based on the primordial assay and the literature, a central composite rotatable design (CCRD) was employed. Four independent variables and their imposed limits were established (Table 7) and twenty-seven assays arranged the experimental design. Four nanoparticles' characterization parameters were considered as response variables: particles' size, PDI, ZP and EE.

Table 7 – Description of experimental design' input variables and their imposed limits

Variable	Minimum	Maximum
Candelilla wax concentration (% w/w)	3.0	5.0
Lecithin concentration (% w/w)	0.0	3.0
Curcumin:wax ratio	3.3	20.0
Tween 80 concentration (% w/w)	0.0	3.0

The SLNs were prepared as indicated in section 3.2.1 while adjusting the concentration of candelilla wax, lecithin, and Tween 80 as well as the ratio of curcumin to wax according to the experimental design established formulation (Table 8).

3.3. Encapsulation of curcumin in pea protein nanoparticles

3.3.1. Nanoparticle preparation

Pea protein isolate (PPI) nanoparticles were prepared based on Fan and colleagues (2020) protocol with some modifications [85]. PPI powder was dissolved in ultrapure water and magnetically stirred for 1 hour at room temperature (400 rpm). The pH of the solution was adjusted to 12 with NaOH (1 M) and kept for 30 min, under magnetic agitation at 400 rpm. Then, the solution was heated in a water bath at 88 °C for 30 min with agitation (200 rpm) and rapidly cooled to room temperature in an iced water bath before pH adjustment (pH 7, 8 or 9). Stock CaCl₂ solution (1 M) was added dropwise to the solution to reach a final concentration of 1 mM, under magnetic stirring (400 rpm). The solution was

kept under agitation (400 rpm) during 2 h to induce nanoparticles formation. The final protein concentration was approximately 1.0 mg/mL.

Table 8 – Composition of the 27 assays of the experimental design

	[Candelilla wax] (%, w/w)	[Lecithin] (%, w/w)	Curcumin : Wax ratio (%, w/w)	[Tween 80] (%, w/w)
E1	3.50	0.75	7.50	0.75
E2	4.50	0.75	7.50	0.75
E3	3.50	2.25	7.50	0.75
E4	4.50	2.25	7.50	0.75
E5	3.50	0.75	15.83	0.75
E6	4.50	0.75	15.83	0.75
E7	3.50	2.25	15.83	0.75
E8	4.50	2.25	15.83	0.75
E9	3.50	0.75	7.50	2.25
E10	4.50	0.75	7.50	2.25
E11	3.50	2.25	7.50	2.25
E12	4.50	2.25	7.50	2.25
E13	3.50	0.75	15.83	2.25
E14	4.50	0.75	15.83	2.25
E15	3.50	2.25	15.83	2.25
E16	4.50	2.25	15.83	2.25
E17	3.00	1.50	11.70	1.50
E18	5.00	1.50	11.70	1.50
E19	4.00	0.00	11.70	1.50
E20	4.00	3.00	11.70	1.50
E21	4.00	1.50	3.30	1.50
E22	4.00	1.50	20.00	1.50
E23	4.00	1.50	11.70	0.00
E24	4.00	1.50	11.70	3.00
E25	4.00	1.50	11.70	1.50
E26	4.00	1.50	11.70	1.50
E27	4.00	1.50	11.70	1.50

3.3.2. Curcumin encapsulation

Curcumin was solubilized in ethanol absolute to obtain a concentrated solution. A certain quantity of curcumin solution was added dropwise to calcium induced PPI nanoparticles solution, under magnetic agitation (400 rpm), to reach the desired final concentration. The mixture was kept on the magnetic stirrer for 6 h in the absence of light. After this time, the solution was kept in the absence of light at 4 °C.

3.4. Nanostructure's characterization

3.4.1. Particle size and polydispersity index

The nanostructures average diameter (size) and polydispersity index (PDI) were determined using DLS (Zetasizer Nano-ZS, Malvern Instruments Ltd., Malvern Hills, UK). The nanostructures were

diluted at a volume ratio of 1:10 with distilled water, at room temperature, and the samples were measured in disposable cuvettes (Zen0040) with three readings for each one of them. The results are given as the average \pm standard deviation of a minimum of six measurements.

3.4.2. ζ -potential

The ζ -potential (ZP) of the nanostructures was determined using DLS (Zetasizer Nano-ZS, Malvern Instruments Ltd., Malvern Hills, UK). The samples were analysed in a folded capillary cell (DTS1070) and the measurements were done in duplicate, with three readings each. The results are presented as the average \pm standard deviation of the values obtained.

3.4.3. Encapsulation efficiency

3.4.3.1. Encapsulation efficiency of SLNs

Encapsulation efficiency (EE) was determined based on Alanchari and colleagues (2021) protocol, with minor alterations. The SLN samples were diluted using a 50 % (w/w) ethanol solution to 1:4 ratio and added to the upper compartment of an ultracentrifuge tube (Amicon Ultra 0.5 mL, NMWL 10 KDa, Merk Millipore Ltd). The samples were then centrifuged at room temperature, during 20 min at 4000 rpm. The absorbance of the filtrated solution, containing the unloaded curcumin, was determined at a wavelength of 430 nm via UV-Vis spectrophotometry (Cytation 3_Biotek). This wavelength was selected once it corresponds to the maximum absorbance of curcumin. The results are presented as the mean average \pm standard deviation of the triplicated measurements.

The encapsulation efficiency equation is the following:

Equation 1:
$$EE(\%) = \frac{W_{Total} - W_{free}}{W_{total}} \times 100$$

Where W_{total} indicated the total amount of curcumin and W_{free} represents the amount of unloaded curcumin.

A calibration curve was established by preparing different dilutions of a 50 % (w/w) ethanol solution with a known quantity of curcumin. Each sample was measured in triplicate in UV-Vis spectrophotometer (Cytation 3_Biotek) at a wavelength of 430 nm. The resulting calibration is indicated in Annex 1 and the corresponding equation is indicated below (Equation 2).

Equation 2:
$$Absorbance(430\text{ nm}) = 61174[Curcumin] \left(\frac{g}{mL}\right) - 0.05$$

When the curcumin absorbance quantified exceeded the quantification limits of the equipment or the volume of free curcumin solution was small, dilutions were done using the 50 % (w/w) ethanol solution. To confirm that the ethanol concentration did not reflect on absorbance values obtained, two samples

with equal concentration of curcumin were prepared in ethanol solutions of 50.0 and 47.5 % (w/w) and the respective absorbance was measured at 430 nm, in sextuplicate. The ethanol concentration of 47.5 (% w/w) was selected considering the maximum dilution required to allow triplicates measurements. Resorting to box plot (coefficient of 0.5), the outliers were removed and OneWay Anova, associated with the mean comparison Tuckey test, was employed confirming no significant differences between samples (Annex 2).

3.4.3.2. Encapsulation efficiency of PPI nanoparticles

EE was determined based on Fan and colleagues (2020) protocol, with minor alterations. The formulation was subjected to centrifugation (Heraeus Multifuge X3R, ThermoFisher Scientific, USA) at 10 000 g for 30 min, at a temperature of 20 °C, to induce the separation of encapsulated and non-encapsulated curcumin. The supernatant was collected and labelled as the fraction containing the non-encapsulated curcumin. The precipitate, containing the encapsulated curcumin, was resuspended in an 2 % (w/w) ethanol solution. The EE was determined based on equation 1.

A calibration curve was established as the absorbance at 430 nm versus the curcumin concentration in ethanol. Each sample was measured in triplicate in an UV-Vis spectrophotometer (Genesys 50, Thermo scientific, USA). The resulting calibration curve is indicated in annex 3, and the corresponding equation is indicated below (Equation 3).

Equation 3:
$$\text{Absorbance (430 nm)} = 186.5 [\text{Curcumin}] \left(\frac{\text{mg}}{\text{mL}} \right) - 0.01$$

3.4.4. Stability assessment during storage of nanostructures

The stability of the nanostructures was determined during storage by assessing changes in size, PDI and ZP using DLS (Zetasizer Nano-ZS, Malvern Instruments Ltd., Malvern Hills, UK). The measurements were done as indicated in sections 3.4.1. and 3.4.2. The results are presented as the average \pm standard deviation of the values obtained.

3.5. *In vitro* digestion

3.5.1. Digestion stock solutions

The selected nanostructures were subjected to a digestion process using the harmonized *in vitro* static digestion model [132]. Simulated salivary fluid (SSF) solution was composed of KCl 15.1 mM, NaHCO₃ 13.6 mM, KH₂PO₄ 3.7 mM, HCl 1.1 mM, MgCl₂(H₂O)₆ 0.15 mM and (NH₄)₂CO₃ 0.06 mM in Milli-Q water. Simulated Gastric Fluid (SGF) solution was composed of NaCl 47.2 mM, NaHCO₃ 25 mM, HCl 15.6 mM, KCl 6.9 mM, KH₂PO₄ 0.9 mM, MgCl₂(H₂O)₆ 0.12 mM, (NH₄)CO₃ 0.5 mM in Milli-Q water.

Simulated intestinal fluid (SIF) solution was prepared with NaHCO_3 85 mM, NaCl 38.4 mM, HCl 8.4 mM, KCl 6.8 mM, KH_2PO_4 0.8 mM, $\text{CaCl}_2(\text{H}_2\text{O})_2$ 0.6 mM and $\text{MgCl}_2(\text{H}_2\text{O})_6$ 0.33 mM in Milli-Q water. All stock solutions were prepared 1.25x concentrated to achieve the final desired concentration after adding water.

3.5.2. *In vitro* static digestion

The oral phase simulation was initiated by the addition of SSF solution, $\text{CaCl}_2(\text{H}_2\text{O})_2$ 0.3 M (final solution concentration of 1.5 M) and Milli-Q water to 5 mL of each sample. The mixture was incubated at 37 °C during 2 min under agitation at 120 rpm. The gastric phase was initiated with the addition of SGF, $\text{CaCl}_2(\text{H}_2\text{O})_2$ 0.3 M (to achieve 0.15 mM in the solution) and pepsin solution (final enzymatic activity of 3593 $\text{U}\cdot\text{mL}^{-1}$). The pH adjustment to 3.0 was performed with HCl (1M) and the SGF solution concentration was adjusted with Milli-Q water. The samples were incubated at 37 °C for 2 h under agitation at 200 rpm. The intestinal phase was simulated by adding SIF, $\text{CaCl}_2(\text{H}_2\text{O})_2$ 0.3 $\text{mol}\cdot\text{L}^{-1}$ (solution concentration of 0.3 mM), bile salts (to reach final concentration of 10 mM) and pancreatic solution (final enzymatic activity of 800 $\text{U}\cdot\text{mL}^{-1}$). The pH was adjusted to 7.0 with NaOH (1 M) or HCl (1 M) and the concentration of SIF was adjusted with Milli-Q water. The incubation occurred over 2 h at 37 °C under agitation at 200 rpm. The selected nanostructures were subjected to the digestion process in triplicate.

3.5.3. Physicochemical characterization

The digested nanostructures were physicochemically characterized in terms of size, PDI and ZP resorting to DLS (Zetasizer Nano-ZS, Malvern Instruments Ltd., Malvern Hills, UK) as described in 2.2.4.1. and 2.2.4.2. A sample was collected after each digestion phase and kept in ice until characterization. Milli-Q water with pH adjusted to 7.0 or 3.0 (according to the sample pH) was employed to dilute the samples at a 1:10 ratio. Three samples of the selected nanostructures were analysed simultaneously, culminating in 9 measurements of each digestion stage. The results are presented as the average \pm standard deviation.

3.5.4. Curcumin bioaccessibility, stability and effective bioavailability

Curcumin bioaccessibility was defined as the fraction of curcumin inside the micelle phase, whilst stability considered the non-transformed curcumin portion present in the whole digesta at the end of the digestion. Effective bioavailability is a curcumin absorption estimative based on the two previous parameters. Bioaccessibility and stability were determined at the end of the digestion based on Liu and colleagues (2018) methodology, with some modifications [133]. The digesta (10 mL) was centrifuged (Heraeus Multifuge X3R, ThermoFisher Scientific, USA) at 18 000 g at 20 °C for 30 min to collect the micelle phase, which was assumed as the supernatant. Then, the whole digesta or micelle phase (5 mL) was mixed in a ratio of 1:1 (v/v) with chloroform, vortexed and centrifuged at 700 g and 20 °C for 10

min. The bottom layer was collected, and the top layer was subjected again to the extraction procedure. The second bottom layer was added to the first one and analysed in an UV-Vis spectrometer (DR 2800, Hach Lange, USA) at 430 nm. A calibration curve was established as the absorbance at 430 nm versus the curcumin concentration in chloroform (Annex 4) and the respective equation is indicated below (equation 4).

$$\text{Equation 4: } \quad \text{Absorbance (430 nm)} = 186.51[\text{Curcumin}] \left(\frac{\text{mg}}{\text{mL}} \right) - 0.01$$

Curcumin bioaccessibility (B), stability (S) and effective bioavailability (BA) were determined using equations 5-7 respectively:

$$\text{Equation 5: } \quad B = \frac{C_{\text{Micelle}}}{C_{\text{Digesta}}} \times 100$$

$$\text{Equation 6: } \quad S = \frac{C_{\text{Digesta}}}{C_{\text{Initial}}} \times 100$$

$$\text{Equation 7: } \quad BA = B \times S$$

Where C_{Micelle} and C_{Digesta} correspond to the curcumin concentration in the micelle phase and whole digesta, respectively. C_{Initial} corresponds to the curcumin concentration in the initial solution prior to digestion.

3.5.5. Nanostructures' digestibility

3.5.5.1. Free fatty acids' release

SLNs digestibility was evaluated by determining the free fatty acids (FFA) release over digestion. To do so, the oral and gastric digestion was performed as described in topic 2.2.3.2 and at the end of the gastric phase, the sample and all salts solutions of the intestinal phase were added to an automatic titration unit (pH stat) (Titrand 902, Metrohm, Switzerland). The pH was measured and adjusted to 6.92 ± 0.02 with NaOH (1 M). Then, the pancreatin enzymatic solution was added and once again the pH was adjusted with NaOH (1 M) or HCl (1 M) to 6.97 ± 0.01 . The solution pH was maintained at 7.0 by the addition of NaOH (0.1 M) using the automatic titration unit during 2 h, under magnetic agitation, in a heated jacket reactor.

The FFA release was determined through equation 8:

$$\text{Equation 8: } \quad \% \text{ FFA} = \left(\frac{(V_{\text{NaOH sample}} - V_{\text{NaOH blank}}) \times m_{\text{NaOH}} \times M_{\text{lipid}}}{w_{\text{lipid}} \times 2} \right) \times 100$$

Where $V_{\text{NaOH sample}}$ and $V_{\text{NaOH blank}}$ are the volume of NaOH added during the titration of the sample and blank assays, respectively, m_{NaOH} is the NaOH titrant' molar concentration, M_{lipid} is the reference molecular weight of candelilla wax (436.84 g/mol) and, w_{lipid} is the initial mass of lipid (g).

3.5.5.2. Protein hydrolysis' degree

PPI nanoparticles digestibility was determined through evaluation of proteins hydrolysis' degree (DH) by Lowry assay method [134]. Samples from the selected PPI nanoparticles were subjected to oral phase followed by the addition of all the salts from the gastric phase according to section 3.5.2. In the automatic titration unit (Titrand 902, Metrohm, Switzerland), the pH of the solution was adjusted to 3.0 followed by the addition of pepsin solution, with final activity of 3600 U/mL⁻¹. The titration was initiated immediately after adding the pepsin solution. For 2 h the temperature was kept at 37 °C using a heated jacketed reactor and the pH was kept at 3.0 by the automatic titration unit, under magnetic agitation.

At the end of the gastric phase, samples were collected for protein DH determination by Lowry assay method [134]. Shortly, the samples were pre-treated with copper ion in alkali solution, incubated in the dark, followed the aromatic amino acids reduction of phosphomolybdatephosphotungstic acid present in the Folin reagent. A calibration curve was development based on bovine serum albumin (BSA) concentration versus absorbance at 750 nm after Folin reaction (Annex 5) and the respective equation is indicated below (Equation 9):

Equation 9:
$$Absorbance (750\text{ nm}) = 0.0027 [Protein] \left(\frac{mg}{L}\right) + 0.0302$$

Lowry method allows to determine the mean degree of dissociation of the carboxylic groups (α_{COOH}) and, conjointly with the final volume of titrant added, the DH (%) can be estimated (Equation 10).

Equation 10:
$$DH (\%) = \frac{(V \times N)}{(m \times h_{tot})} \times \frac{1}{1 - \alpha_{COOH}} \times 100$$

Where V and N are the volume (mL) and normality (N) of acid titrant, m is the mass of protein in the sample (g) and h_{tot} (9.6) is the number of peptide bonds per mass of pea protein [128].

3.6. Statistical analysis

All the data was statistically analysed using analysis of variance (ANOVA) and Tukey mean comparison test ($p < 0.05$), resorting to Origin Pro 8 software (Massachusetts, USA). The outliers were removed based on box plot analysis, with a coefficient of 0.5, and the experimental results are presented as the mean values \pm standard deviation.

3.6.1. Experimental design' statistical treatment

The software Protimiza Experimental Design was used to generate the experimental design as well as analysing the experimental data based on experimental planning methodology and resourcing to central composite rotatable design. This methodology was employed instead of central composite design

since the location of the optimum point within the region of interest is not known [135]. Hence, the same magnitude of prediction errors was given to all points. The ED centre replicates provide an independent estimate of the experimental design error.

Further statistical treatment was done through multivariable linear regression (MLR) and Partial Least squares (PLS). MLR is a statistical technique which attempts to analyse the correlation between a single dependent variable and several independent variables [136]. PLS is a multivariate statistical technique that attempts to establish connections between multiple independent and dependent variables, by identifying the underlying factors, a linear combination of the independent variables with the best response to the independent variables [137]. It was designed to be employed on small datasets, with missing values or with possibility of collinearity [137].

4. Results and discussion

4.1. Solid lipid nanoparticles for curcumin encapsulation

4.1.1. Preliminary assay: production of SLNs

The development of SLNs required a lipid matrix, a surfactant (i.e. lecithin), a surfactant/co-emulsifier, Tween 80, as well as the bioactive compound, curcumin. In this work, a preliminary assay was conducted to determine a suitable lipid core to encapsulate curcumin among three available plant waxes: candelilla, carnauba and rice bran wax. For the SLNs production, a procedure developed by Kheradmandnia and colleagues (2010) was used, replacing the beeswax by the respective plant wax.

The size, PDI as well as the ZP are important parameters used to characterize lipid-based nanoparticles [10], [34], [110], [113], [119]. The determination of the mean particle size combined with PDI substantiates if the desired dimensions were achieved but also if they are maintained during storage. The nanoparticles' characteristics were determined using DLS and the results are indicated in Figure 3.

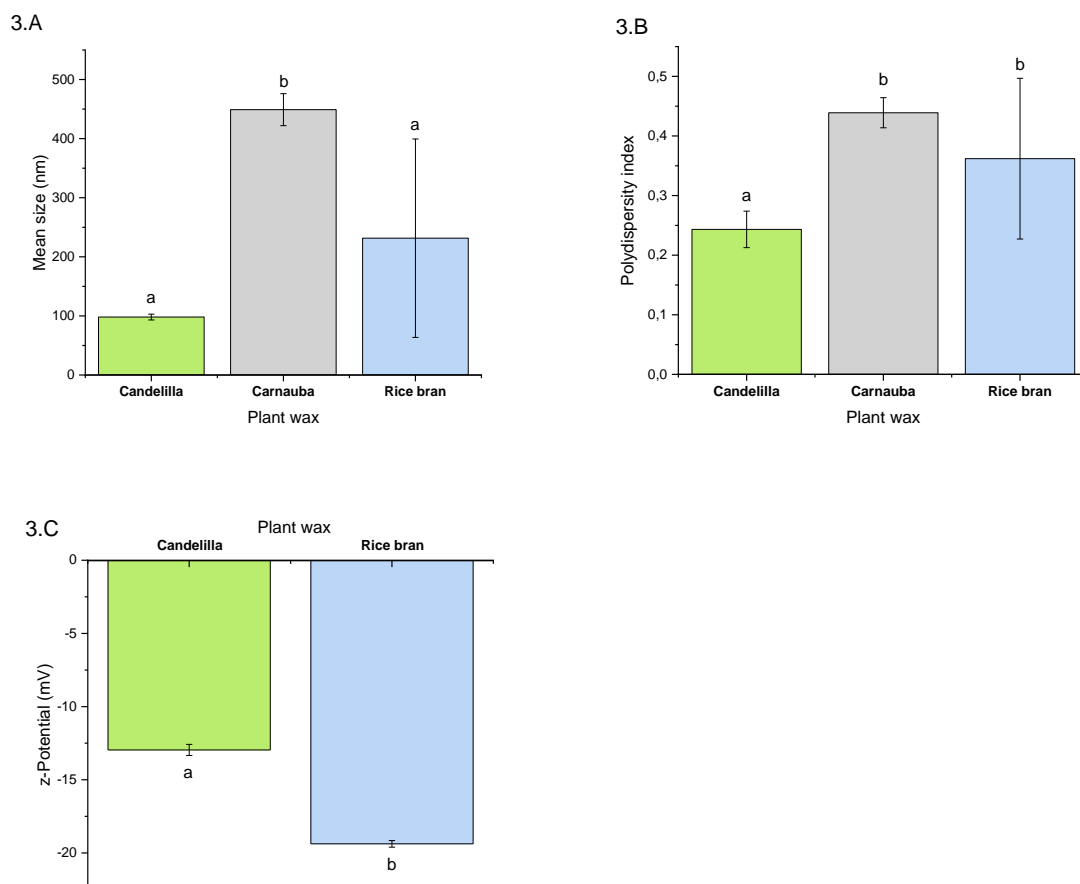


Figure 3 – Nanoparticles' size (A), polydispersity index (PDI) (B) and ζ -Potential (C). Statistically significant differences ($p > 0.05$) among plant waxes, for each parameter, are indicated in lower case letters. Equal letters indicate that no statistically significant difference was identified through Tukey Mean comparison test.

The purpose of the preliminary assay was performed to select a suitable wax formulation, from the available plant waxes, to use in the SLNs formulation which was optimized using an experimental design. In this sense, the formulation which exhibited a stable reduced size (i.e. inferior to 200 nm) as well as monodisperse (i.e. PDI inferior to 0.5) was selected. Carnauba wax formulation culminated in a mean particle size of 449.0 ± 27.07 nm and PDI of 0.439 ± 0.025 , therefore it was categorised as non-suitable. The ZP of this formulation wasn't measured since it was immediately discarded due to the high size. Rice Bran wax formulation demonstrated a higher (in modulus) ZP (-19.4 ± 0.224 mV), an indicator of a more stable formulation however the high variability in size measurements (231.6 ± 167.9 nm, i.e. high standard deviation) and PDI (0.361 ± 0.134) did not validate the selection of this plant wax.

Candelilla wax formulation provided the most interesting results, specifically a reduced mean particle size (98.09 ± 4.86 nm) and PDI (0.243 ± 0.030). Comparatively with Gonçalves and colleagues (2021) studies, in which SLNs based on beeswax with the same procedure and components' concentration, the developed nanoparticles demonstrated smaller size (98.09 ± 4.86 nm vs 145.4 ± 8.1 nm), PDI (0.243 ± 0.030 vs 0.253 ± 0.010) and ZP ($-13.0 \pm 0,8$ mV vs -23.6 ± 1.3 mV). The candelilla wax ZP value could be indicative of destabilization, nonetheless, this plant wax formulation was selected and subjected to physical stability assessment for 37 days (Figure 4). Up to day 27, the nanoparticles exhibited no significant changes in the measured parameters (i.e. particle size, PDI and ZP). At day 37, a small but statistically significant ($p > 0.05$) size change was detected. The nanoparticles were not considered stable after the day 27 since it was observed the formation of lumps (Figure 5), an indicator of particles disturbance.

4.1.2. Experimental design

The ED was applied in this study with the main objective of developing an optimal candelilla wax' nanoparticle formulation with reduced size (< 200 nm) and PDI (< 0.5). Encapsulation efficiency was also chosen as a response parameter since it is intended to maximize the curcumin beneficial effects while avoiding wasting this nutraceutical. ZP was evaluated due to its association with nanoparticles stability. The concentration of wax, emulsifier, and co-emulsifier as well as the ratio of the bioactive compound to wax were considered as independent variables (section 3.2.2.2.). The preliminary assay formulation was used as reference to the experimental design as well as the literature.

Surfactants stabilize SLNs by decreasing surface tension between the aqueous solution and the lipid. Even though, it was reported that higher concentrations of surfactants tend to reduce the nanoparticles size, they are more prone to induce toxicity, especially when ionic surfactants are use [91], [138]. Tween

80, a non-ionic surfactant, and lecithin, a zwitterionic surfactant and co-emulsifier, were kept from the preliminary assay. A maximum and minimum value of 3 and 0 % (w/v) was established since the non-ionic surfactant is synthetically produced, which contradicts with the sustainability aspect of this work.

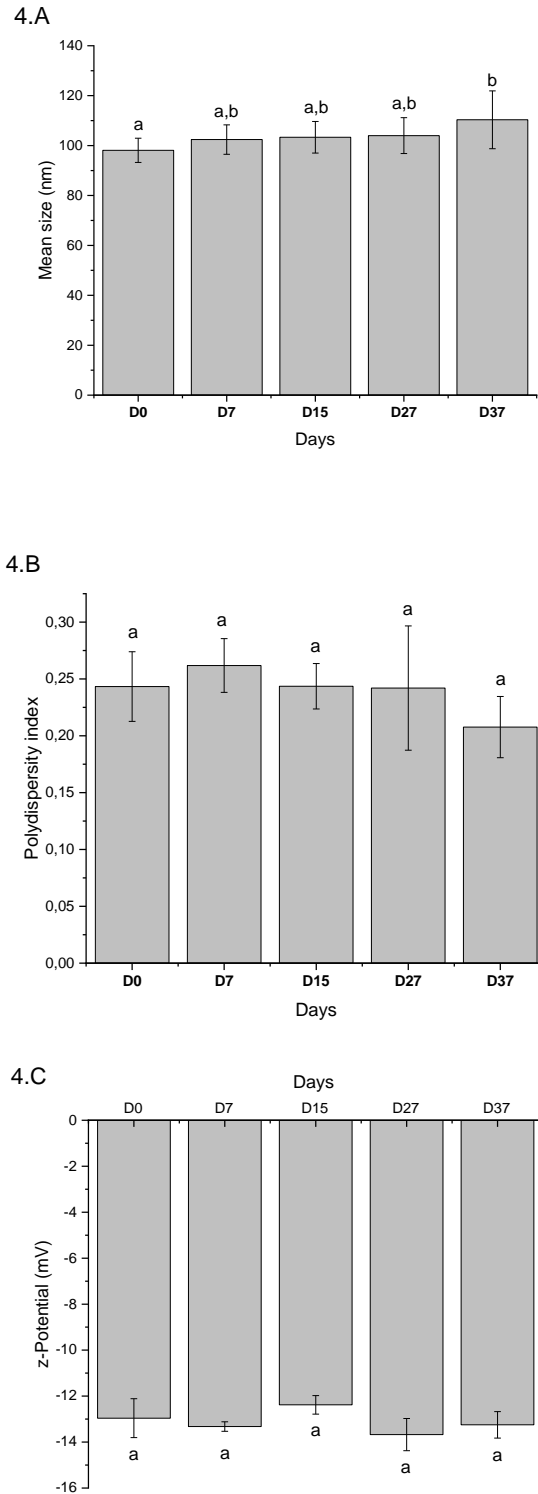


Figure 4 – Stability assessment of solid lipid nanoparticle formulation based on candelilla wax. The particle size (A), polydispersity index (PDI) (B) and ζ -Potential (C) were evaluated during 37 days of storage. The formulation is composed of 3 % (w/w) candelilla wax, 0.10 % (w/w) curcumin and 1.5 % (w/w) of lecithin and Tween 80. Statistically significant differences ($p > 0.05$) among values obtained for each

parameter on the analysed days are indicated in lower case letters. Equal letters indicate that no statistically significant difference was identified through Tuckey Mean comparison test.

The candelilla wax concentration was determined as a minimum of 3 % (w/w), such as the preliminary assay, and a maximum of 5 % (w/w), based on the literature [50], [138]. The maximum ratio of curcumin to candelilla wax was accessed through a solubility test, consisting of candelilla wax and lecithin ratio of 1:1, as well as an increasing quantity of curcumin. The maximum solubility was achieved at a curcumin to wax ratio of 21.3 % (w/w). An analogous approach was employed by Slavomira and colleagues (2017) for determining curcumin's affinity to different lipidic dispersions. The experimental design was composed of 27 assays whose formulations are indicated in Table 8 (Section 3.2.2.2.).

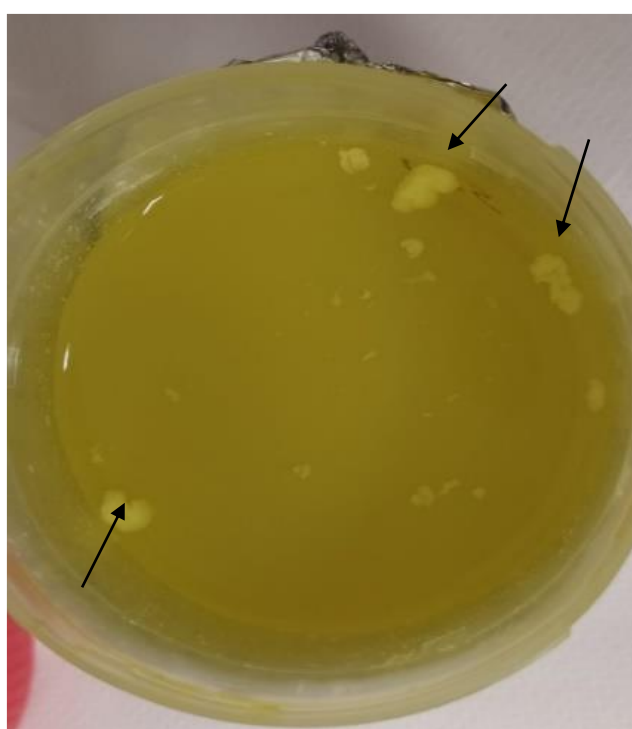


Figure 5 – Nanoparticles apparent destabilization, indicated by black arrows, verified on day 27 after formulation. The formulation is composed of 3 % (w/w) candelilla wax, 0.10 % (w/w) curcumin and 1.5 % (w/w) of lecithin and Tween 80.

4.2.1. Physicochemical characterization

4.2.1.1. Particle size

DLS is an effective technique and standard method that has been widely used to measure particle size and particle size distribution at submicron scale [116], [139]. On formulation day, the 27 assays (whose formulation is indicated in Table 8 in section 3.2.2.2.) were characterized in terms of size resorting to DLS. The same parameter was measured after 30 and 60 days of storage to assess formulation's stability (Table 9).

Table 9 – Particle mean size (nm), and respective standard deviation of solid lipid nanoparticles formulations based on with candelilla wax (27 formulations from experimental design). Statistically significant differences ($p > 0.05$) among values obtained for each parameter on the analysed days are indicated in lower case letters. Equal letters indicate that no statistically significant difference was identified through Tuckey Mean comparison test

Samples' name	Day		
	Size \pm Standard deviation (nm)		
	Day 0	Day 30	Day 60
E1	156.7 ^a \pm 7.5	145.8 ^b \pm 1.9	144.6 ^b \pm 1.2
E2	153.8 ^a \pm 3.3	148.4 ^b \pm 2.7	151.4 ^a \pm 4.3
E3	447.3 ^a \pm 32.5	411.1 ^a \pm 2.4	462.5 ^a \pm 37.9
E4	430.1 ^a \pm 16.0	426.9 ^a \pm 21.3	416.9 ^a \pm 11.5
E5	179.2 ^a \pm 4.0	186.4 ^b \pm 5.1	176.7 ^a \pm 2.6
E6	357.1 ^a \pm 20.9	333.8 ^b \pm 11.7	313.7 ^b \pm 6.2
E7	273.0 ^a \pm 7.5	303.6 ^a \pm 8.1	286. ^c \pm 6.1
E8	536.6 ^a \pm 42.0	512.8 ^{a,b} \pm 7.0	482.5 ^b \pm 20.0
E9	349.6 ^a \pm 14.5	93.5 ^b \pm 3.1	84.8 ^b \pm 1.7
E10	458.8 ^a \pm 115.7	196.7 ^b \pm 55.4	171.1 ^b \pm 6.9
E11	586.5 ^a \pm 218.9	234.4 ^b \pm 81.3	250.0 ^b \pm 61.6
E12	961.7 ^a \pm 206.5	738.5 ^a \pm 189.0	920.1 ^a \pm 203.8
E13	747.8 ^a \pm 211.6	159.9 ^b \pm 68.5	118.8 ^b \pm 34.8
E14	708.9 ^a \pm 124.7	344.9 ^b \pm 64.8	409.5 ^b \pm 109.9
E15	1066 ^a \pm 331.4	477.3 ^b \pm 237.6	872.4 ^{a,b} \pm 537.1
E16	551.1 ^a \pm 72.04	342.4 ^b \pm 21.1	375.2 ^b \pm 44.5
E17	164.6 ^a \pm 11.33	151.2 ^b \pm 3.3	150.9 ^b \pm 2.7
E18	378.6 ^a \pm 15.05	330.7 ^b \pm 5.1	312.7 ^b \pm 4.4
E19	6378.0 ^b \pm 2372	1078.0 ^b \pm 319.3	890.7 ^c \pm 240.4
E20	673.9 ^a \pm 90.93	953.9 ^b \pm 217.6	667.1 ^a \pm 161.1
E21	307.1 ^a \pm 16.46	292.6 ^a \pm 17.9	296.2 ^a \pm 12.3
E22	325.9 ^a \pm 27.11	299.3 ^{a,b} \pm 10.7	294.0 ^b \pm 9.4
E23	260.0 ^a \pm 13.03	253.7 ^a \pm 19.2	248.0 ^a \pm 4.2
E24	361.6 ^a \pm 111.5	93.4 ^b \pm 6.5	114.0 ^b \pm 25.8
E25	352.3 ^a \pm 12.44	337.3 ^a \pm 19.7	289.5 ^b \pm 21.8
E26	344.2 ^a \pm 38.09	333.2 ^a \pm 13.7	274.5 ^b \pm 12.8
E27	376.6 ^a \pm 41.36	432.7 ^a \pm 104.6	285.7 ^b \pm 11.0

4.2.1.2. Polydispersity Index

PDI determines the width of a particle size distribution, being values higher than 0.6 indicators of polydispersity and values under 0.3 indicators of mono-dispersity, but also the distribution of the particles in the matrix [34], [113], [116]. PDI of all 27 assays was measured simultaneously with particles size through to DLS technique at formulation day, after 30 and 60 days (Table 10).

Table 10 – Polydispersity index, and respective standard deviation, of solid lipid nanoparticles formulated with candelilla wax (27 formulations from experimental design). Statistically significant differences ($p > 0.05$) among values obtained for each parameter on the analysed days are indicated in lower case letters. Equal letters indicate that no statistically significant difference was identified through Tuckey Mean comparison test

Samples' name	Day	Polydispersity index \pm standard deviation (nm)		
		Day 0	Day 30	Day 60
E1		0.202 ^a \pm 0.033	0.186 ^{a,b} \pm 0.011	0.161 ^b \pm 0.006
E2		0.214 ^a \pm 0.043	0.213 ^a \pm 0.014	0.199 ^b \pm 0.035
E3		0.484 ^{a,b} \pm 0.036	0.468 ^a \pm 0.043	0.567 ^b \pm 0.065
E4		0.468 ^a \pm 0.025	0.473 ^a \pm 0.024	0.418 ^a \pm 0.046
E5		0.191 ^a \pm 0.008	0.202 ^a \pm 0.004	0.197 ^a \pm 0.007
E6		0.450 ^a \pm 0.039	0.416 ^a \pm 0.014	0.410 ^a \pm 0.008
E7		0.290 ^a \pm 0.029	0.327 ^{a,b} \pm 0.043	0.349 ^a \pm 0.024
E8		0.483 ^a \pm 0.052	0.486 ^a \pm 0.008	0.457 ^a \pm 0.017
E9		0.407 ^a \pm 0.040	0.414 ^a \pm 0.044	0.333 ^b \pm 0.030
E10		0.526 ^a \pm 0.054	0.448 ^{a,b} \pm 0.101	0.401 ^b \pm 0.030
E11		0.628 ^a \pm 0.151	0.495 ^{a,b} \pm 0.055	0.446 ^b \pm 0.071
E12		0.810 ^a \pm 0.064	0.749 ^a \pm 0.039	0.726 ^a \pm 0.069
E13		0.795 ^a \pm 0.181	0.324 ^a \pm 0.045	0.369 ^b \pm 0.062
E14		0.718 ^a \pm 0.127	0.583 ^a \pm 0.068	0.626 ^{a,b} \pm 0.025
E15		0.909 ^a \pm 0.103	0.567 ^b \pm 0.165	0.701 ^{a,b} \pm 0.249
E16		0.641 ^a \pm 0.031	0.821 ^b \pm 0.196	0.878 ^b \pm 0.081
E17		0.289 ^a \pm 0.050	0.239 ^b \pm 0.012	0.271 ^{a,b} \pm 0.023
E18		0.390 ^a \pm 0.037	0.373 ^{a,b} \pm 0.035	0.340 ^b \pm 0.018
E19		1.000 ^a \pm 0.000	0.858 ^b \pm 0.110	0.789 ^b \pm 0.039
E20		0.661 ^{a,b} \pm 0.013	0.795 ^a \pm 0.125	0.640 ^b \pm 0.029
E21		0.435 ^a \pm 0.068	0.384 ^a \pm 0.007	0.423 ^a \pm 0.063
E22		0.461 ^a \pm 0.054	0.417 ^a \pm 0.006	0.417 ^a \pm 0.032
E23		0.349 ^{a,b} \pm 0.013	0.359 ^a \pm 0.015	0.334 ^a \pm 0.005
E24		0.431 ^a \pm 0.097	0.349 ^{a,b} \pm 0.007	0.333 ^b \pm 0.096
E25		0.408 ^a \pm 0.036	0.400 ^a \pm 0.024	0.393 ^a \pm 0.044
E26		0.419 ^a \pm 0.027	0.417 ^a \pm 0.021	0.371 ^b \pm 0.019
E27		0.473 ^a \pm 0.037	0.516 ^a \pm 0.078	0.439 ^a \pm 0.052

4.2.1.3. ζ -potential

The ZP of each formulation was determined at day 0, 30 and 60 of storage. A high value (positive or negative) is indicative that the particles are electrically stabilized while low values ($< \pm 20$ mV) can lead to van der Waals interparticle attraction, resulting in flocculation or aggregation [119], [120]. All the data collected is indicated in Table 11.

Table 11 - ζ -Potential (mV), and respective standard deviation, of solid lipid nanoparticles formulated with candelilla wax (27 formulations from experimental design). Statistically significant differences ($p > 0.05$) among values obtained for each parameter on the analysed days are indicated in lower case letters. Equal letters indicate that no statistically significant difference was identified through Tuckey Mean comparison test

Samples' name	Day	ζ -Potential \pm Standard deviation (mV)		
		Day 0	Day 30	Day 60
E1		-18.5 ^a \pm 0.7	-18.0 ^a \pm 1.8	-19.7 ^a \pm 0.8
E2		-19.3 ^a \pm 0.7	-19.6 ^a \pm 1.7	-20.4 ^a \pm 3.3
E3		-19.3 ^{ab} \pm 0.8	-18.7 ^a \pm 0.3	-19.9 ^b \pm 0.9
E4		-20.0 ^a \pm 0.6	-22.0 ^b \pm 0.4	-20.1 ^a \pm 0.6
E5		-20.4 ^a \pm 0.3	-19.0 ^a \pm 1.1	-20.4 ^a \pm 1.3
E6		-19.5 ^a \pm 0.5	-19.2 ^a \pm 1.2	-18.7 ^a \pm 0.4
E7		-16.6 ^a \pm 0.6	-17.4 ^a \pm 0.6	-19.5 ^b \pm 0.5
E8		-21.4 ^a \pm 0.8	-20.9 ^a \pm 0.7	-23.2 ^b \pm 0.4
E9		-13.6 ^a \pm 0.2	-13.3 ^{ab} \pm 0.3	-12.7 ^b \pm 0.3
E10		-13.4 ^a \pm 0.5	-12.9 ^a \pm 0.2	-11.5 ^b \pm 0.5
E11		-14.9 ^a \pm 0.5	-15.7 ^a \pm 1.1	-16.2 ^a \pm 3.0
E12		-13.0 ^a \pm 0.4	-13.3 ^a \pm 0.1	-17.2 ^b \pm 0.7
E13		-11.5 ^a \pm 0.6	-11.5 ^a \pm 0.3	-14.4 ^b \pm 0.5
E14		-13.7 ^a \pm 0.7	-11.6 ^b \pm 0.8	-14.3 ^a \pm 1.2
E15		-13.3 ^a \pm 1.0	-11.8 ^b \pm 0.4	-13.6 ^a \pm 0.6
E16		-11.6 ^a \pm 0.4	-13.3 ^b \pm 0.4	-14.8 ^c \pm 1.1
E17		-12.7 ^a \pm 0.6	-14.0 ^b \pm 0.6	-15.3 ^c \pm 1.0
E18		-17.0 ^a \pm 0.7	-17.9 ^{ab} \pm 1.3	-19.1 ^b \pm 0.8
E19		-13.4 ^a \pm 0.1	-16.9 ^b \pm 0.2	-15.6 ^c \pm 0.6
E20		-16.0 ^a \pm 0.7	-17.4 ^a \pm 2.7	-20.3 ^b \pm 1.0
E21		-17.3 ^a \pm 0.5	-17.1 ^a \pm 0.7	-17.2 ^a \pm 1.5
E22		-16.9 ^a \pm 0.9	-17.1 ^a \pm 0.9	-17.2 ^a \pm 1.1
E23		-25.9 ^a \pm 0.4	-25.8 ^a \pm 0.6	-26.0 ^a \pm 0.7
E24		-10.4 ^a \pm 0.7	-12.7 ^b \pm 0.5	-13.1 ^b \pm 1.0
E25		-15.6 ^a \pm 0.9	-16.8 ^{ab} \pm 1.6	-17.7 ^b \pm 0.2
E26		-16.0 ^a \pm 0.8	-16.8 ^{ab} \pm 0.8	-17.3 ^b \pm 0.3
E27		-14.1 ^a \pm 0.6	-14.0 ^a \pm 1.1	-17.0 ^b \pm 0.8

4.2.1.4. Encapsulation efficiency

Encapsulation efficiency is considered one of the most important parameters for bioactive compounds' delivery [140]. EE was quantified on day 0 of the formulations' production to determine the curcumin encapsulation limitations imposed by each formulation conditions (Table 12).

Table 12 – Encapsulation efficiency, of solid lipid nanoparticles formulated with candelilla wax (27 formulations from experimental design)

Sample' name	Encapsulation efficiency (%)
E1	100.0 ± 1.4
E2	100.0 ± 1.3
E3	100.0 ± 0.9
E4	100.0 ± 1.7
E5	100.0 ± 0.6
E6	100.0 ± 0.0
E7	100.0 ± 0.2
E8	100.0 ± 4.4
E9	100.0 ± 0.0
E10	100.0 ± 0.6
E11	100.0 ± 0.0
E12	100.0 ± 0.3
E13	100.0 ± 0.0
E14	100.0 ± 0.0
E15	100.0 ± 0.0
E16	100.0 ± 0.0
E17	67.5 ± 0.0
E18	100.0 ± 0.0
E19	97.4 ± 0.0
E20	100.0 ± 0.0
E21	38.3 ± 0.0
E22	90.6 ± 0.0
E23	99.4 ± 0.0
E24	73.7 ± 0.0
E25	85.7 ± 0.0
E26	87.4 ± 0.0
E27	83.3 ± 0.0

4.2.2. Experimental design data analysis

4.2.2.1. Central composite rotatable design methodology

The selection of the most adequate design of experiment strategy is mainly dependent on the number of independent variables studied as well as the initial knowledge on the process that it is intended to optimize [141]. CCRD methodology was applied to evaluate the possible results of the initial data (Day 0). For each dependent variable, a regression equation and respective determination coefficient (r^2) was obtained (Table 13) after removal of statistically non-significant coefficients (p -value > 0.05), as confirmed by Pareto's graph.

Table 13 – Central composite rotatable design methodology employed on experimental design' data. The regression equation and respective determination coefficient for each dependent variable was attained by removal of non-statistically significant coefficients (p -value < 0.05)

Dependent variable	Regression equation	Determination coefficient (r^2) (%)
Encapsulation efficiency	$EE = 89.15 + 5.21 L^2 + 5.10 R$	26.1
Z-potential	$\zeta\text{-potential} = - 15.51 + 3.37 T - 0.70 T^2$	85.7
Size	Mean particle size = $- 13.30 - 402.86 L + 760.25 L^2$	55.3
Polydispersity index	$PDI = 0.41 + 0.11 L^2 + 0.12 T$	54.7

Note: The abbreviation EE corresponds to encapsulation efficiency, L to lecithin, R to curcumin to wax ratio and T to Tween 80.

R^2 is a statistical measure that represents the proportion of the variance for a dependent variable that is explained by an independent variable or variables in a regression model. EE regression equation indicates that both lecithin concentration and curcumin to wax ratio could be influential in EE variation, however the low explained variance percentage (26.1 %) suggests low suitability. Subedi and colleagues (2009) reported that EE is influenced by the compound solubility in the lipid as well as the lipid content, since it increases the interface of interaction between compound and lipid [142].

Particle size and PDI demonstrated r^2 of 55.3 and 54.7 %, respectively, indicating some correlation between the independent variables and the dependent variables variation. Lecithin concentration demonstrates to influence both dependent variables, based on their regression' equations. Size reduction was verified by Smith and colleagues (2020) when lecithin was added to SLNs formulations which previously only contained Tween 80 as surfactant. Schuber and colleagues (2005) also concluded that the presence of lecithin facilitates the formation of a lipid/water interface, and consequently reduced the particles size [143]. High contents of lecithin (> 30 %) caused an opposite effect since the high content of lecithin did not energetically reduce the size of the particles and may as well accumulate in multilayers. Among all dependent variables, ZP demonstrated the highest r^2 , specifically of 85.7 %, indicating that it is adequate to evaluate ZP value variance justified on Tween 80 concentration. The increase in negative particle charge with the increase of Tween 80 concentration was also observed by Alanchari and colleagues (2021) [144].

Due to the high variability of some assays as well as the bigger size of some measurements the experimental design was not able to predict with certainty the significant influence of all parameters. Although, DLS has the capacity to determine particle size distribution of a broad size range (0.3 nm to 10 μ m) and enables the comparison of particles quantity in different samples, it is susceptible to multiple light scattering. High particle concentration, particles' clustering, non-transparency of samples or minor

amounts of large particles can disturb the scattering properties of the solution, resulting in increased polydispersity and peak broadening [113], [114], [116]. Simultaneously, when a sample has various particles' groups with similar size ranges, this method may not distinguish between size groups or between single particles and small aggregates, culminating in a global distribution [115]. Centrifugation, filtration, or chromatographic methods can be effective in reducing light scattering disturbance [114]. Additionally, the development of a second design of experiment with an adjusted range for each studied variable, conceivably would allow to calculate their effect on dependent variables, as well as analyse the response surface [141].

To determine if some of the data had useful information on the relationship between the independent and dependent variables, a multiple linear regression (MLR) and a partial least squares (PLS) analysis were applied. A PDI superior to 0.5 was established as exclusion parameter since it is indicative of high variability in the composition and lower quality in the measurements.

4.2.2.2. Multiple linear regression

MLR was employed to 18 essays from the experimental design, whose selection was based on PDI value ($PDI < 0.5$). To each dependent variable, linear regressions with one to four independent variables combinations were employed to determine their influence on the dependent variables results. All the resulting data is indicated in Table 14.

In what concerns to PDI and ζ - potential, the combination of all four variables or the combined effect of candelilla wax, lecithin and Tween 80 concentration are the same, specifically of 52.6 % and 84.7 %. A similar effect was verified for particle size, in which the r^2 value, for all variables and the three variables mentioned, is 62.3 % and 62.1 %, respectively. Thus, under the evaluated boundaries, curcumin to candelilla wax ratio does not demonstrate a significant influence on these dependent variables.

The positive effect of lecithin and Tween 80 on particles' size and PDI may be due to the intercalation of the non-ionic surfactant on the phospholipid monolayer, forming a closely packed mixed film [145]. Similar effect was verified for mean particle size whose outcome was majorly determined by candelilla wax and Tween 80 concentration merge. Nonetheless, a nanoparticles' size and PDI increase was indicated in different research papers [144], [146] when lipid concentration increased, possibly due to an increase in the viscosity and insufficient surfactant concentration. Üner (2016) also indicated that an increase in surfactant/lipid ratio typically induces nanoparticles' size reduction [147].

Regarding to EE, it demonstrated the lowest adjustment to linear regression (i.e. 37.1 %). Curcumin to candelilla wax ratio combined with Tween 80 concentration demonstrates to influence the most the

experimental versus calculated encapsulation efficient with a r^2 of 33.3 %. Concerning the ZP, Tween 80 concentration alone account for 79.9 % of the variability observed in this dependent variable experimental data. This result is in accordance with CCDR methodology analysis since Tween 80 concentration was identified as an influential independent variable on ZP variance.

Table 14 – Multiple linear regressions' determination coefficients obtained for each dependent variable. based on the combination of one to four independent variables

Dependent variable Independent variables combination	Determination coefficient (%)			
	ZP	Size	PDI	EE
CLRT	84.7	62.3	52.6	37.1
CLR	9.2	55.0	37.9	20.1
LRT	80.0	44.1	39.7	34.8
CRT	84.6	25.2	24.3	35.3
CLT	84.7	62.1	52.6	23.8
CL	8.9	54.9	37.9	4.3
RT	79.9	3.5	8.8	33.3
CT	84.5	24.5	24.0	22.6
CR	8.9	21.1	13.6	19.3
LT	80.0	43.7	39.7	21.1
LR	1.1	38.5	27.0	16.8
C	8.6	20.7	13.6	3.9
L	0.7	38.3	27.0	0.2
R	0.5	0.8	0.2	16.2
T	79.9	2.4	8.3	20.0

Note: ZP refers to ζ -Potential; PDI to polydispersity index; EE to encapsulation efficiency; C to candelilla wax concentration; L to lecithin concentration; T to Tween 80 concentration and R to curcumin to candelilla wax ratio.

4.2.2.3. Partial Least squares

Further analysis of the experimental data was done through PLS. A standardised World's iteration method was employed, and the results are indicated in Table 15. No dimensional reduction was verified, and thus four factors were provided from the four independent variables. All four factors demonstrated similar variance for x effects, as a result no relationship between these elements is apparent. It is postulated that the cumulative effect of the variance explained for Y responses should correspond to approximately 100 %, so that it can explain all the results variability [137]. However, in this PLS, the cumulative effect of the four factors represents only 59.2 % of the dependent variance. Thus, the remaining variability may derive from other variables outside the evaluated ones.

Table 15 – Partial least squares analysis employed on the selected assays from the experimental design (PDI <0.5). The resulting factors, variance explained from X effects and for Y responses, resulting from a standardized worlds iteration method, are indicated

Factor	Variance explained for X effects (%)	Variance Explained for Y responses (%)
1	26.2	30.0
2	26.9	26.1
3	23.4	2.9
4	23.5	0.1

Additionally, a Variance importance in projection (VIP) plot was established for all four independent variables (Figure 6). Three of four independent variables demonstrated to have a significant influence in the dependent variable's variance, i.e., the VIP for each independent variable is superior to the standardized value of 0.8. Curcumin to candelilla wax ratio did not demonstrate to be an influential parameter in dependent variable variance, which is in accordance with MLR results.

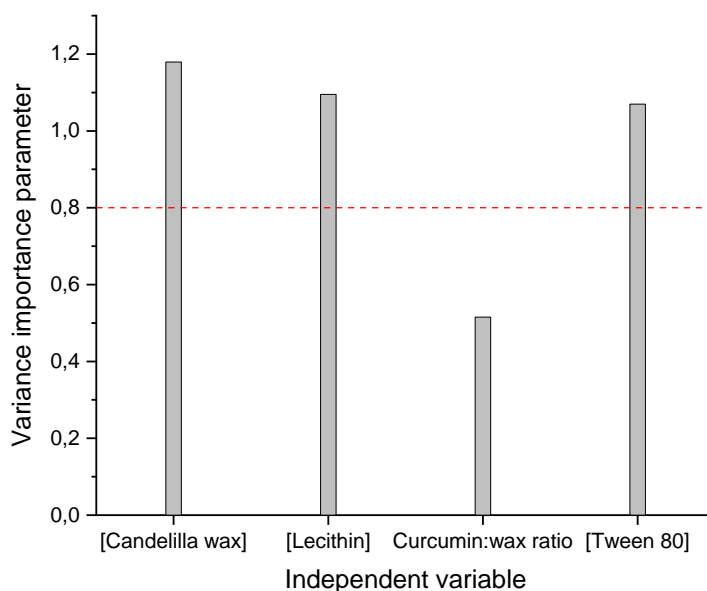


Figure 6 – Variable importance in projection plot obtained as result of Partial Least Squares analysis of the selected experimental design assays.

Although the experimental design was not employed to determine an optimal formulation, as it was initially intended, the supplementary statistical analysis demonstrated that three of the four independent variables (i.e. Candelilla wax, lecithin, and Tween 80 concentration) significantly influence the dependent variables variance. The influence of Tween 80 concentration on ZP variance was evident in all statistical treatments, with the highest r^2 values. This is indicative of a sustained association between these variables, under the studied conditions.

4.2.2.4. Formulation selection

The low quality of the experimental design did not allow to conceptualize an optimal formulation, however 3 of the 27 assays' formulations demonstrated characteristics within the initial objectives. These formulations were selected as candidates to proceed with the *in vitro* digestion analysis (i.e. formulation E1, E2 and E5), based primarily on size and PDI. These formulations are composed by 0.75 % (w/w) of lecithin and Tween 80, which could indicate an ideal ratio between emulsifiers, in the imposed conditions. The lower Tween 80 concentration provides a more sustainable alternative, when compared with the preliminary assay formulation. Furthermore, the reduction of surfactant and emulsifier concentration is also advantageous since it complies with the food sector limitations regarding the maximum acceptable amount [146].

The formulations E1 and E5 are identical except on the ratio of curcumin to wax. which was higher for the latest. Formulation E5 was able to encapsulate more curcumin while having the smallest PDI (0.191 ± 0.008), a reduced size (179.2 ± 4.0 nm) and the most negative ζ -potential (-20.4 ± 0.3 mV) of the three formulations. Even though formulation E2 demonstrated smaller size (153.8 ± 3.3 nm), reduced PDI (0.214 ± 0.043) as well as a high ZP (-19.3 ± 0.7 mV), when comparing this formulation with E1 and E5, it required a higher amount of wax.

The stability of the formulations was also a determining factor in the selection. The formulations demonstrated small, but statistically significant differences on particle mean size at day 30 comparatively with day 0 (Table 9). Formulation E1 demonstrated a continuous reduction of PDI from the day 0 to the last, verifying a statistically significant difference at day 60. On the contrary, formulations E2 and E5 did not demonstrate significant variations in PDI value, however, it should be noticed that the PDI of formulation E2 for each measurement demonstrated wider standard deviation (Table 10). None of the formulations demonstrate significant variations in ZP measurements (Table 11).

Subsequently, formulation E5 (4.2 % (w/w) candelilla wax, 0.7 % (w/w) curcumin and 0.9 % (w/w) lecithin and Tween 80) was selected for *in vitro* simulated digestion analysis since it had the desired characteristics in terms of size (< 200 nm) and PDI (< 0.3), while encapsulating the highest quantity of curcumin. The ZP was also a good indicator of stability which was verified on the stability assessment. The particle size variation at day 30 was not considered relevant. The storage stability of this formulation was also measured at day 148, revealing no significant alterations in ZP (-20.4 ± 0.3 mV vs -18.7 ± 0.2 mV) and PDI (0.191 ± 0.008 vs 0.202 ± 0.026). The size of the nanoparticles remained below 200 nm,

however a significantly increase (179.2 ± 4.0 nm vs 190.5 ± 11.3 nm) was observed, comparatively with day 0.

4.3.2. *In vitro* digestion analysis

In vitro simulated gastrointestinal digestion is widely used for evaluating the gastrointestinal behaviour of food and pharmaceuticals. The utilization of a standardized model allows not only to enjoy the general advantages of *in vitro* digestion (e.g. fast, less expensive and no ethical restrictions) but also make it more reproducible due to the controlled conditions [132].

4.3.2.1. Particles characterization

Samples were collected at the end of each digestion phase and kept in ice, for particles' characterization in DLS. The *in vitro* digestion analysis was done in triplicates and the sample were characterize in terms of mean particles size, PDI and ζ -potential resulting in 9 measurements for each digestion phase. The outliers were removed based on box plot analysis, with a coefficient of 0.5 and the resultant mean values and standard deviation are indicated in Table 16.

Oral phase simulated conditions did not demonstrate a significant impact on mean particle size and PDI of SLNs with formulation E5, however a slight, but significant ($p > 0.05$) negative increase of ZP values was observed. The presence of salt ions on simulated salivary fluids as well as the slight pH alterations may have induced electrostatic screening effects [118], [132], [148].

Table 16 - Mean particle size, polydispersity index and ζ -Potential of the selected solid lipid nanoparticles (formulation E5), with respective standard deviation value, in the different *in vitro* gastrointestinal digestion phases. Different lowercase letters indicate statistically significant differences between digestion phases measurements

Digestion phase	Mean particle size (nm)	Polydispersity index	ζ -potential (mV)
Initial	$186.4^a \pm 5.1$	$0.202^a \pm 0.004$	$-19.0^a \pm 1.1$
Oral	$199.9^a \pm 6.3$	$0.275^{a,b} \pm 0.024$	$-22.9^b \pm 0.5$
Gastric	$2900.0^b \pm 2034.3$	$0.403^c \pm 0.064$	$2.6^c \pm 1.3$
Intestinal	$856.4^a \pm 144.5$	$0.363^{b,c} \pm 0.127$	$-17.7^a \pm 1.0$

During gastric phase, all measured parameters demonstrated significant differences comparatively with the previous phase and initial formulation. A significant size and PDI increase occurred at this digestion phase, possibly resulting from low pH and high ionic strength which decreases the repulsion between the SLNs and consequently, promotes aggregation through coalescence [149]. Furthermore, lower quality characterization can occur in samples with aggregates or in high salt conditions [116], [150]. ZP

demonstrated a positive value at the end of this digestion phase, which could be due to pH change to 3.0 as well as the strong ionic strength [118].

At the end of intestinal phase, mean particle size and PDI decreased significantly. ZP reverted to negative without significant difference when compared with the initial and oral phase, which could be due to the presence of various anionic colloidal particles after digestion. Gonçalves and colleagues (2020) observed a similar behaviour when SLNs composed of 3 % of beeswax, 1.5 % lecithin and 1.5 % Tween 80 were subjected to simulated *in vitro* digestion, although the size increase was smaller at the gastric and intestinal phases (from 145 to 489 nm) [149]. Sislioglu and colleagues (2021) analysed a formulation with 5 % (w/w) candelilla wax and 2 % (w/v) of Tween 80 under digestion, verifying an increase in the initial size from, approximately, 150 nm to 400 nm at the gastric phase, and the maintenance of a relatively large size in intestinal phase. At gastric phase, the ZP became close to zero.

4.3.2.2. Bioaccessibility, stability and effective bioavailability determination

The formulation E5 demonstrated a bioaccessibility of 67.4 ± 14.4 % which indicates that, more than half from of the curcumin initially present was in the micellar portion after digestion, which means that it is available for absorption. The curcumin stability at the end of *in vitro* digestion was 5.3 ± 0.4 % and, as result, the effective bioavailability was 3.6 ± 0.6 %. Commonly, free curcumin demonstrates poor oral bioavailability (< 1 %) due to significant metabolic transformations that occur during digestion therefore, the encapsulation of curcumin in the SLNs seems to increase curcumin's bioavailability [151]. Compared with the present work, Gonçalves and colleagues (2020) verified a smaller value of bioaccessibility (53 %) with a higher stability (29.3 %) when curcumin was incorporated in beeswax SLNs. In previous studies, SLNs demonstrated lower bioaccessibility when compared to particles produced with only liquid lipids or both types of lipids [149], [152]. The highly ordered structure of SLNs not only may promote the expulsion of some hydrophobic compounds during storage but also the burst release under acidic conditions [50], [92], [153]. These effects as well as the surface adsorption of curcumin onto SLNs expose it to the environmental conditions, making it more susceptible to degradation [153], [154]. Adytya and colleagues (2014) compared SLNs, nanostructured lipid carriers and nanoemulsions' influence on quercetin release, verifying that the tightly and densely packed lipids in SLNS may hinder the hydrophobic compound release [152].

The inhibition of the burst release effect in the gastric phase could allow the delivery of a larger amount of curcumin to the intestine. Baek and colleagues (2017) verified a curcumin *in vitro* release reduction from 40 % to 6 % when glyceryl monostearate based SLNs surface was modified with N-carboxymethyl

chitosan [155]. The utilization of surfactants, such as lecithin and Tween 80, also demonstrates to positively affect the intestinal membrane permeability and lipid particles affinity to intestinal membrane [38], [151].

The quantification of the free curcumin immediately before digestion analysis could allow to determine if nutraceutical expulsion from nanoparticles occurred during storage. Additionally, the assessment of *curcumin* release at each *in vitro* digestion step would be opportune to determine if a burst release occurs in gastric conditions. Moreover, surface modification of the candelilla wax formulation could be employed to attempt to increase the stability and the effective bioavailability, thus enhancing the beneficial effects of curcumin encapsulation.

4.3.2.3. SLNs digestibility

After simulated intestinal digestion, candelilla wax formulation demonstrated a total production of FFA of 14.25 ± 6.38 %. The physical state and fatty acids chain length of candelilla wax may hinder the enzymes access to SLNs surface reducing the hydrolyse rate and capacity [50], [152], [156]. Sislioglu and colleagues (2021) indicated that candelilla wax SLNs could not be hydrolysed since this wax is not digestible.

Some of the total FFA production could be due to the presence of lecithin, that is composed by a mixture of neutral lipids and phospholipids, and of the surfactant Tween 80. Heider and colleagues (2016) evaluated the digestion of pure surfactants, in the same concentration added to SLNs formulations, verifying that Tween 80 and the blank assay showed a significantly difference on the digestion degree [157]. It is also mentioned that misleading results could be obtained from the pH-stat method by overestimating the lipid digestion due to the formation of other acidic molecules (e.g lecithin and bile acids esters). Further studies should be developed on the relationship between the lower digestibility of SLNs, comparatively with other lipidic nanostructures, and the control of food intake [152].

4.2. Encapsulation of curcumin in pea protein isolate nanoparticles

4.2.1. Formulation optimization

4.2.1.1. Particles characterization

The development of pea protein nanoparticles intended to encapsulate the maximum amount of curcumin while complying to a reduced size (< 200 nm), small PDI (< 0.3) and high stability during storage. An initial formulation (E1) was produced as indicated before and a final concentration of 1 mg/mL of curcumin was added. Nanoparticles with a size of 3526.0 ± 620.9 nm, PDI of 0.869 ± 0.131

and ZP of -23.6 ± 3.6 mV were obtained. To infer if the increased size and PDI were due to the formulation procedure, three new essays were developed in parallel, and samples were analysed without curcumin added (Section 3.3.1.). Two of the formulations were started in a tenth of the total volume, and the remaining volume was added after CaCl_2 (E2) or after the two hours of agitation (E4). The third formulation had eighty-five percent of the total volume of the solution from the beginning (E3). Formulations E2 and E4 did not demonstrate statistical difference between them ($p < 0.05$) in terms of size (Figure 7.A) and PDI (Figure 7.B). However, the utilization of a larger initial volume led to a smaller size with larger PDI. In what concerns ZP, in all formulations as well as replicates, a significant difference was observed (Figure 7.C). This could be due to protein content variations in charged amino acids and the respective response to environmental conditions. Pea protein nanoparticles of size inferior to 200 nm and PDI lower than 0.35 were also obtained through pH shifting and thermal treatment, calcium induced cross-linking and potassium metabisulfite induced self-assembly [79], [81], [85]. It was concluded that the increased size and PDI verified on the initial formulation (E1) did not result from cross-linking process employed but from the curcumin addition procedure.

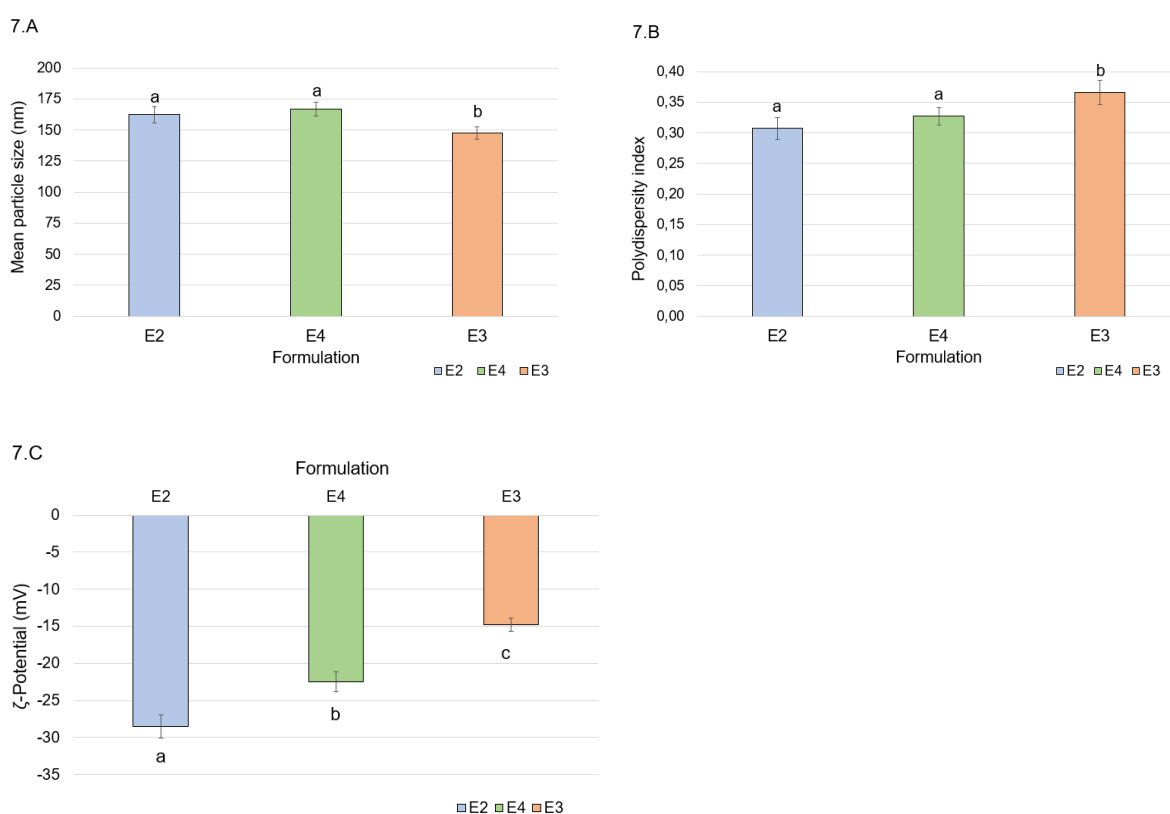


Figure 7 – Particles physical characterization of formulations E2, E3 and E4 of PPI nanoparticles. Mean particle size (A), polydispersity index (B) and ζ -Potential (C) were determined for each formulation. Formulation E2 and E4 correspond to the formulation's procedures initiated in a tenth of the total volume and in which the remaining water volume was added immediately or 2h after the calcium dichloride cross-linking. Formulation E3 has 85 % of the total volume from the beginning. Different lowercase letters indicate significant difference ($p > 0.05$) between formulations.

Hence, further concurrent experiments were conducted based on formulation E4 given that no statistical significance was determined in size and PDI comparatively with formulation E2, and a larger ZP was observed comparatively with E1. The ZP of E2 and E4 was similar, although statistically significant ($p > 0.5$) which could be due to experimental variations or slight protein composition differences. Five experiments were conducted to assess which factor was significant during curcumin's encapsulation, in this sense the curcumin concentration and ethanol percentage was altered (Table 17).

Table 17 – Experimental assays established conditions for determining the influence of final curcumin concentration (mg/mL) and final ethanol percentage (% w/v) on formulation E4

Formulation name	[Curcumin]_{final} (mg/mL)	[Ethanol]_{final} (% w/v)
T1	0.567	8.95
T2	0.567	0.00
T3	0.113	8.95
T4	0.000	8.95
T5	0.013	2.00

Note: In formulation T2, the curcumin powder was added directly to the pea protein isolate nanoparticles.

After 6 hours of agitation, the formulations' characteristics were evaluated through DLS (Figure 8). Formulation T4, in which only ethanol was added, demonstrated no statistical difference in all measured parameters ($p > 0.05$) comparatively with E4. Therefore, the ethanol concentration added must not have affected the initial formulation. When free curcumin was added (T2), an increase on size (166.9 ± 5.5 nm to 1491 ± 223.9 nm) and PDI (0.327 ± 0.014 to 0.991 ± 0.013) was verified. Formulation T1 and T2 demonstrated to be significantly differences in all parameters, hence the comparatively smaller particle size and PDI, and larger ZP of T1 could be an indicator that not only the curcumin concentration in the solution induced the particle size increase verified in the initial formulation but also that ethanol might have a stabilizing effect on the nanoparticles during encapsulation.

Formulations T1 and T3 wherein the curcumin concentration was altered, did not demonstrate significant differences in particles' size, although PDI and ZP were statistically different. Formulation T5 demonstrated interesting results since the size and ZP did not differ significantly from formulation E4. Additionally, the PDI value slight but significant increase could be a possible repercussion of curcumin's encapsulation. Okagu and colleagues (2021) also obtained particles with reduced size (166 nm) when a solution of curcumin with a final concentration of 0.01 mg/mL was added to PPI nanoparticles. The polydispersity of the particles was significantly higher (0.49) and the ZP more negative (-46.8 mV), comparing to the results of the present work.

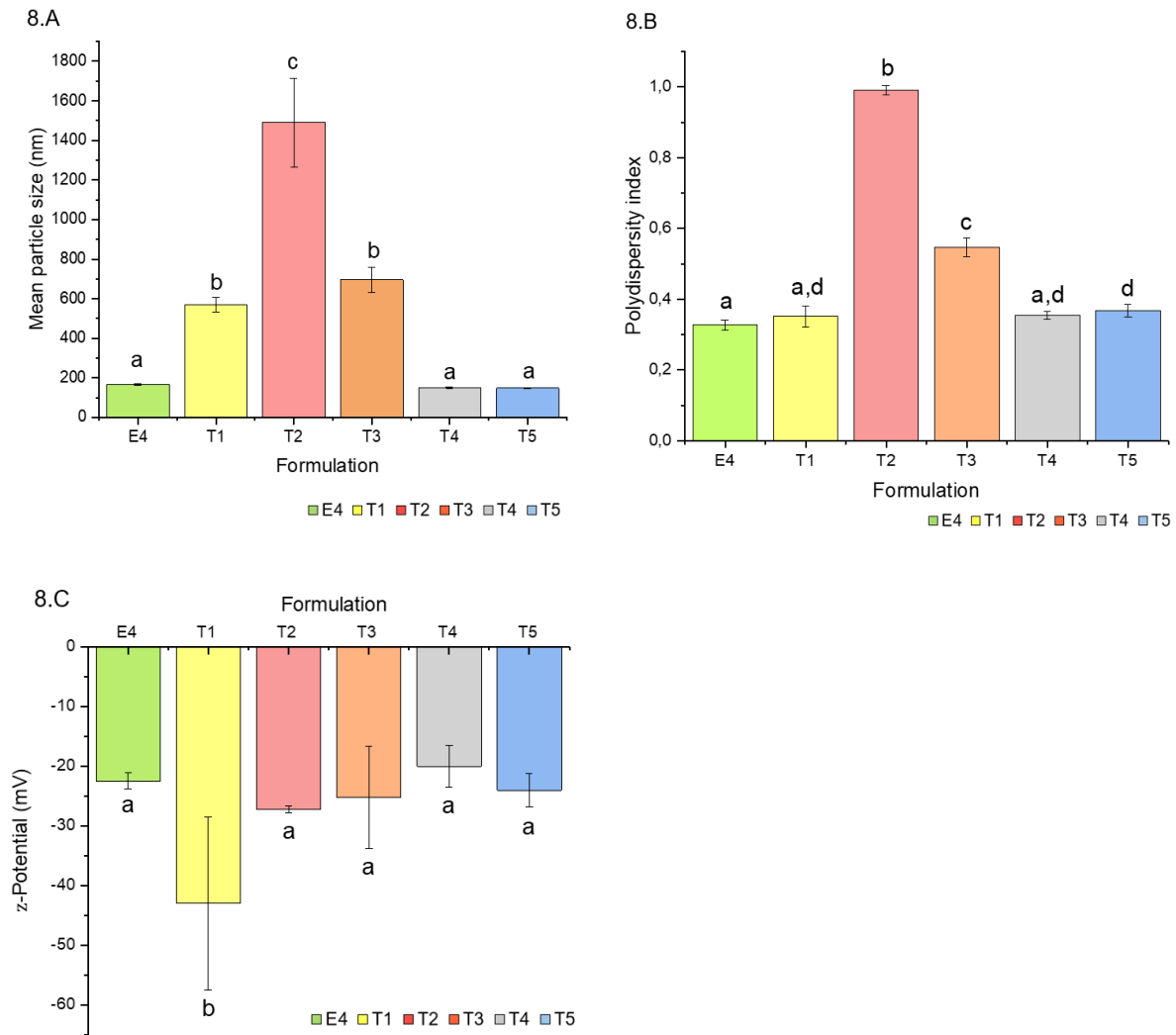


Figure 8 –Mean particle size (A), polydispersity index (B) and ζ -Potential (C) of different PPI nanoparticles' formulations. E4 indicates the formulation without curcumin added while experiments T1, T3 and T4 had a final curcumin concentration of, respectively, 0.567, 0.113 and 0.000 mg/mL in final ethanol concentration of 8.95 % (w/v). In experiment T2, a final curcumin concentration of 0.567 mg/mL was obtained by direct addition of curcumin powder. T5 has a final curcumin and ethanol composition of 0.013 mg/mL and 2 % (w/v). Different lowercase letters indicate significant difference ($p > 0.05$) between formulations.

In a posterior experiment, the effect of adding curcumin before or after the nanoparticle's formation was evaluated. The same amount of curcumin was added before the addition of CaCl_2 and after two hours of homogenization. No statistical difference was assessed in particles size and ZP from adding curcumin before or after CaCl_2 cross-linking (Figure 9), however, a decrease of PDI and EE from $0,373 \pm 0,011$ to $0,332 \pm 0,027$ and from 49.02 ± 1.39 to 37.55 ± 0.74 %, respectively was observed. The lower encapsulation efficiency could be due to curcumin and PPI repulsion in the inauspicious hydrophilic environment.

Guo and colleagues (2021) produced curcumin-loaded protein-surfactant complexes through pH driven method, obtaining a size of 135 and 145 nm with and without curcumin encapsulated [77]. This

phenomenon was associated with the expulsion of water from the complex by curcumin, a hydrophobic compound, leading to a more compact structure and smaller particle size [77], [158]. This effect was also noticeable in this experiment in which a lower concentration of curcumin was used.

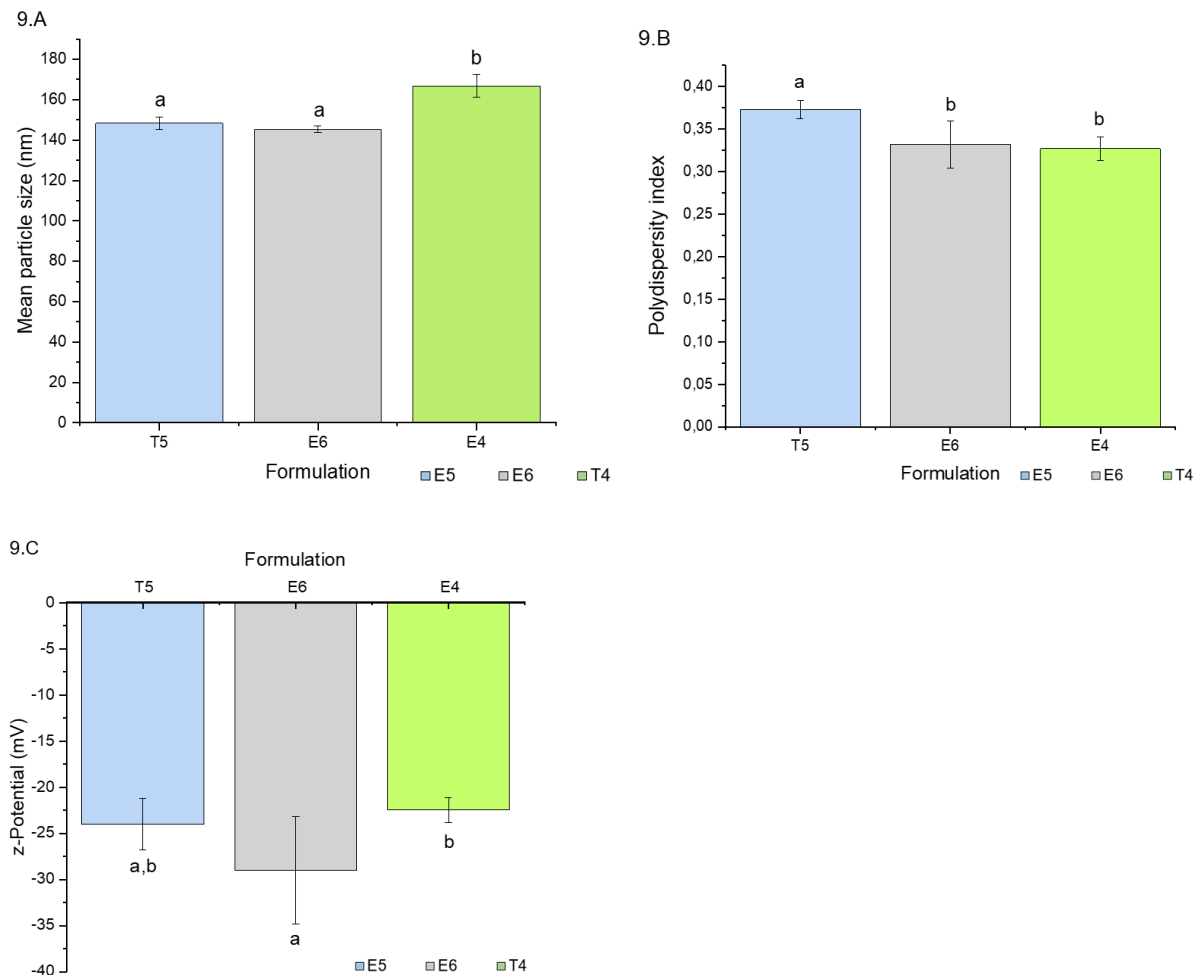


Figure 9 – PPI nanoparticles mean particle size (A), polydispersity index (B) and ζ -Potential (C). Formulation E4 (green) corresponds to the formulation without curcumin, E6 (grey) and T5 (blue) correspond to the formulation with 0.013 mg/mL of curcumin added, respectively, before and after nanoparticles cross-linking induced by CaCl_2 . Different lowercase letters indicate statistically significant differences between formulations measurements ($p > 0.05$).

Based on formulation T5, composed of 1 mg/mL of PPI, 1mM of CaCl_2 and 0.013 mg/mL of curcumin, the nutraceutical concentration was increased to 0.034 mg/mL and 0.078 mg/mL (i.e. formulation E8T1 and E8T2). E8T1 and E8T2 formulations exhibited reduced particle sizes (< 200 nm), PDI inferior to 0.4 and ZP values between -20 and -31 mV, an indicator of good stability (Figure 10). No statistically significant differences were observed on the measured parameters ($p > 0.05$) between the three formulations. Similar results were reported for curcumin encapsulated in zein nanoparticles stabilized with sodium caseinate and sodium alginate [159]. The authors demonstrated that zein nanoparticles'

particle size decreased at low concentrations of curcumin (from 171 to 136 nm), followed by an increase with curcumin concentration (to 151 nm). In the present work this connection was not evident.

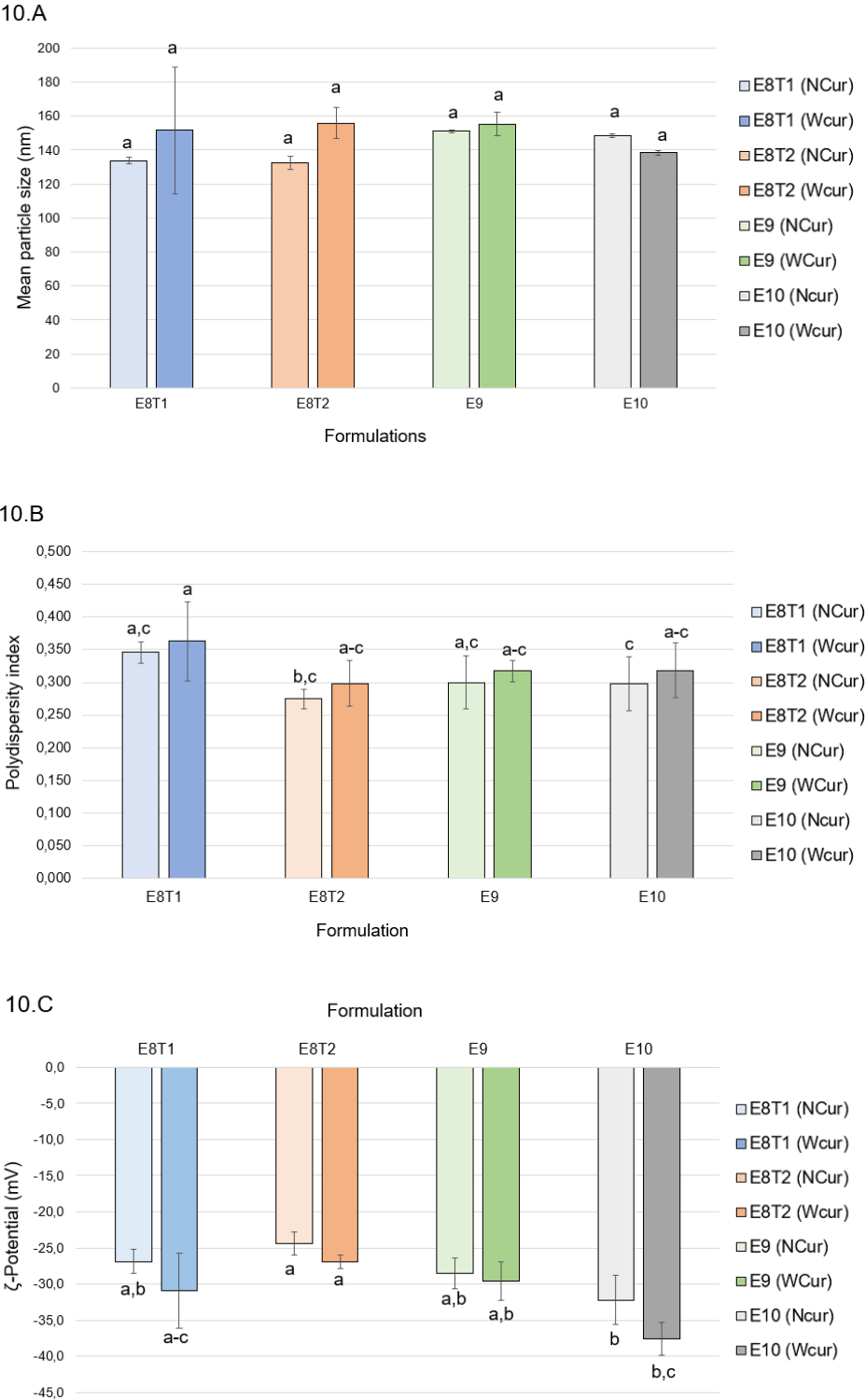


Figure 10 –Mean particle size (A), polydispersity index (B) and ζ -Potential (C) of different PPI nanoparticles' formulations. For formulations E8T1 (blue) and E8T2 (orange) crosslinking with CaCl_2 occurred at pH 7, with an initial curcumin concentration of 0.034 mg/mL and 0.078 mg/mL, respectively. For formulation E9 (green) and E10 (grey) crosslinking occurred at pH 8 and 9, respectively, and both formulations

had an initial concentration of curcumin of 0.034 mg/mL. The formulations without curcumin (NCur) are represented in lighter colour tone while the formulations with curcumin encapsulated (WCur) are represented in a darker colour tone. Different lowercase letters indicate statistically significant differences between formulations measurements ($p > 0.05$).

The alteration of pH from 7 to 8 and 9 during formulation process (i.e. E9 and E10), while maintaining curcumin's concentration of 0.034 mg/mL, did not demonstrate to significantly impact the size and PDI of the formulations comparatively with E8T1 (Figure 10). ZP of formulation E10, the largest value of all formulations, was significantly different from the one quantified for formulation E8T2, which could be due to the environmental conditions' influence on the particles' surface exposed amino acids.

4.2.1.2. Encapsulation efficiency

Since all four formulations (i.e. E8T1, E8T2, E9 and E10) demonstrated similar physicochemical characteristics, the EE was used to select which formulation should be used to proceed with the *in vitro* simulated gastrointestinal digestion (Table 18). Formulation E10 demonstrated the lowest EE, specifically of 54.74 ± 0.68 %. This value could be due to curcumin's degradation and/or repel due to the highly negative charge of the nanoparticles which is promoted at alkaline conditions [160]. E8T1 and E8T2 showed similar EE values, approximately 68 %, while E9 had the highest value (80.29 ± 8.54 %).

Table 18 –Curcumin's encapsulation efficiency. and respective standard deviation obtained for different formulations

Formulation name	Encapsulation efficiency (%)
E8T1	68.19 ± 0.82
E8T2	67.68 ± 0.23
E9	80.29 ± 8.54
E10	54.74 ± 0.68

Chen and colleagues (2015) verified an EE decrease from 98 to 78 % when curcumin concentration increased from 0.032 to 1.35 mg/mL Jiang and colleagues (2020), encapsulated curcumin in PPI-methoxyl pectin microcomplexes and verified a gradual decrease of EE, approximately 92 to 65 %, when curcumin's concentration increased from 25 to 300 $\mu\text{g/mL}$ [79]. Additionally, this effect was also evident in curcumin-loaded zein nanoparticles [158], [161]. This effect was not verified the present experiment when curcumin concentration was increased from 0.013 to 0.079 mg/mL (E5, E8T1 and E8T2).

The protein hydrophobicity influences the binding type and stability of hydrophobic nutraceuticals' encapsulation [72]. Okagu and coworkers (2021) demonstrated an encapsulation efficiency of approximately 35 % for native PPI nanoparticles, while the protein succinylation and coating with chitosan demonstrated to, respectively, decrease (i.e. 25 %) and increase (i.e. 85 %) the EE [162]. Curcumin binding affinity is majorly dependent on surface hydrophobicity, therefore the EE decrease was associated

with the three-fold decrease on surface hydrophobicity when PPI was succinated. Okagu and associates (2022) also determined that pea protein fractions soluble in alkaline and in salt conditions strongly bonded with curcumin, which reflected in EE increase from 43 % to 95 and 75 %, respectively [72]. This effect is supported by the increase of the surface hydrophobicity which promotes the interaction with curcumin and, consequently, improves the EE.

Similar effects in EE were observed by Guo and colleagues (2021) when anionic and non-ionic surfactants were complexed to PPI, since low quantities of surfactants increased the exposure of hydrophobic groups. The increase of surfactants concentration demonstrated to reduce EE when an anionic or a non-ionic surfactant and increase with the cationic surfactant. The latest effect was associated with curcumin and cationic surfactant electrostatic attraction.

4.2.1.3. Stability of PPI nanoparticles over time

Curcumin's stability on PPI nanoparticles is one of the most important factors to determine for commercial food and beverages applications [84]. The PPI nanoparticles stability over time was determined based on particles size, PDI and ZP (Figure 11). Formulation E8T1 demonstrated a significantly different size and PDI at day 1. Formulation E4T5 exhibited significant differences in all measured parameters while the PDI of formulation E6 destabilized at day 30. Formulation E8T2 suffered a significant increase in ZP from -24.4 ± 1.5 mV up to -34.2 ± 3.4 mV at day 30. Due to time restrictions, formulation E9 and E10 measurements were limited to day 13 and 15. E10's PDI and ZP significantly increased at day 15.

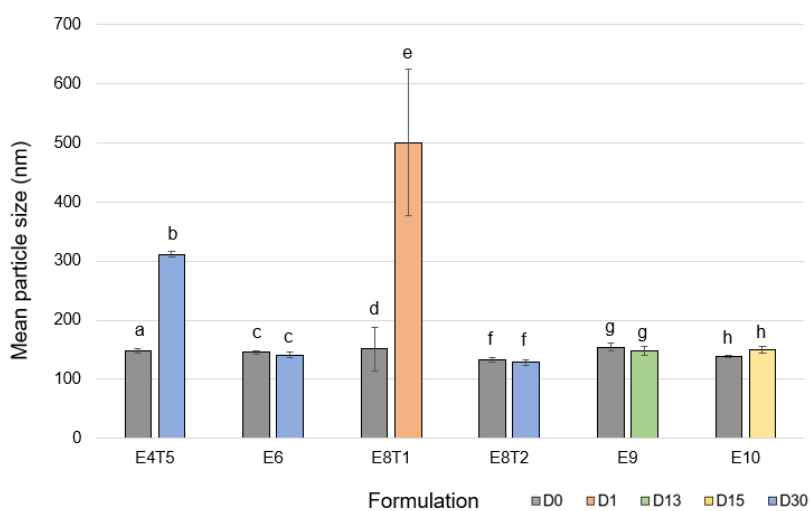
Although, formulation E9 demonstrated a slight but significant ($p > 0.05$) increase in PDI at day 13, this formulation was selected for *in vitro* static digestion analysis, since it demonstrated the desired characteristics as well as the highest EE, which was established as the selection parameter.

4.2.2. In vitro digestion of PPI nanoparticles

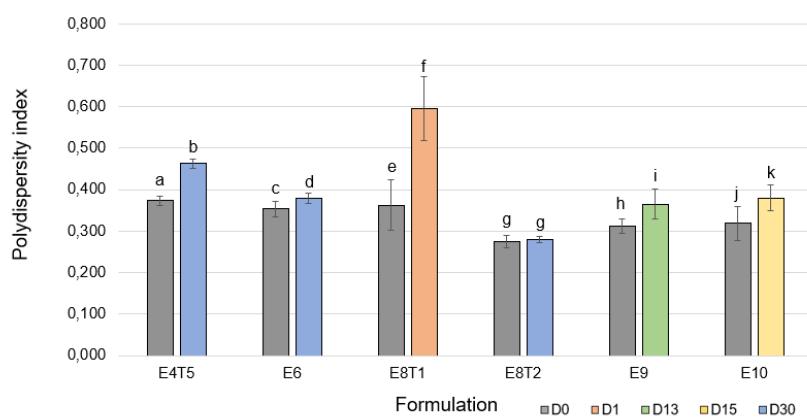
4.2.2.1. Particles characterization

Delivery systems are subjected to various pH and ionic strength conditions during digestion, therefore the alterations on particles characteristics must be evaluated. Formulation E9 was subjected to *in vitro* simulated digestion, as indicated in section 3.5.2. At the end of each digestion phase, samples were collected for particles' characterization through DLS technique (Table 19). In the oral phase, size and PDI alterations were insignificant, possible due to the short residence time [77]. The significant ZP reduction ($p < 0.05$) could be derived from slight pH adjustment and salts concentration.

11.A



11.B



11.C

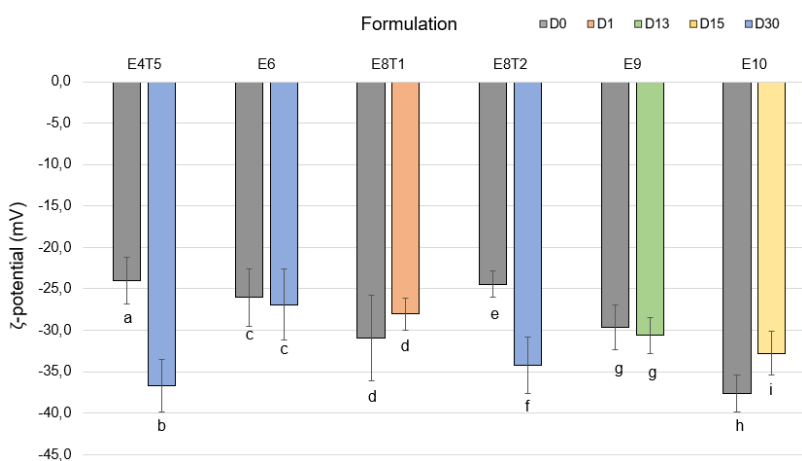


Figure 11 – Mean particle size (A), polydispersity index (B) and ζ -potential (C) of different PPI nanoparticles' formulations. The formulations E6 and E4T5 curcumin adding of 0.013 mg/mL occurred, respectively, before and after nanoparticles cross-linking induced by CaCl₂ at pH7. Formulations E8T1 and E8T2 crosslinking with CaCl₂ occurred at pH 7, with an initial curcumin concentration of 0.034 mg/mL and 0.078 mg/mL, correspondingly. For formulation E9 and E10 crosslinking occurred at pH 8 and 9, respectively, and both formulations had

an initial concentration of curcumin of 0.034 mg/mL. The measurement days are colour coded: dark grey as day 0, orange as day 1, green as day 13, yellow as day 15 and blue as day 30. Different lowercase letters indicate statistically significant differences between measurement days of the same formulation ($p < 0.05$).

The protein hydrophobicity alteration in the gastric phase, due to high ionic conditions and low pH, is a determining factor in the protein-curcumin bond strength and, subsequent complex stability [77], [162]. In the gastric phase, statistically significant alterations ($p > 0.05$) in particles size, PDI and ZP were observed. Wei and co-workers (2020) also verified a decrease in pea protein surface charge, when pH decreased from 7.0 to 3.5. The pH decrease, at the gastric phase was associated with particles' aggregation due to the pH proximity with the protein isoelectric point, and resulted in a decrease of particles' repulsion [86]. Similarly, particle size increase and ZP decrease results were associated with surface charge decrease of PPI-curcumin complexes and therefore weaker repulsive forces [77]. Furthermore, one of the major globulins in pea protein, Vicilin has its subunits held together by hydrophobic bonds, being susceptible to reversible aggregation in high ionic strength conditions [72].

Table 19 - Mean particle size, polydispersity index and ζ -Potential of PPI nanoparticles (formulation E9), in different *in vitro* gastrointestinal digestion phases. Different lowercase letters indicate statistically significant differences between digestion phases measurements ($p < 0.05$)

Digestion phase	Mean particle size (nm)	Polydispersity index	Z-Potential (mV)
Initial	154.6 ^a ± 6.5	0.312 ^a ± 0.018	-29.6 ^a ± 2.7
Oral	189.6 ^a ± 13.7	0.433 ^{a,b} ± 0.021	-16.5 ^b ± 0.9
Gastric	2407 ^b ± 2508.6	0.620 ^b ± 0.289	-0.8 ^c ± 9.2
Intestinal	1273 ^{a,b} ± 107.8	0.445 ^{a,b} ± 0.072	-12.7 ^b ± 1.8

In the intestinal phase, a significant size and PDI reduction were observed, possibly reflecting the ionic strength. Other studies with zein nanoparticles, demonstrated that particle size and ZP alteration was mainly due to pH, while at pH 7, the aggregation was induced by salt concentration [163], [164]. The decrease in particles' size could also be associated with bile salts strong emulsifying activity that can inhibit protein aggregation, as well as protein hydrolysis [158]. The ZP of oral and intestinal phase did not demonstrate a significant alteration, which could also be due to solutions' pH.

4.2.2.2. Curcumin's bioaccessibility, stability and effective bioavailability

The curcumin encapsulated in PPI nanoparticles (formulation E9) exhibited a bioaccessibility of 46.6 ± 27.7 %, a stability of 14.1 ± 2.9 % and an effective bioavailability of 5.0 ± 1.3 %. Chen and colleagues (2015) verified a curcumin bioaccessibility of nearly 60 and 90 % when heated and non-heated soy protein nanocomplexes were digested in the presence of enzymes. The bioaccessibility differences were attributed to differences in protein hydrolysis and protein aggregation. Both curcumin-loaded insect

protein and PPI nanoparticles revealed over 90 % of bioaccessibility [24], [162]. Lower curcumin' bioaccessibility values (10 – 33 %) were also reported in the literature for zein or whey protein nanoparticles [159], [165]–[167].

The digestion process involves drastic environmental conditions (e.g. low pH and high ionic strength) that can reverberate in nanoparticles' characteristics as well as curcumin's stability and bioaccessibility [168]. If the encapsulated curcumin is susceptible to the digestion process, the stability of curcumin could greatly impact the bioaccessibility [168]. Guo and colleagues (2021) verified that curcumin-PPI complexes released 70 % of curcumin at the gastric phase, while the surfactant-modified complexes mainly released curcumin at the intestinal phase, therefore improving curcumin stability [77].

4.2.2.3. PPI nanoparticles digestibility

The PPI nanoparticles' DH was determined in an auto titration unit, in which a minimum volume of HCl (0.5 M) was added to keep the solution's pH (pH=3.0). The equation 10 was employed to determine DH based on the acid volume added, the h_{tot} of 9.6 and an experimental α_{COOH} of 0.9993. Formulation E9 showed a DH of 70.1 ± 16.6 % (Figure 12).

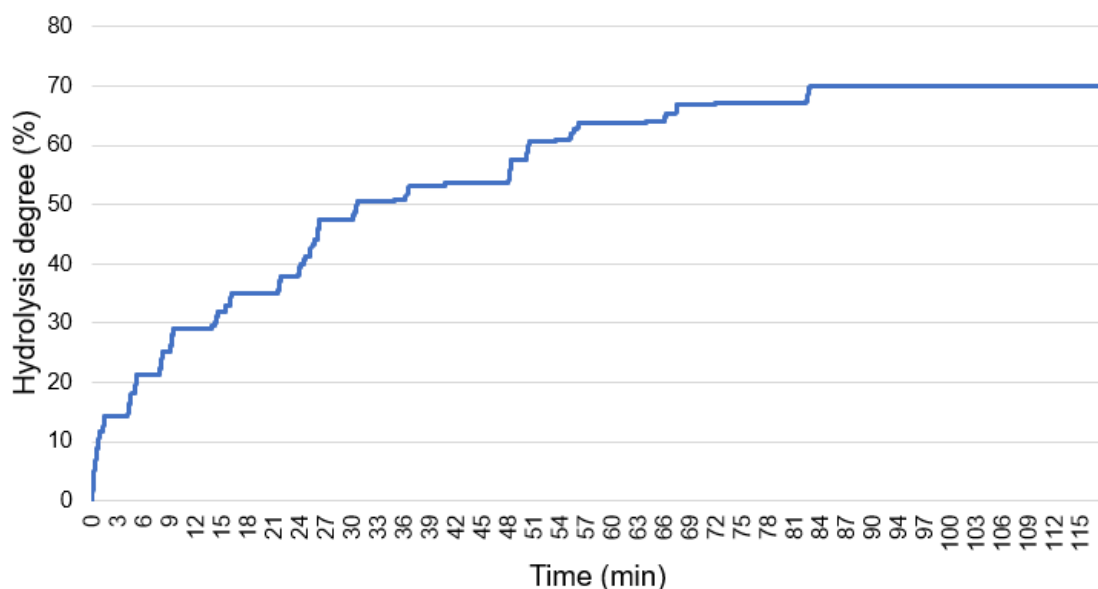


Figure 12 – Degree of hydrolysis over time of PPI nanoparticles (formulation E9) at gastric phase of *in vitro* digestion.

PPI is mainly composed of 7S and 11S globulins, specifically legumin (11S), vicilin (7S) and convicilin (7S) [169]. On one hand, Globulins 11S tend to not be completely digested and broken into aminoacids, on the other hand protease susceptibility and/or *in vitro* digestibility of vicilins was positively affected by heat-induced denaturation and negatively affected by protein aggregation [168], [170], [171]. The

susceptibility to proteolysis is also influenced by slight variations in the 7S proteins of different legume species, resulting in different conformational changes under similar environments [172].

Opazo-Navarrete and colleagues (2019) determined the DH of quinoa protein isolate and protein enriched fractions obtaining values inferior to 16 %. The authors observed a diminishment of DH on heat treated samples, which induced protein denaturation and, consequently, led to aggregation in the gastric phase [173]. In green peas, this effect was confirmed by undesirable conformational changes of vicilin upon heating, increasing the protein resistance to hydrolysis [172].

Jimenez-Munoz and colleagues (2023) evaluated the DH of two commercially available PPI, during *in vitro* digestion. The DH of both samples during gastric phase, approximately 18 and 25 %, are not in accordance with results of this work. Moreover, the experimental values obtained demonstrate more similarity to those of commercially available PPI after 15 min of intestinal digestion (approximately 70 %) [174]. Furthermore, the experimental work demonstrated higher similarity in DH value to other legumin proteins. Anitha and colleagues (2019) It was reported DH values of 70 % and 80 % for two pigeon pea as well as 80 % and 89 % for chickpea protein flours [175]. In another study, a DH of 50 % was reported for pigeon pea protein isolate [176]. It should be noticed that DH variability was observed within same legume species.

Carbonaro and colleagues (2012) reported the digestibility of the plant proteins of common bean (74 %), chickpea (77 %), lentil (79 %), soybean (80 %), barley (78 %) and emmer wheat (83 %) [177]. In this work, was also observed that the utilization of autoclaving induced more severe changes in legume protein's secondary structure than dry heating, which culminated in higher digestion value of legume proteins due to destabilization of β -sheets structures. β -sheets in their native state tend to form stable complexed which are resistant to proteolysis [177]. Nevertheless, the digestibility of proteins can also be affected by the complexation with phenolic compounds, enhancing or diminishing it [168]. Chen and colleagues (2015) demonstrated that curcumin encapsulation in heated and non-heated treated soy protein nanoparticles increased the protein digestibility.

5. Conclusions and future remarks

5.1. Conclusions

The focus of this work was to develop sustainable BBNDs based on plants, characterize them and evaluating their behaviour during *in vitro* digestion. Ideally, the developed nanoparticles should have a reduced size (< 200 nm) and PDI (< 0.3) as well as a ZP close to ± 30 mV, to indicate a good stability, and high EE. Two different plant-based nanodelivery systems have been developed to encapsulate curcumin: a lipidic system - solid lipid nanoparticles and a protein-based system - pea protein nanoparticles. For the development of SLNs, an experimental design was created with the intention of designing an optimal formulation base on the connections established between independent and dependent variables by CCRD methodology. Due to experimental design low quality, this was not possible. However, the statistical treatment with MLR and PLS analysis allowed to conclude that curcumin, lecithin and Tween 80 concentrations significantly influenced the dependent variables variability. The conjoint effect of the four factors obtained by PLS analysis could only explain 59.2 % of the dependent variable's variability, therefore the remaining variance originated from non-analysed variables. Tween 80 concentration alterations demonstrated a high correlation with ZP variability in the evaluated conditions. Formulation E5, composed of 4.2 % candelilla wax, 0.7 % curcumin and 0.9 % lecithin and Tween 80, was selected from the experimental design since it demonstrated a reduced size (179.2 ± 4.0 nm) and PDI (0.191 ± 0.008) and a ZP value (-20.4 ± 0.3 mV) indicative of a good stability. Simultaneously, this formulation exhibited a high EE (100.0 ± 0.6 %). During the stability assessment, a small but significant size change was noticed, although no statistically significant alterations were evident after 60 days of storage. Additionally, the reduction of surfactants concentration (Tween 80) comparatively with the initial formulation positively contributes to the sustainable aspect of this work. During digestion of the SLNs, significant alterations in all parameters were evident during gastric phase, possibly due to aggregation induced by pH reduction and high ionic strength. At the end of intestinal phase, the bioaccessibility, stability and effective bioavailability of curcumin was determined, obtaining as result 67.4 ± 14.4 %, 5.3 ± 0.4 % and 3.6 ± 0.6 %, respectively. The low stability could be caused by a burst release of curcumin during gastric phase, a recurring event with SLNs, or from a premature exposure of curcumin to environmental conditions as it can be adsorbed on SLNs surface. In what concerns to the FFA release, a value of 14.25 ± 6.38 % was obtained, which is higher that indicated in the literature since candelilla wax is considered non-digestible.

Pea protein nanoparticles were developed, and different tests have been performed to optimize their formulation, such as the increase in curcumin concentration (from 0.013 mg/mL to 0.078 mg/mL) and

pH alteration (from pH 7 to pH 9). At pH 7, the alteration of curcumin concentration was not reflected in statistical differences in particle characteristics. At pH 9, there was an increase in the ZP level and a reduction in encapsulation efficiency compared to tests with the same curcumin concentration and different pH. Formulation E9 (pea protein concentration of 1.0 mg/mL, CaCl₂ of 1 mM produced at pH 8 and with curcumin concentration of 0.034 mg/mL) was selected to proceed with the *in vitro* digestion analysis since it demonstrated a size of 154.6 ± 6.5 nm, PDI 0.312 ± 0.018 and ZP -29.6 ± 2.7 mV. Additionally, it offered the highest EE of 80.29 ± 8.54 % among the formulations tested. At day 13 the size and ZP were maintained and the PDI showed a slight but significant increase. During digestion, a significant increase in the characteristics of the PPI nanoparticles in the gastric phase of *in vitro* digestion has occurred, similarly with candelilla wax SLNs digestion behaviour. At the end of *in vitro* digestion, a bioaccessibility of 46.6 ± 27.7 %, a stability of 14.1 ± 2.9 % and effective bioavailability of 5.0 ± 1.3 % was observed. The digestibility of PPI nanoparticles was 70.1 ± 16.6 %.

Both BBNDs developed attained the proposed physical characteristics, with low particle size, high EE, and stability over time and relatively high bioaccessibility. Pea protein nanoparticles demonstrated better results during *in vitro* digestion in what refers to nanoparticles digestibility and, most importantly, in effective bioavailability. Nonetheless, comparatively with SLNs, this formulation demonstrated a wither PDI, and the storage stability was determined in a shorter interval. Although, the nanoparticles SLNs and PPI nanoparticles demonstrated to aggregate at acid conditions, it is still possible to employ these formulations in food and beverages products with neutral pH, such as nutritional beverages or dairy-based products.

5.2. Future remarks

The BBNDs developed demonstrated promising results and further formulations improvements may be employed to enhance their effective bioavailability, while maintaining the desired physical characteristics. Further experimentation may include:

1. Experimental design development to determine independent variables influence on dependent variables variability.
2. Evaluation of nanostructures' stability under different storage conditions and for longer periods of time.
3. Quantification of free curcumin alteration during storage, and consequently the impact on EE.
4. Incorporation of nanostructures in food matrixes with different characteristics, and evaluation of their physical properties.

5. Lecithin and Tween 80 digestibility during *in vitro* digestion to evaluate their interference on SLNs digestibility values.
6. Determination of PPI nanoparticles' DH without encapsulated curcumin, to assess the influence of this polyphenol during digestion.
7. Quantification of curcumin release in each digestion step, identifying a possible burst release during gastric phase.
8. Determination of nanostructures' digestibility during gastric and intestinal phase.
9. Surface modification or coating of nanostructures with the purpose of increasing the bioaccessibility, stability and effective bioavailability of curcumin.
10. Comparative studies of curcumin's bioaccessibility in *in vitro* and *in vivo* digestion systems.
11. *In vitro* cytotoxicology assays of assess the nanostructures' toxicity.

6. References

- [1] A. K. Pandey, P. Kumar, P. Singh, N. N. Tripathi, and V. K. Bajpai, "Essential oils: Sources of antimicrobials and food preservatives," *Front. Microbiol.*, vol. 7, no. JAN, pp. 1–14, 2017.
- [2] R. F. S. Gonçalves, J. T. Martins, C. M. M. Duarte, A. A. Vicente, and A. C. Pinheiro, "Advances in nutraceutical delivery systems: from formulation design for bioavailability enhancement to efficacy and safety evaluation," *Trends Food Sci. Technol.*, vol. 78, no. June, pp. 270–291, 2018.
- [3] S. A. Ashraf *et al.*, "Innovations in nanoscience for the sustainable development of food and agriculture with implications on health and environment," *Sci. Total Environ.*, vol. 768, p. 144990, 2021.
- [4] Z.-L. L. Wan, J. Guo, and X.-Q. Q. Yang, "Plant protein-based delivery systems for bioactive ingredients in foods," *Food Funct.*, vol. 6, no. 9, pp. 2876–2889, 2015.
- [5] L. de Souza Simões, D. A. Madalena, A. C. Pinheiro, J. A. Teixeira, A. A. Vicente, and Ó. L. Ramos, "Micro- and nano bio-based delivery systems for food applications: in vitro behavior," *Adv. Colloid Interface Sci.*, vol. 243, pp. 23–45, 2017.
- [6] A. P. Maurya, J. Chauhan, D. K. Yadav, R. Gangwar, and V. K. Maurya, "Nutraceuticals and their impact on human health," in *Preparation of Phytopharmaceuticals for the Management of Disorders*, Elsevier Inc., 2021, pp. 229–254.
- [7] S. M. Dizaj *et al.*, "Curcumin nanoformulations: Beneficial nanomedicine against cancer," *Phyther. Res.*, vol. 36, no. 3, pp. 1156–1181, 2022.
- [8] A. B. Kunnumakkara *et al.*, "Curcumin, the golden nutraceutical: multitargeting for multiple chronic diseases," *Br. J. Pharmacol.*, vol. 174, no. 11, pp. 1325–1348, 2017.
- [9] S. Doktorovova, E. B. Souto, and A. M. Silva, "Hansen solubility parameters (HSP) for prescreening formulation of solid lipid nanoparticles (SLN): in vitro testing of curcumin-loaded SLN in MCF-7 and BT-474 cell lines," *Pharm. Dev. Technol.*, vol. 23, no. 1, pp. 96–105, 2018.
- [10] S. Khorasani, M. Danaei, and M. R. Mozafari, "Nanoliposome technology for the food and nutraceutical industries," *Trends Food Sci. Technol.*, vol. 79, no. July 2018, pp. 106–115, 2018.
- [11] X. Li and T. Wang, "Plant proteins make a difference," *J. Agric. Food Res.*, vol. 9, no. April, p. 100318, 2022.
- [12] A. Gomes and P. J. D. A. Sobral, "Plant protein-based delivery systems: An emerging approach for increasing the efficacy of lipophilic bioactive compounds," *Molecules*, vol. 27, no. 1, pp. 1–30, 2022.
- [13] L. I. Atanase, "Micellar Drug Delivery Systems Based on Natural Biopolymers," *Polymers (Basel)*, vol. 13, no. 3, pp. 1–33, Feb. 2021.
- [14] H. R. Sharif *et al.*, "Current progress in the utilization of native and modified legume proteins as emulsifiers and encapsulants – a review," *Food Hydrocoll.*, vol. 76, pp. 2–16, 2018.
- [15] Z. L. Wan, J. Guo, and X. Q. Yang, "Plant protein-based delivery systems for bioactive ingredients in foods," *Food Funct.*, vol. 6, no. 9, pp. 2876–2889, 2015.
- [16] K. Sampathkumar, K. X. Tan, and S. C. J. Loo, "Developing nano-delivery systems for agriculture and food applications with nature-derived polymers," *iScience*, vol. 23, no. 5, p.

101055, 2020.

- [17] M. H. Abd El-Salam and S. El-Shibiny, *Natural biopolymers as nanocarriers for bioactive ingredients used in food industries*. Elsevier Inc., 2016.
- [18] D. Paolino *et al.*, “Nanonutraceuticals: the new frontier of supplementary food,” *Nanomaterials*, vol. 11, no. 3, pp. 1–20, 2021.
- [19] A. C. Pinheiro, R. F. Gonçalves, D. A. Madalena, and A. A. Vicente, “Towards the understanding of the behavior of bio-based nanostructures during in vitro digestion,” *Curr. Opin. Food Sci.*, vol. 15, pp. 79–86, 2017.
- [20] S. Gottardo *et al.*, “Towards safe and sustainable innovation in nanotechnology: State-of-play for smart nanomaterials,” *NanoImpact*, vol. 21, no. January, 2021.
- [21] A. Santini *et al.*, “Nutraceuticals: opening the debate for a regulatory framework,” *Br. J. Clin. Pharmacol.*, vol. 84, no. 4, pp. 659–672, 2018.
- [22] B. Kumar and K. Smita, *Scope of Nanotechnology in Nutraceuticals*. Elsevier Inc., 2017.
- [23] T. Tsuda, “Curcumin as a functional food-derived factor: degradation products, metabolites, bioactivity, and future perspectives,” *Food Funct.*, vol. 9, no. 2, pp. 705–714, 2018.
- [24] O. D. Okagu, O. Verma, D. J. McClements, and C. C. Udenigwe, “Utilization of insect proteins to formulate nutraceutical delivery systems: encapsulation and release of curcumin using mealworm protein-chitosan nano-complexes,” *Int. J. Biol. Macromol.*, vol. 151, pp. 333–343, 2020.
- [25] M. Zhao *et al.*, “Current innovations in nutraceuticals and functional foods for intervention of non-alcoholic fatty liver disease,” *Pharmacol. Res.*, vol. 166, no. November 2020, p. 105517, 2021.
- [26] A. Rauf, M. Imran, H. A. R. Sulera, B. Ahmad, D. G. Peters, and M. S. Mubarak, “A comprehensive review of the health perspectives of resveratrol,” *Food Funct.*, vol. 8, no. 12, pp. 4284–4305, 2017.
- [27] P. Fernández-Palanca, F. Fondevila, C. Méndez-Blanco, M. J. Tuñón, J. González-Gallego, and J. L. Mauriz, “Antitumor effects of quercetin in hepatocarcinoma in vitro and in vivo models: a systematic review,” *Nutrients*, vol. 11, no. 12, pp. 1–31, 2019.
- [28] M. Eggersdorfer and A. Wyss, “Carotenoids in human nutrition and health,” *Arch. Biochem. Biophys.*, vol. 652, no. June, pp. 18–26, 2018.
- [29] A. Rajasekaran, G. Sivagnanam, and R. Xavier, “Nutraceuticals as therapeutic agents : a review,” *Res. J. Pharm. Tech*, vol. 1, no. 4, pp. 328–340, 2008.
- [30] S. Kumar, B. Sharma, P. Bhadwal, P. Sharma, and N. Agnihotri, *Lipids as Nutraceuticals: a Shift in Paradigm*, no. January. 2018.
- [31] G. G. L. Gianfranceschi, G. G. L. Gianfranceschi, L. Quassinti, and M. Bramucci, “Biochemical requirements of bioactive peptides for nutraceutical efficacy,” *J. Funct. Foods*, vol. 47, no. June, pp. 252–263, 2018.
- [32] G. R. Gibson *et al.*, “Expert consensus document: the international scientific association for probiotics and prebiotics (ISAPP) consensus statement on the definition and scope of

- prebiotics," *Nat. Rev. Gastroenterol. Hepatol.*, vol. 14, no. 8, pp. 491–502, 2017.
- [33] C. Hill *et al.*, "Expert consensus document: the international scientific association for probiotics and prebiotics consensus statement on the scope and appropriate use of the term probiotic," *Nat. Rev. Gastroenterol. Hepatol.*, vol. 11, no. 8, pp. 506–514, 2014.
- [34] M. Pateiro *et al.*, "Nanoencapsulation of promising bioactive compounds to improve their absorption, stability, functionality and the appearance of the final food products," *Molecules*, vol. 26, no. 6, p. 1547, 2021.
- [35] M. Rodriguez-Concepcion *et al.*, "A global perspective on carotenoids: metabolism, biotechnology, and benefits for nutrition and health," *Prog. Lipid Res.*, vol. 70, no. April, pp. 62–93, 2018.
- [36] K. Zaheer and M. Humayoun Akhtar, "An updated review of dietary isoflavones: nutrition, processing, bioavailability and impacts on human health," *Crit. Rev. Food Sci. Nutr.*, vol. 57, no. 6, pp. 1280–1293, 2017.
- [37] D. Barreca *et al.*, "Food flavonols: nutraceuticals with complex health benefits and functionalities," *Trends Food Sci. Technol.*, no. September 2020, 2021.
- [38] X. Y. Mao, M. Z. Jin, J. F. Chen, H. H. Zhou, and W. L. Jin, "Live or let die: neuroprotective and anti-cancer effects of nutraceutical antioxidants," *Pharmacol. Ther.*, vol. 183, no. October 2017, pp. 137–151, 2018.
- [39] A. M. Alves-Santos, C. S. A. Sugizaki, G. C. Lima, and M. M. V. Naves, "Prebiotic effect of dietary polyphenols: a systematic review," *J. Funct. Foods*, vol. 74, no. August, p. 104169, 2020.
- [40] L. Křížová, K. Dadáková, J. Kašparovská, and T. Kašparovský, "Isoflavones," *Molecules*, vol. 24, no. 6, 2019.
- [41] S. J. Choi and D. J. McClements, "Nanoemulsions as delivery systems for lipophilic nutraceuticals: strategies for improving their formulation, stability, functionality and bioavailability," *Food Sci. Biotechnol.*, vol. 29, no. 2, pp. 149–168, 2020.
- [42] H. Rostamabadi, S. R. Falsafi, and S. M. Jafari, "Starch-based nanocarriers as cutting-edge natural cargos for nutraceutical delivery," *Trends Food Sci. Technol.*, vol. 88, no. December 2018, pp. 397–415, 2019.
- [43] K. S. Swanson *et al.*, "The International Scientific Association for Probiotics and Prebiotics (ISAPP) consensus statement on the definition and scope of synbiotics," *Nat. Rev. Gastroenterol. Hepatol.*, vol. 17, no. 11, pp. 687–701, 2020.
- [44] G. Novik and V. Savich, "Beneficial microbiota. probiotics and pharmaceutical products in functional nutrition and medicine," *Microbes Infect.*, vol. 22, no. 1, pp. 8–18, 2020.
- [45] D. Mohanty, S. Misra, S. Mohapatra, and P. S. Sahu, "Prebiotics and synbiotics: recent concepts in nutrition," *Food Biosci.*, vol. 26, no. November 2017, pp. 152–160, 2018.
- [46] M. A. Núñez-Sánchez, F. M. Herisson, G. L. Cluzel, and N. M. Caplice, "Metabolic syndrome and synbiotic targeting of the gut microbiome," *Curr. Opin. Food Sci.*, vol. 41, pp. 60–69, 2021.
- [47] S. M. T. Gharibzahedi and S. M. Jafari, "The importance of minerals in human nutrition: Bioavailability, food fortification, processing effects and nanoencapsulation," *Trends Food Sci. Technol.*, vol. 62, pp. 119–132, 2017.

- [48] S. Khorasani *et al.*, *Recent Trends in the Nanoencapsulation Processes for Food and Nutraceutical Applications*. Elsevier, 2021.
- [49] D. J. McClements, "Recent advances in the production and application of nano-enabled bioactive food ingredients," *Curr. Opin. Food Sci.*, vol. 33, no. December 2019, pp. 85–90, 2020.
- [50] K. Sislioglu, C. E. Gumus, C. K. W. Koo, I. Karabulut, and D. J. McClements, "In vitro digestion of edible nanostructured lipid carriers: impact of a Candelilla wax gelator on performance," *Food Res. Int.*, vol. 140, no. December 2020, p. 110060, 2021.
- [51] T. A. Comunian, M. P. Silva, and C. J. F. Souza, "The use of food by-products as a novel for functional foods: their use as ingredients and for the encapsulation process," *Trends Food Sci. Technol.*, vol. 108, no. November 2020, pp. 269–280, 2021.
- [52] R. N. Roy, A. Finck, G. J. Blair, and H. L. S. Tandon, *Plant nutrition for food security. In FAO fertilizer and plant nutrition bulletin*. 2006.
- [53] K. Kaderides and A. M. Goula, "Encapsulation of pomegranate peel extract with a new carrier material from orange juice by-products," *J. Food Eng.*, vol. 253, pp. 1–13, 2019.
- [54] M. Azam, M. Saeed, I. Pasha, and M. Shahid, "A prebiotic-based biopolymeric encapsulation system for improved survival of *Lactobacillus rhamnosus*," *Food Biosci.*, vol. 37, p. 100679, 2020.
- [55] D. Santoyo-Aleman, L. T. Sanchez, and C. C. Villa, "Citric-acid modified banana starch nanoparticles as a novel vehicle for β -carotene delivery," *J. Sci. Food Agric.*, vol. 99, no. 14, pp. 6392–6399, Nov. 2019.
- [56] Y. Panahi, A. Khosroshhi, A. Sahebkar, and H. R. Heidari, "Impact of Cultivation Condition and Media Content on *Chlorella vulgaris* Composition," *Adv. Pharm. Bull.*, vol. 9, no. 2, pp. 182–194, 2019.
- [57] K.-I. Jang and H. G. Lee, "Stability of chitosan nanoparticles for L-Ascorbic Acid during heat treatment in aqueous solution," *J. Agric. Food Chem.*, vol. 56, no. 6, pp. 1936–1941, Mar. 2008.
- [58] J. Gomez-Estaca, M. P. Balaguer, R. Gavara, and P. Hernandez-Munoz, "Formation of zein nanoparticles by electrohydrodynamic atomization: effect of the main processing variables and suitability for encapsulating the food coloring and active ingredient curcumin," *Food Hydrocoll.*, vol. 28, no. 1, pp. 82–91, 2012.
- [59] R. Penalva, I. Esparza, M. Agüeros, C. J. Gonzalez-Navarro, C. Gonzalez-Ferrero, and J. M. Irache, "Casein nanoparticles as carriers for the oral delivery of folic acid," *Food Hydrocoll.*, vol. 44, pp. 399–406, 2015.
- [60] N. Walia and L. Chen, "Pea protein based vitamin D nanoemulsions: Fabrication, stability and in vitro study using Caco-2 cells," *Food Chem.*, vol. 305, p. 125475, 2020.
- [61] C. Bustos-Garza, J. Yáñez-Fernández, and B. E. Barragán-Huerta, "Thermal and pH stability of spray-dried encapsulated astaxanthin oleoresin from *Haematococcus pluvialis* using several encapsulation wall materials," *Food Res. Int.*, vol. 54, no. 1, pp. 641–649, 2013.
- [62] A. Pezeshki, B. Ghanbarzadeh, M. Mohammadi, I. Fathollahi, and H. Hamishehkar,

- “Encapsulation of vitamin A palmitate in Nanostructured Lipid Carrier (NLC)-effect of surfactant concentration on the formulation properties,” *Adv Pharm Bull*, vol. 4, no. 6, pp. 563–568, Dec. 2014.
- [63] D. F. Silva, C. S. Favaro-Trindade, G. A. Rocha, and M. Thomazini, “MICROENCAPSULATION OF LYCOPENE BY GELATIN–PECTIN COMPLEX COACERVATION,” *J. Food Process. Preserv.*, vol. 36, no. 2, pp. 185–190, Apr. 2012.
- [64] A. Jain, D. Thakur, G. Ghoshal, O. P. Katare, and U. S. Shivhare, “Microencapsulation by complex coacervation using whey protein isolates and gum Acacia: an approach to preserve the functionality and controlled release of β -carotene,” *Food Bioprocess Technol.*, vol. 8, no. 8, pp. 1635–1644, 2015.
- [65] Z. Zhang *et al.*, “Encapsulation of curcumin in polysaccharide-based hydrogel beads: impact of bead type on lipid digestion and curcumin bioaccessibility,” *Food Hydrocoll.*, vol. 58, pp. 160–170, 2016.
- [66] M. P. Silva, F. L. Tulini, F. E. Matos-Jr, M. G. Oliveira, M. Thomazini, and C. S. Fávoro-Trindade, “Application of spray chilling and electrostatic interaction to produce lipid microparticles loaded with probiotics as an alternative to improve resistance under stress conditions,” *Food Hydrocoll.*, vol. 83, pp. 109–117, 2018.
- [67] O. C. Paucar, F. L. Tulini, M. Thomazini, J. C. C. Balieiro, E. M. J. A. Pallone, and C. S. Favaro-Trindade, “Production by spray chilling and characterization of solid lipid microparticles loaded with vitamin D3,” *Food Bioprod. Process.*, vol. 100, pp. 344–350, 2016.
- [68] E. A. Cortés-Morales, G. Mendez-Montealvo, and G. Velazquez, “Polysaccharide-protein complexes as encapsulation materials: a review,” *Adv. Colloid Interface Sci.*, vol. 292, p. 102398, 2021.
- [69] D. J. McClements, E. A. Decker, Y. Park, and J. Weiss, *Structural design principles for delivery of bioactive components in nutraceuticals and functional foods*, vol. 49, no. 6. 2009.
- [70] O. D. Okagu, B. Wang, C. Acquah, and C. C. Udenigwe, *Protein-based nanodelivery systems for food applications*. Elsevier, 2018.
- [71] N. Reddy and M. Rapisarda, “Properties and applications of nanoparticles from plant proteins,” *Materials (Basel)*, vol. 14, no. 13, pp. 1–41, 2021.
- [72] O. D. Okagu and C. C. Udenigwe, “Molecular Interactions of Pea Globulin, Albumin and Glutelin With Curcumin: Formation and Gastric Release Mechanisms of Curcumin-loaded Bio-nanocomplexes,” *Food Biophys.*, vol. 17, no. 1, pp. 10–25, 2022.
- [73] M. B. J. Maviah *et al.*, “Food Protein-Based Nanodelivery Systems for Hydrophobic and Poorly Soluble Compounds,” *AAPS PharmSciTech*, vol. 21, no. 3, 2020.
- [74] N. P. Aditya, Y. G. Espinosa, and I. T. Norton, “Encapsulation systems for the delivery of hydrophilic nutraceuticals: Food application,” *Biotechnol. Adv.*, vol. 35, no. 4, pp. 450–457, 2017.
- [75] L. Le Roux *et al.*, “Are faba bean and pea proteins potential whey protein substitutes in infant formulas? An in vitro dynamic digestion approach,” *Foods*, vol. 9, no. 3, 2020.
- [76] Y. Ji, C. Han, E. Liu, X. Li, X. Meng, and B. Liu, “Pickering emulsions stabilized by pea protein

- isolate-chitosan nanoparticles: fabrication, characterization and delivery EPA for digestion in vitro and in vivo," *Food Chem.*, vol. 378, p. 132090, 2022.
- [77] Q. Guo *et al.*, "Fabrication and characterization of curcumin-loaded pea protein isolate-surfactant complexes at neutral pH," *Food Hydrocoll.*, vol. 111, no. 17, p. 106214, 2021.
- [78] S. M. T. Gharibzahedi and B. Smith, "Legume proteins are smart carriers to encapsulate hydrophilic and hydrophobic bioactive compounds and probiotic bacteria: A review," *OMPRESHENSIVE Rev. FOOD Sci. FOOD Saf.*, vol. 20, no. 2, pp. 1250–1279, 2021.
- [79] J. Yi, H. Huang, Y. Liu, Y. Lu, Y. Fan, and Y. Zhang, "Fabrication of curcumin-loaded pea protein-pectin ternary complex for the stabilization and delivery of β -carotene emulsions," *Food Chem.*, vol. 313, no. August 2019, p. 126118, 2020.
- [80] X.-L. Li, W.-J. Liu, B.-C. Xu, and B. Zhang, "Simple method for fabrication of high internal phase emulsions solely using novel pea protein isolate nanoparticles: Stability of ionic strength and temperature," *Food Chem.*, vol. 370, p. 130899, 2022.
- [81] X. L. Li, Q. T. Xie, W. J. Liu, B. C. Xu, and B. Zhang, "Self-Assembled Pea Protein Isolate Nanoparticles with Various Sizes: Explore the Formation Mechanism," *J. Agric. Food Chem.*, vol. 69, no. 34, pp. 9905–9914, 2021.
- [82] C. D. Doan and S. Ghosh, "Formation and stability of pea proteins nanoparticles using ethanol-induced desolvation," *Nanomaterials*, vol. 9, no. 7, 2019.
- [83] E. Schulman, W. Wu, and D. Liu, "Two-dimensional zeolite materials: Structural and acidity properties," *Materials (Basel)*, vol. 13, no. 8, 2020.
- [84] H. Zhang, T. Wang, F. He, and G. Chen, "Fabrication of pea protein-curcumin nanocomplexes via microfluidization for improved solubility, nano-dispersibility and heat stability of curcumin: Insight on interaction mechanisms," *Int. J. Biol. Macromol.*, vol. 168, pp. 686–694, 2021.
- [85] Y. Fan, X. Zeng, J. Yi, and Y. Zhang, "Fabrication of pea protein nanoparticles with calcium-induced cross-linking for the stabilization and delivery of antioxidative resveratrol," *Int. J. Biol. Macromol.*, vol. 152, pp. 189–198, 2020.
- [86] Y. Wei *et al.*, "Core-shell pea protein-carboxymethylated corn fiber gum composite nanoparticles as delivery vehicles for curcumin," *Carbohydr. Polym.*, vol. 240, no. January, p. 116273, 2020.
- [87] C. Montes, M. J. Villaseñor, and Á. Ríos, "Analytical control of nanodelivery lipid-based systems for encapsulation of nutraceuticals: achievements and challenges," *Trends Food Sci. Technol.*, vol. 90, no. February, pp. 47–62, 2019.
- [88] F. Keivani Nahr, B. Ghanbarzadeh, H. Hamishehkar, and H. Samadi Kafil, "Food grade nanostructured lipid carrier for cardamom essential oil: preparation, characterization and antimicrobial activity," *J. Funct. Foods*, vol. 40, pp. 1–8, 2018.
- [89] O. Tarhan and M. J. Spotti, "Nutraceutical delivery through nano-emulsions: General aspects, recent applications and patented inventions," *Colloids Surfaces B Biointerfaces*, vol. 200, no. December 2020, 2021.
- [90] M. M. Mehanna and A. T. Mneimneh, "Formulation and applications of lipid-based nanovehicles: Spotlight on self-emulsifying systems," *Adv. Pharm. Bull.*, vol. 11, no. 1, pp. 56–67, 2021.
- [91] R. Chutoprapat, P. Kopongpanich, and L. W. Chan, "A Mini-Review on Solid Lipid Nanoparticles

- and Nanostructured Lipid Carriers: Topical Delivery of Phytochemicals for the Treatment of Acne Vulgaris,” *Molecules*, vol. 27, no. 11, 2022.
- [92] A. Beloqui, A. del Pozo-Rodríguez, A. Isla, A. Rodríguez-Gascón, and M. Á. Solinís, “Nanostructured lipid carriers as oral delivery systems for poorly soluble drugs,” *J. Drug Deliv. Sci. Technol.*, vol. 42, pp. 144–154, 2017.
- [93] Y. Soleimani, S. A. H. Goli, A. Shirvani, A. Elmizadeh, and A. G. Marangoni, “Wax-based delivery systems: Preparation, characterization, and food applications,” *Comprehensive Reviews in Food Science and Food Safety*, vol. 19, no. 6. pp. 2994–3030, 2020.
- [94] D. J. McClements and B. Öztürk, “Utilization of nanotechnology to improve the handling, storage and biocompatibility of bioactive lipids in food applications,” *Foods*, vol. 10, no. 2, pp. 1–17, 2021.
- [95] V. Nahum and A. J. Domb, “Recent developments in solid lipid microparticles for food ingredients delivery,” *Foods*, vol. 10, no. 2, pp. 1–25, 2021.
- [96] X. Hong, Q. Zhao, J. Chen, T. Ye, L. Fan, and J. Li, “Fabrication and characterization of oleogels and temperature-responsive water-in-oil emulsions based on candelilla (*Euphorbia cerifera*) wax,” *Food Chem.*, vol. 397, no. July, p. 133677, 2022.
- [97] D. Sahu, D. Bharti, D. Kim, P. Sarkar, and K. Pal, “Variations in microstructural and physicochemical properties of candelilla wax/rice bran oil–derived oleogels using sunflower lecithin and soya lecithin,” *Gels*, vol. 7, no. 4, 2021.
- [98] A. D. Palaparthi, “Potential applications of lipid nanoparticles in edible packaging and nutraceutical delivery,” *Rutgers Univ. Community Repos.*, 2016.
- [99] N. E. Aranda-Ledesma *et al.*, “Candelilla wax: Prospective suitable applications within the food field,” *Lwt*, vol. 159, 2022.
- [100] I. C. Núñez-García *et al.*, “Candelilla Wax Extracted by Traditional Method and an Ecofriendly Process: Assessment of Its Chemical, Structural and Thermal Properties,” *Molecules (Basel, Switzerland)*, vol. 27, no. 12. Departamento de Ings. Química-Bioquímica, TecNM/Instituto Tecnológico de Durango, Blvd. Felipe Pescador 1830 Ote., Nueva Vizcaya, Durango 34080, Durango, Mexico., p. 3735, 2022.
- [101] M. A. Cerqueira *et al.*, “Design of Bio-nanosystems for Oral Delivery of Functional Compounds,” *Food Eng. Rev.*, vol. 6, no. 1–2, pp. 1–19, 2014.
- [102] IKA-Werke GmbH & Co. KG, “IKA ULTRA-TURRAX ® T 25 digital.” pp. 1–10.
- [103] X. Hua, S. Xu, M. Wang, Y. Chen, H. Yang, and R. Yang, “Effects of high-speed homogenization and high-pressure homogenization on structure of tomato residue fibers,” *Food Chem.*, vol. 232, pp. 443–449, 2017.
- [104] H. C. Mai, T. S. V. Nguyen, T. H. N. Le, D. C. Nguyen, and L. G. Bach, “Evaluation of conditions affecting properties of Gac (*Momordica Cochinchinensis* Spreng) oil-loaded solid lipid nanoparticles (SLNs) synthesized using high-speed homogenization process,” *Processes*, vol. 7, no. 2, 2019.
- [105] M. D. Triplett and J. F. Rathman, “Optimization of β -carotene loaded solid lipid nanoparticles preparation using a high shear homogenization technique,” *J. Nanoparticle Res.*, vol. 11, no. 3,

- pp. 601–614, 2009.
- [106] E. B. Souto, S. Doktorovova, A. Zielinska, and A. M. Silva, “Key production parameters for the development of solid lipid nanoparticles by high shear homogenization,” *Pharm. Dev. Technol.*, vol. 24, no. 9, pp. 1181–1185, 2019.
- [107] A. Kharlamova, T. Nicolai, and C. Chassenieux, “Calcium-induced gelation of whey protein aggregates: Kinetics, structure and rheological properties,” *Food Hydrocoll.*, vol. 79, pp. 145–157, 2018.
- [108] A. I. Bourbon, R. N. Pereira, L. M. Pastrana, A. A. Vicente, and M. A. Cerqueira, “Protein-based nanostructures for food applications,” *Gels*, vol. 5, no. 1, pp. 1–17, 2019.
- [109] A. C. Alting, *Cold gelation of globular proteins*. 2003.
- [110] S. M. Jafari, A. Faridi Esfanjani, I. Katouzian, and E. Assadpour, *Release, characterization, and safety of nanoencapsulated food ingredients*. Elsevier Inc., 2017.
- [111] S. Castro Coelho, B. Nogueiro Estevinho, and F. Rocha, “Encapsulation in food industry with emerging electrohydrodynamic techniques: electrospinning and electrospraying – A review,” *Food Chem.*, vol. 339, no. July 2020, p. 127850, 2021.
- [112] M. Danaei *et al.*, “Impact of particle size and polydispersity index on the clinical applications of lipidic nanocarrier systems,” *Pharmaceutics*, vol. 10, no. 2, pp. 1–17, 2018.
- [113] H. Nolte, C. Schilde, and A. Kwade, “Determination of particle size distributions and the degree of dispersion in nanocomposites,” *Compos. Sci. Technol.*, vol. 72, no. 9, pp. 948–958, 2012.
- [114] S. Falke and C. Betzel, “Dynamic Light Scattering (DLS),” in *Radiation in Bioanalysis*, Springer International Publishing, 2019, pp. 173–193.
- [115] F. Caputo *et al.*, “Measuring Particle Size Distribution by Asymmetric Flow Field Flow Fractionation: A Powerful Method for the Preclinical Characterization of Lipid-Based Nanoparticles,” *Mol. Pharm.*, vol. 16, no. 2, pp. 756–767, 2019.
- [116] F. Babick, “Dynamic light scattering (DLS),” in *Characterization of Nanoparticles: Measurement Processes for Nanoparticles*, Elsevier Inc., 2019, pp. 137–172.
- [117] D. S. Auld, J. Inglese, and J. L. Dahlin, “Assay Interference by Aggregation Flowchart Abbreviations Introduction and Background Introduction,” *The Assay Guidance Manual*, no. NIH. pp. 1–28, 2017.
- [118] G. W. Lu and P. Gao, “Emulsions and Microemulsions for Topical and Transdermal Drug Delivery,” in *Handbook of Non-Invasive Drug Delivery Systems*, 2010, pp. 59–94.
- [119] A. J. Shnoudeh *et al.*, *Synthesis, Characterization, and Applications of Metal Nanoparticles*. Elsevier Inc., 2019.
- [120] K. Rajpoot and R. K. Tekade, “Chapter 10 - Microemulsion as drug and gene delivery vehicle: an inside story,” in *Advances in Pharmaceutical Product Development and Research*, R. K. B. T.-D. D. S. Tekade, Ed. Academic Press, 2019, pp. 455–520.
- [121] J. Nsor-Atindana, M. Yu, H. D. Goff, M. Chen, and F. Zhong, “Analysis of kinetic parameters and mechanisms of nanocrystalline cellulose inhibition of α -amylase and α -glucosidase in simulated digestion of starch,” *Food Funct.*, vol. 11, no. 5, pp. 4719–4731, 2020.

- [122] E. Joseph and G. Singhvi, "Chapter 4 - Multifunctional nanocrystals for cancer therapy: a potential nanocarrier," A. M. B. T.-N. for D. D. and T. Grumezescu, Ed. William Andrew Publishing, 2019, pp. 91–116.
- [123] D. J. McClements, "Advances in edible nanoemulsions: Digestion, bioavailability, and potential toxicity," *Prog. Lipid Res.*, vol. 81, no. December 2020, p. 101081, 2021.
- [124] I. Sensoy, "A review on the food digestion in the digestive tract and the used in vitro models," *Curr. Res. Food Sci.*, vol. 4, no. April, pp. 308–319, 2021.
- [125] C. Li, W. Yu, P. Wu, and X. D. Chen, "Current in vitro digestion systems for understanding food digestion in human upper gastrointestinal tract," *Trends Food Sci. Technol.*, vol. 96, pp. 114–126, 2020.
- [126] L. Egger *et al.*, "The harmonized INFOGEST in vitro digestion method : from knowledge to action," *Food Res. Int.*, vol. 88, pp. 217–225, 2016.
- [127] A. Brodkorb *et al.*, "INFOGEST static in vitro simulation of gastrointestinal food digestion," *Nat. Protoc.*, vol. 14, no. 4, pp. 991–1014, 2019.
- [128] D. J. L. Mat, T. Cattenoz, I. Souchon, C. Michon, and S. Le Feunteun, "Monitoring protein hydrolysis by pepsin using pH-stat: in vitro gastric digestions in static and dynamic pH conditions," *Food Chem.*, vol. 239, pp. 268–275, 2018.
- [129] S. Kheradmandnia, E. Vashghani-Farahani, M. Nosrati, and F. Atyabi, "Preparation and characterization of ketoprofen-loaded solid lipid nanoparticles made from beeswax and carnauba wax," *Nanomedicine Nanotechnology, Biol. Med.*, vol. 6, no. 6, pp. 753–759, 2010.
- [130] S. N. Politis, P. Colombo, G. Colombo, and D. M. Rekkas, "Design of experiments (DoE) in pharmaceutical development," *Drug Dev. Ind. Pharm.*, vol. 43, no. 6, pp. 889–901, 2017.
- [131] T. K. Gündođdu, Ęrem Deniz, G. alıřkan, E. S. řahin, and N. Azbar, "Experimental design methods for bioengineering applications," *Crit. Rev. Biotechnol.*, vol. 36, no. 2, pp. 368–388, 2016.
- [132] M. Minekus *et al.*, "A standardised static in vitro digestion method suitable for food – an international consensus," *Food Funct.*, vol. 5, no. 6, pp. 1113–1124, 2014.
- [133] W. Liu, J. Wang, D. J. McClements, and L. Zou, "Encapsulation of β -carotene-loaded oil droplets in caseinate/alginate microparticles: Enhancement of carotenoid stability and bioaccessibility," *J. Funct. Foods*, vol. 40, pp. 527–535, 2018.
- [134] O. H. LOWRY, N. J. ROSEBROUGH, A. L. FARR, and R. J. RANDALL, "Protein measurement with the Folin phenol reagent.," *J. Biol. Chem.*, vol. 193, no. 1, pp. 265–275, 1951.
- [135] G. Cukor, Z. Jurković, and M. Sekulić, "Rotatable central composite design of experiments versus Taguchi method in the optimization of turning," *Metallurgija*, vol. 50, no. 1, pp. 17–20, 2011.
- [136] P. Roback and J. Legler, *Beyond Multiple Linear Regression*. CRC Press, 2021.
- [137] D. M. Pirouz, "An Overview of Partial Least Squares," *SSRN Electron. J.*, no. October 2006, 2012.
- [138] T. Smith *et al.*, "Application of smart solid lipid nanoparticles to enhance the efficacy of 5-

- fluorouracil in the treatment of colorectal cancer,” *Sci. Rep.*, vol. 10, no. 1, pp. 1–14, 2020.
- [139] M. Wang *et al.*, “Particle size measurement using dynamic light scattering at ultra-low concentration accounting for particle number fluctuations,” *Materials (Basel)*, vol. 14, no. 19, 2021.
- [140] U. Badilli, M. Gumustas, B. Uslu, and S. A. Ozkan, “Lipid-based nanoparticles for dermal drug delivery,” in *Organic Materials as Smart Nanocarriers for Drug Delivery*, Elsevier Inc., 2018, pp. 369–413.
- [141] M. I. Rodrigues and A. F. Lemma, *Planejamento de experimentos e otimização de processos*, 3rd ed. Caritas Editora, 2014.
- [142] R. K. Subedi, K. W. Kang, and H. K. Choi, “Preparation and characterization of solid lipid nanoparticles loaded with doxorubicin,” *Eur. J. Pharm. Sci.*, vol. 37, no. 3–4, pp. 508–513, 2009.
- [143] M. A. Schubert and C. C. Müller-Goymann, “Characterisation of surface-modified solid lipid nanoparticles (SLN): Influence of lecithin and nonionic emulsifier,” *Eur. J. Pharm. Biopharm.*, vol. 61, no. 1–2, pp. 77–86, 2005.
- [144] M. Alanchari *et al.*, “Optimization and antimicrobial efficacy of curcumin loaded solid lipid nanoparticles against foodborne bacteria in hamburger patty,” *J. Food Sci.*, vol. 86, no. 6, pp. 2242–2254, 2021.
- [145] I. Katouzian, A. Faridi Esfanjani, S. M. Jafari, and S. Akhavan, “Formulation and application of a new generation of lipid nano-carriers for the food bioactive ingredients,” *Trends Food Sci. Technol.*, vol. 68, pp. 14–25, 2017.
- [146] R. Shtay, C. P. Tan, and K. Schwarz, “Development and characterization of solid lipid nanoparticles (SLNs) made of cocoa butter: A factorial design study,” *J. Food Eng.*, vol. 231, pp. 30–41, 2018.
- [147] M. Üner, “Characterization and imaging of solid lipid nanoparticles and nanostructured lipid carriers,” in *Handbook of Nanoparticles*, Springer International Publishing, 2015, pp. 118–137.
- [148] R. M. Bao, H. M. Yang, C. M. Yu, W. F. Zhang, and J. B. Tang, “An efficient protocol to enhance the extracellular production of recombinant protein from *Escherichia coli* by the synergistic effects of sucrose, glycine, and Triton X-100,” *Protein Expr. Purif.*, vol. 126, pp. 9–15, 2016.
- [149] R. F. S. Gonçalves *et al.*, “Lipid-based nanostructures as a strategy to enhance curcumin bioaccessibility: behavior under digestion and cytotoxicity assessment,” *Food Res. Int.*, vol. 143, no. October 2020, 2021.
- [150] A. Parupudi, S. H. R. Mulagapati, and J. A. Subramony, “Chapter 1 - Nanoparticle technologies: Recent state of the art and emerging opportunities,” P. Kesharwani and K. K. B. T.-N. T. Singh, Eds. Academic Press, 2022, pp. 3–46.
- [151] V. Kakkar, S. K. Muppu, K. Chopra, and I. P. Kaur, “Curcumin loaded solid lipid nanoparticles: An efficient formulation approach for cerebral ischemic reperfusion injury in rats,” *Eur. J. Pharm. Biopharm.*, vol. 85, no. 3 PART A, pp. 339–345, 2013.
- [152] N. P. Aditya *et al.*, “Development and evaluation of lipid nanocarriers for quercetin delivery: A comparative study of solid lipid nanoparticles (SLN), nanostructured lipid carriers (NLC), and

- lipid nanoemulsions (LNE)," *LWT - Food Sci. Technol.*, vol. 59, no. 1, pp. 115–121, 2014.
- [153] C. Qian, E. A. Decker, H. Xiao, and D. J. McClements, "Impact of lipid nanoparticle physical state on particle aggregation and β -carotene degradation: Potential limitations of solid lipid nanoparticles," *Food Res. Int.*, vol. 52, no. 1, pp. 342–349, 2013.
- [154] R. S. Mulik, J. Mönkkönen, R. O. Juvonen, K. R. Mahadik, and A. R. Paradkar, "Transferrin mediated solid lipid nanoparticles containing curcumin: Enhanced in vitro anticancer activity by induction of apoptosis," *Int. J. Pharm.*, vol. 398, no. 1, pp. 190–203, 2010.
- [155] J. S. Baek and C. W. Cho, "Surface modification of solid lipid nanoparticles for oral delivery of curcumin: Improvement of bioavailability through enhanced cellular uptake, and lymphatic uptake," *Eur. J. Pharm. Biopharm.*, vol. 117, pp. 132–140, 2017.
- [156] Y. Li *et al.*, "A comparative study: The impact of different lipid extraction methods on current microalgal lipid research," *Microb. Cell Fact.*, vol. 13, no. 1, pp. 1–9, 2014.
- [157] M. Heider, G. Hause, and K. Mäder, "Does the commonly used pH-stat method with back titration really quantify the enzymatic digestibility of lipid drug delivery systems? A case study on solid lipid nanoparticles (SLN)," *Eur. J. Pharm. Biopharm.*, vol. 109, pp. 194–205, 2016.
- [158] L. Dai, Y. Wei, C. Sun, L. Mao, D. J. McClements, and Y. Gao, "Development of protein-polysaccharide-surfactant ternary complex particles as delivery vehicles for curcumin," *Food Hydrocoll.*, vol. 85, no. 17, pp. 75–85, 2018.
- [159] Q. Liu, Y. Jing, C. Han, H. Zhang, and Y. Tian, "Encapsulation of curcumin in zein/caseinate/sodium alginate nanoparticles with improved physicochemical and controlled release properties," *Food Hydrocoll.*, vol. 93, no. August 2018, pp. 432–442, 2019.
- [160] O. Naksuriya, M. J. Vansteenberg, J. S. Torano, S. Okonogi, and W. E. Hennink, "A kinetic degradation study of curcumin in its free form and loaded in polymeric micelles," *AAPS J.*, vol. 18, no. 3, pp. 777–787, 2016.
- [161] A. Patel, Y. Hu, J. K. Tiwari, and K. P. Velikov, "Synthesis and characterisation of zein-curcumin colloidal particles," *Soft Matter*, vol. 6, no. 24, pp. 6192–6199, 2010.
- [162] O. D. Okagu, J. Jin, and C. C. Udenigwe, "Impact of succinylation on pea protein-curcumin interaction, polyelectrolyte complexation with chitosan, and gastrointestinal release of curcumin in loaded-biopolymer nano-complexes," *J. Mol. Liq.*, vol. 325, p. 115248, 2021.
- [163] K. Hu and D. J. McClements, "Fabrication of biopolymer nanoparticles by antisolvent precipitation and electrostatic deposition: Zein-alginate core/shell nanoparticles," *Food Hydrocoll.*, vol. 44, pp. 101–108, 2015.
- [164] L. Dai, H. Zhou, Y. Wei, Y. Gao, and D. J. McClements, "Curcumin encapsulation in zein-rhamnolipid composite nanoparticles using a pH-driven method," *Food Hydrocoll.*, vol. 93, no. February, pp. 342–350, 2019.
- [165] S. Hu, T. Wang, M. L. Fernandez, and Y. Luo, "Development of tannic acid cross-linked hollow zein nanoparticles as potential oral delivery vehicles for curcumin," *Food Hydrocoll.*, vol. 61, pp. 821–831, 2016.
- [166] J. Xue, Y. Zhang, G. Huang, J. Liu, M. Slavin, and L. (Lucy) Yu, "Zein-caseinate composite nanoparticles for bioactive delivery using curcumin as a probe compound," *Food Hydrocoll.*, vol.

83, pp. 25–35, 2018.

- [167] M. Mohammadian, M. Salami, F. Alavi, S. Momen, Z. Emam-Djomeh, and A. A. Moosavi-Movahedi, “Fabrication and Characterization of Curcumin-Loaded Complex Coacervates Made of Gum Arabic and Whey Protein Nanofibrils,” *Food Biophys.*, vol. 14, no. 4, pp. 425–436, 2019.
- [168] F. P. Chen, B. S. Li, and C. H. Tang, “Nanocomplexation between Curcumin and Soy Protein Isolate: Influence on Curcumin Stability/Bioaccessibility and in Vitro Protein Digestibility,” *J. Agric. Food Chem.*, vol. 63, no. 13, pp. 3559–3569, 2015.
- [169] H.-T. Chang, C.-Y. Lin, L.-S. Hsu, and S.-T. Chang, “Thermal degradation of linalool-chemotype Cinnamomum osmophloeum leaf Essential Oil and its stabilization by microencapsulation with β -cyclodextrin,” *Molecules*, vol. 26, no. 2, p. 409, 2021.
- [170] M. Adachi *et al.*, “Crystal structure of soybean 11S globulin: Glycinin A3B4 homohexamer,” *Proc. Natl. Acad. Sci.*, vol. 100, no. 12, pp. 7395–7400, Jun. 2003.
- [171] D. Drulyte and V. Orlien, “The effect of processing on digestion of legume proteins,” *Foods*, vol. 8, no. 6, 2019.
- [172] S. S. Deshpande and S. Damodaran, “Structure-Digestibility Relationship of Legume 7S Proteins,” *J. Food Sci.*, vol. 54, no. 1, pp. 108–113, 1989.
- [173] M. Opazo-Navarrete, D. Tagle Freire, R. M. Boom, and A. E. M. Janssen, “The Influence of Starch and Fibre on In Vitro Protein Digestibility of Dry Fractionated Quinoa Seed (Riobamba Variety),” *Food Biophys.*, vol. 14, no. 1, pp. 49–59, 2019.
- [174] L. Jiménez-Munoz, M. Torp Nielsen, L. Roman, and M. Corredig, “Variation of in vitro digestibility of pea protein powder dispersions from commercially available sources,” *Food Chem.*, vol. 401, no. September 2022, 2023.
- [175] S. Anitha, M. Govindaraj, and J. Kane-Potaka, “Balanced amino acid and higher micronutrients in millets complements legumes for improved human dietary nutrition,” *Cereal Chem.*, vol. 97, no. 1, pp. 74–84, 2020.
- [176] A. Tapal, G. E. Vegarud, A. Sreedhara, and P. Kaul Tiku, “Nutraceutical protein isolate from pigeon pea (: *Cajanus cajan*) milling waste by-product: Functional aspects and digestibility,” *Food Funct.*, vol. 10, no. 5, pp. 2710–2719, 2019.
- [177] M. Carbonaro, P. Maselli, and A. Nucara, “Relationship between digestibility and secondary structure of raw and thermally treated legume proteins: A Fourier transform infrared (FT-IR) spectroscopic study,” *Amino Acids*, vol. 43, no. 2, pp. 911–921, 2012.

7. Annexes

Annex 1 – Calibration curve of curcumin in ethanol - absorbance at 430 nm versus curcumin concentration

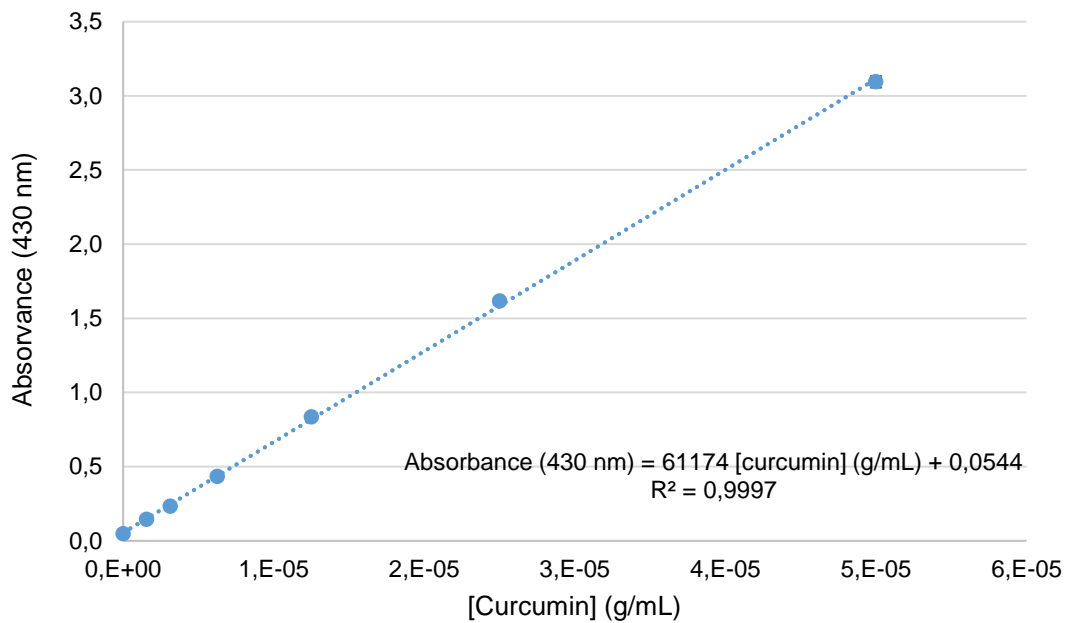


Figure A.1. – Calibration curve of curcumin in ethanol - absorbance at 430 nm versus curcumin concentration ($\mu\text{g/mL}$). The calibration curve equation is: $\text{Absorbance (430 nm)} = 61174 [\text{Curcumin}] (\mu\text{g/mL}) + 0.0544$ and the respective determination coefficient is 0.9997. The absorbance measurements were obtained in Cytation 3_Biotec equipment.

Annex 2 – Statistical evaluation of ethanol percentage influence in curcumin absorbance at 430 nm

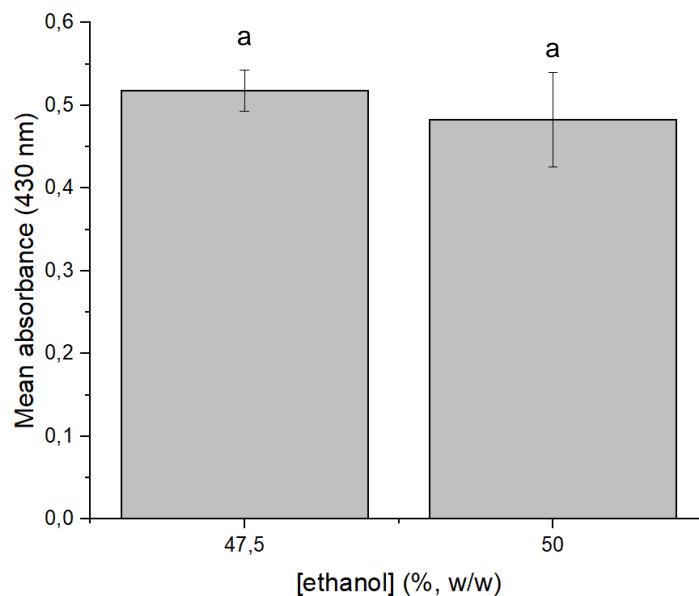


Figure A.2. – Demonstration of curcumin mean absorbance at 430 nm, solubilized in 47.5 and 50 % (w/v) of ethanol. Different lower case letters are indicative of statistically significant differences ($p > 0.5$).

Annex 3 – Calibration curve of curcumin in ethanol - absorbance at 430 nm versus curcumin concentration

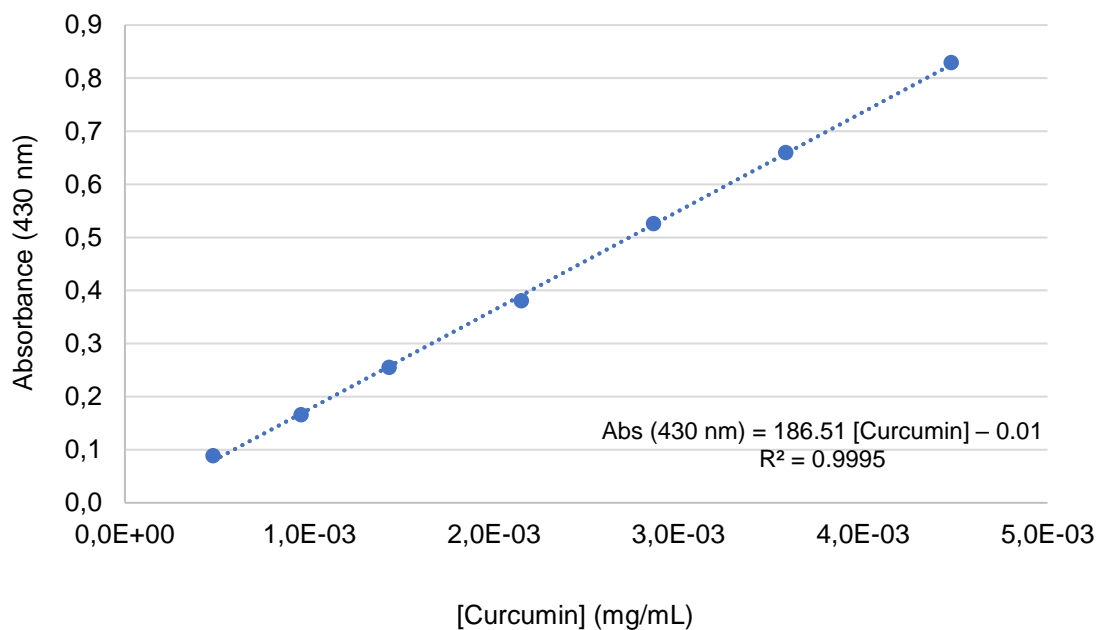


Figure A.3. – Calibration curve of curcumin in ethanol - absorbance at 430 nm versus curcumin concentration ($\mu\text{g/ml}$). The calibration curve equation is: $Absorbance(430\text{ nm}) = 186.51 [Curcumin] (\text{g/mL}) - 0.01$ and the respective determination coefficient is 0.9995. The absorbance measurements were obtained in Genesys 50 (Thermo scientific, USA) UV-Vis spectrophotometer.

Annex 4 – Calibration curve of curcumin in chloroform - absorbance at 430 nm versus curcumin concentration

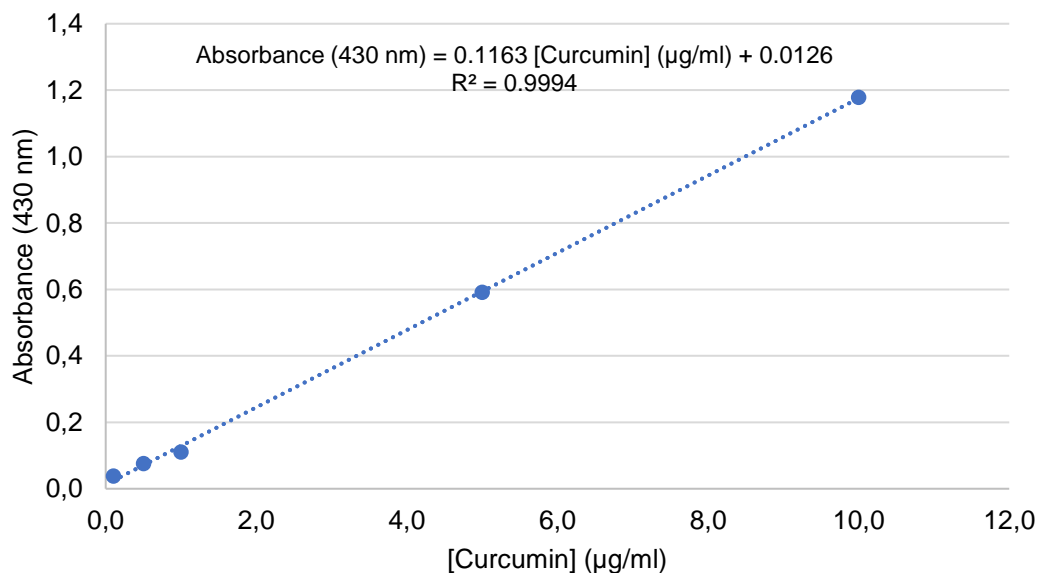


Figure A.4. – Calibration curve of curcumin in chloroform – absorbance at 430 nm versus curcumin concentration ($\mu\text{g/ml}$). The calibration curve equation is: $Absorbance(430\text{ nm}) = 0.1163 [Curcumin] (\mu\text{g/ml}) + 0.0126$ and the respective determination coefficient is 0.9994. The absorbance measurements were obtained in DR 2800 (Hach Lange, USA) UV-Vis spectrophotometer.

Annex 5 – Calibration curve of protein - absorbance at 750 nm versus protein concentration

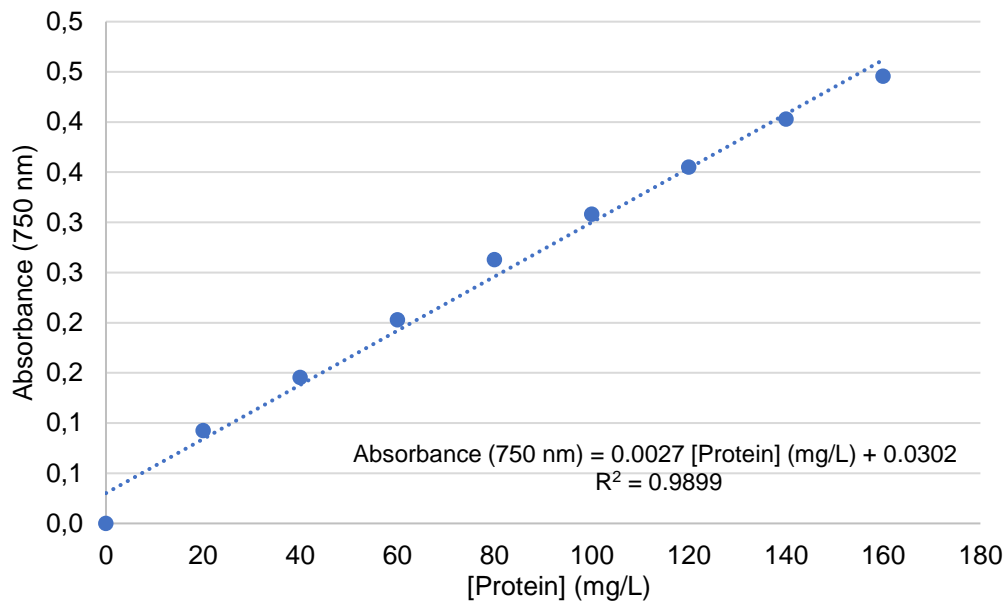


Figure A.5. – Calibration curve of protein - absorbance at 750 nm versus BSA concentration ($\mu\text{g/ml}$) resultant from Lowry assay method. The calibration curve equation is the following: $\text{Absorbance (750 nm)} = 0.0027 [\text{Protein}] (\text{mg/L}) + 0.0302$ and the respective determination coefficient is 0.9899. The absorbance measurements were obtained in Cytation 3_Byotek equipment.